A PROBABILISTIC MODEL OF SPECTRUM OCCUPANCY, USER ACTIVITY, AND SYSTEM THROUGHPUT FOR OFDMA BASED COGNITIVE RADIO SYSTEMS

A Dissertation

by

NARIMAN RAHIMIAN

Submitted to the Office of Graduate Studies of
Texas A&M University
in partial fulfillment of the requirements for the degree of

DOCTOR OF PHILOSOPHY

Approved by:

Chair of Committee,	Costas N. Georghiades
Co-Chair of Committee,	Khalid A. Qaraqe
Committee Members,	Jose Silva-Martinez
	Natarajan Gautam
Department Head,	Chanan Singh

May 2013

Major Subject: Electrical Engineering

ABSTRACT

With advances in communications technologies, there is a constant need for higher data rates. One possible solution to overcome this need is to allocate additional bandwidth. However, due to spectrum scarcity this is no longer feasible. In addition, the results of spectrum measurement campaigns discovered the fact that the available spectrum is under-utilized. One of the most significant solutions to solve the under-utilization of radio-frequency (RF) spectrum is the cognitive radio (CR) concept. A valid mathematical model that can be applied for most practical scenarios and also captures the random fluctuations of the spectrum is necessary. This model provides a significant insight and also a better quantitative understanding of such systems and this is the topic of this dissertation. Compact mathematical formulations that describe the realistic spectrum usage would improve the recent theoretical work to a large extent. The data generated for such models, provide a mean for a more realistic evaluation of the performance of CR systems. However, measurement based models require a large amount of data and are subject to measurement errors. They are also likely to be subject to the measurement time, location, and methodology.

In the first part of this dissertation, we introduce cognitive radio networks and their role on solving the problem of under-utilized spectrum.

In the second part of this dissertation, we target the random variable which accounts for the fraction of available subcarriers for the secondary users in an OFDMA based CR system. The time and location dependency of the traffic is taken into account by a non-homogenous Poisson Point Process (PPP).

In the third part, we propose a comprehensive statistical model for user activity, spectrum occupancy, and system throughput in the presence of mutual interference

in an OFDMA-based CR network which accounts for the sensing procedure of spectrum sensor, spectrum demand-model and spatial density of primary users, system objective for user satisfaction which is to support as many users as possible, and environment-dependent conditions such as propagation path loss, shadowing, and channel fading.

In the last part of this dissertation, unlike the second and the third parts that the modeling is theoretical and based on limiting assumptions, the spectrum usage modeling is based on real data collected from an extensive measurement.

DEDICATION

I lovingly dedicate this dissertation to my parents, Narges and Nojan.

ACKNOWLEDGEMENTS

I would like to express my appreciations to Dr. Khalid A. Qaraqe and Dr. Costas N. Georghiades, for their precious support during the whole length of my program. I'm honored to have them as my advisor and appreciate the freedom I had to pursue different research areas. I also acknowledge the efforts of my defense committee members Dr. Jose Silva-Martinez and Dr. Natarajan Gautam on providing feedback at the defending phase. Indeed their comments enhanced this work. I would like to thank Dr. Zeeshan Shakir and Dr. Hasari Celebi for their precious support, collaborations and encouragements during my PhD program. Finally, I thank my parents and friends for sharing their love all these years. I owe all my success to their blessings and encouragement. I especially thank Sabit Ekin, for his help in preparation of this work. Last but not least, I thank to Qatar Telecom (Qtel) and Qatar National Research Fund (an initiative of Qatar Foundation) for their valuable supports to this research.

NOMENCLATURE

AWGN	Additive White Gaussian Noise
CDF	Cumulative Distribution Function
CR	Cognitive Radio
DFS	Dynamic Frequency Selection
DSA	Dynamic Spectrum Access
FCC	Federal Communications Commission
ISP	Internet Service Provider
MGF	Moment Generating Function
Ofcom	Office of Communications
OFDMA	Orthogonal Frequency-Division Multiple Access
PDF	Probability Density Function
PMF	Probability Mass Function
PPP	Poisson Point Process
PR	Primary Receiver
PU	Primary User
QoS	Quality of Service
RF	Radio Frequency
SINR	Signal-to-Interference-plus-Noise Ratio
SNR	Signal-to-Noise Ratio
SR	Secondary Receiver
SU	Secondary User
TPS	Transmit Power Control

TABLE OF CONTENTS

LIST OF FIGURES

LIST OF TABLES

TABLE Page

1. INTRODUCTION

1.1 Cognitive Radio Networks

In this section, we introduce cognitive radio networks and their role on solving the problem of under-utilized spectrum. Since the multiple access method is assumed to be orthogonal frequency multiple access (OFDMA) throughout this dissertation, we provide an overview on the technical aspects and benefits of this multiple access method. Next, related works on modeling the spectrum usage on CR networks are introduced. Finally, an overview on several standards supporting cognitive radio and dynamic spectrum access is provided.

Radio frequency (RF) spectrum can be considered as one of the most precious and rare resources in wireless communication systems. Therefore, regulatory agencies exclusively allocate each band in spectrum to a specific user and guarantee that this licensed user will be protected from any interference. Under these strict frequency allocation policies and the requirement of high data rates, the RF spectrum has turned into a very valuable resource especially with the vast applications of wireless technologies and the emergence of new wireless services. On the other hand, recent spectrum measurement campaigns, performed by Federal Communications Commission (FCC), reported that the RF spectrum is being used in an inefficient and unbalanced manner [2, 11, 27, 37]. Hence, efficient utilization of the spectrum is considered as the most important issue.

The idea of cognitive radios (CRs) is a promising approach for the efficient utilization of spectrum. Opportunistic spectrum access creates the opening of under-utilized portions of the licensed spectrum for reuse, provided that the transmissions of secondary radios do not cause harmful interference to primary users. For secondary

users to accurately detect and access the idle spectrum, CR has been proposed as an enabling technology. Generally, in CR networks the usage of spectrum by cognitive (secondary) users is maintained by three approaches:

In interweave cognitive networks secondary users opportunistically access the idle spectrum. Therefore, primary and secondary users are not allowed to operate simultaneously.

In underlay cognitive networks both primary and secondary users share the spectrum. However, PUs are allocated a higher priority to use the spectrum than SUs, and the coexistence of primary and secondary users is allowed under the PU's predefined interference constraint which is called interference temperature. In this networks, a minimum quality of service (QoS) for the primary network must be guaranteed..

In overlay cognitive networks, SUs and PUs are allowed to transmit simultaneously. This is possible with the application of advanced coding techniques [28]. Combinations of the interweave (opportunistic access) and underlay (spectrum sharing) approaches are called hybrid CR networks [31].

Information acquisition about the spectrum occupancy of PUs is among the most challenging issues in the implementation of CR networks [5,15,61]. Utilizing efficient spectrum sensing algorithms is difficult due to the uncertainties in the propagation channels at device and network-level, the hidden PU problem as the result of deep fading and shadowing conditions, and the limited sensing duration. There exist a large number of contributions that investigate the possible solutions for the current challenges and issues. In [70] and references therein, a comprehensive survey on the spectrum sensing algorithms and CR applications is conducted and the design and implementation challenges are addressed in detail. Various aspects of spectrum sensing problem are studied from a cognitive radio perspective and multi-dimensional

spectrum sensing concept is introduced.

1.2 Overview on Orthogonal Frequency Division Multiple Access

In orthogonal frequency division multiple access (OFDMA) systems, the radio frequency spectrum is divided into non-overlapping bands, called subcarriers. Subsets of subcarriers are assigned to individual users or different cells. This allows simultaneous low data rate transmission from several users. Different numbers of sub-carriers can be assigned to different users, in view to support differentiated Quality of Service (QoS), i.e. to control the data rate and error probability individually for each user. OFDMA can be seen as an alternative to combining orthogonal frequency division multiplexing (OFDM) with time division multiple access (TDMA) or time-domain statistical multiplexing, i.e. packet mode communication. Low-data-rate users can send continuously with low transmission power instead of using a "pulsed" high-power carrier. Constant delay, and shorter delay, can be achieved. This technique can also be described as a combination of frequency domain and time domain multiple access, where the resources are partitioned in the time-frequency space, and slots are assigned along the OFDM symbol index as well as OFDM sub-carrier index. OFDMA is considered as highly suitable for broadband wireless networks, due to advantages including scalability and MIMO-friendliness, and ability to take advantage of channel frequency selectivity [69].

In spectrum sensing cognitive radio, OFDMA is a possible approach to filling free radio frequency bands adaptively. In [65], a spectrum pooling system is proposed in which free bands sensed by nodes were immediately filled by OFDMA subbands. In OFDMA, the main idea is to send the transmitted data over many different orthogonal subchannels [25]. Since the bandwidth of each subcarrier is less than the channel coherence bandwidth, the channel fading model in each subcarrier is assumed to be

flat fading model. Therefore, the inter-symbol-interference (ISI) on each subcarrier is considerably negligible, and it can be completely eliminated through the use of cyclic prefix [25]. Cyclic prefix does not only eliminate ISI but also turns the whole transmitter-channel-receiver system into a linear time-invariant (LTI) systems [63] in the frequency domain, a result which is often expressed alternatively as a transformation of a frequency-selective channel into a multitude of at-fading channels.

Since the early establishment of cellular mobile communication networks, efficient sharing of the radio spectrum among the users has been an essential system design problem. There have been always numerous criteria such as fair spectrum allocation or minimum QoS satisfaction. In traditional OFDMA systems, the universal frequency reuse is assumed, i.e., the same set of subcarriers can be used in different cells while assuring that the subcarriers assigned to users in each cell are orthogonal to each other. Therefore, one of the main challenges is subcarrier collisions for cell edge users. In [4, 9, 16], stochastic subcarrier collision models have been proposed to investigate the performance of various scheduling and utilization schemes, and to evaluate the inter-cell-interference for cell-edge users.

1.3 Related Work

After Mitola's originating work [40], CRs have drawn large amount of attention and turned into a promising solution to solve and enhance the problem of under utilized spectrum see, e.g., [11, 72]. Many spectrum occupancy measurement campaigns have been conducted so far [10, 12, 17, 30, 36, 45, 54, 67]. These studies can be categorized as single band monitoring, time - frequency analysis, and indoor vs. outdoor measurements. For instance, in [36], the spectrum occupancy over time and frequency is studied while [67] studies the spectrum occupancy for indoor vs. outdoor considering time and frequency domains. In [24] a novel spectrum occupancy model

designed to generate accurate temporal and frequency behavior of various wireless transmissions is proposed. In [34], an empirical time-dimension model of spectrum use that is appropriate for dynamic spectrum access and CR is presented. Concretely, a two-state discrete-time Markov chain with novel deterministic and stochastic duty cycle models is proposed as an adequate mean to accurately describe spectrum occupancy in the time domain.

The data from the spectrum occupancy measurement can be considered as the observations of a random process. There are random variables such as amplitude of the measured spectrum, number of the occupied channels, bandwidth of the occupied channels, and center frequency of the occupied channels that can be mathematically characterized by evaluating their distribution. In [66] a spectrum use model has been introduced which is basically an amplitude distribution model. In [48] the spectrum usage is characterized by evaluating the PMF of the number of occupied channels at four geographically different locations based on an extensive measurement conducted in the State of Qatar. These random variables are important since the secondary users in CR networks are constantly sensing the spectrum for availability. Hence, having a valid mathematical distribution of the mentioned random variables provides a significant insight to the secondary users about the dynamic nature of the spectrum so they can adjust their sensing and transmitting specifications accordingly. All the so far conducted measurement campaigns have provided models which are heavily dependent on the time and geographical location of the measurement, therefore the results may not be applicable to other times and spots. Based on this argument, a rigorous model that can be applied for most practical scenarios and also captures the random fluctuations of the spectrum is essential. This randomness is mostly covered by the mentioned random variables.

The Poisson point process model (PPP) has been used for spatial node distribu-

tions in various wireless networks, such as random access, ad-hoc, relay, cognitive radio and femtocell networks [8,13,14,18,22,23,29,38,52,57,64] . It represents a good trade-off between the complexity of the model and its ability to represent practical scenarios. In this dissertation, we consider primary users spatially scattered according to a homogeneous PPP in a finite two-dimensional plane where the monitoring spectrum sensor is located in the center of the region. Note that the spectrum sensor can be considered as a sensing secondary user searching for spectrum holes.

There exits numerous contributions that address the challenges due to RF spectrum sharing, and to investigate various aspects of CR networks, such as performance evaluation, implementation issues, etc such as [5] and references therein. Information acquisition about the spectrum occupancy of PUs is one of the implementation issues. In [49], optimal cooperation strategies for spectrum sensing to combat the effects of destructive channels and malfunctioning devices are presented. The proposed method conducts spectrum sensing based on the linear combination of local test statistics from individual secondary users. In [20], collaborative spectrum sensing is proposed as a mean to combat the effects of shadowing or fading.

To understand the performance constraints of a spectrum sharing system, SU throughput is a very useful performance measure. The ergodic and outage capacities of CR systems in Rayleigh fading channels are studied in [44], and a comprehensive study considering different conditions of power constraints and channel fading types is performed in [32]. In [21], considering a point-to-point communication scenario, the closed form equations for the average throughput of a single SU assuming the existence of a single PU and no mutual interference are derived for different channel fading types such as Rayleigh, Nakagami-m and Log-normal. In [60], which is the extension of [21], the SU throughput and the average bit error rate effected by PU's interference and imperfect channel knowledge, in a Rayleigh channel are

derived. In [50], a new statistical model for aggregate interference of a cognitive network, which accounts for the sensing procedure, secondary spatial reuse protocol, and environment-dependent conditions such as path loss, shadowing, and channel fading is proposed. In [71], the average sum capacity of SUs with multiple access and broadcast fading channels is derived applying optimal power allocation.

1.4 Overview on IEEE Standards Supporting Cognitive Radio and Dynamic Spectrum Access

Standardization is key to the success of many technologies. CR radio is no exception. CR techniques are being applied in many different communications systems. They promise to improve the utilization of radio frequencies making room for new and additional commercial data, emergency, and military communications services [39, 42]. In the United States these techniques are being considered by the Federal Communications Commission (FCC) for communications services in unlicensed VHF and UHF TV bands. Similar consideration is being given elsewhere in the world such as Office of Communications (Ofcom) in the United Kingdom. Standardization is the main building block of cognitive radio's successes. This section provides a survey of cognitive radio standardization activities, their past and present, and discusses prospects and issues for future standardization. The the institute of electrical and electronics engineers (IEEE) has two well-known standards activities in this area - SCC41 (formerly known as P1900) and IEEE 802.22. However, there are lesser known related activities within IEEE as well. One of the indirect topics related to the CR systems is "co-existence" which, for many years has been considered in various standards. The ability to "co-exist" with other radios using different protocols in the same bands is important for many radios. This is particularly true in unlicensed bands where a wide variety of unrelated protocols are applied includ-

ing such IEEE standards as the IEEE 802.11, IEEE 802.15, and the IEEE 802.16. Techniques such as dynamic frequency selection (DFS) and power control (PC) have been developed and standardized to deal with co-existence issues. The co-existence techniques developed and being developed for these bands are similar to those for dynamic spectrum access (DSA). In some regards, the application of CR/DSA techniques can be thought of as an evolution of co-existence techniques. Planned systems such as 802.16e and m, with well defined cellular architectures as well as frequency allocations have an easier problem in dealing with self co-existence. However, systems such as 802.22, where primary users of the spectrum such as wireless micro-phones can dynamically come on and off, as well as secondary users such as the internet service providers (ISP) compete for the same available frequency (White space), the co-existence issue is difficult to solve.

Figure 1.1 shows a time-line for the evolution of cognitive standards within IEEE that takes coexistence standards as a starting point. Initial coexistence standards provided methods of measuring interference and mitigating interference through manual coordination. These standards started being developed as early as 1999. Eventually it was realized that many of these techniques could be automated, and a second generation of standards resulted, including capabilities such as DFS and PC. Today CR/DSA standards are being developed that address issues such as coexistence. The specific standards and their time-lines are depicted in Fig. 1.1.

The completed standards activities to date include the IEEE 802.16.2-2001, IEEE 802.15.2-2003, IEEE 802.15.4-2003, IEEE 802.11h-2003, IEEE 802.16a-2003 and IEEE 802.16.2-2004. More information on the descriptions and comparison of the standards can be found in [56]. All the completed standards to date deal with co-existence of one form or another. Co-existence standards that depend on manual co-ordination are included because they define what constitutes interference, and

mechanisms to mitigate it. These laid the ground work for the automated detection and spectrum sharing techniques that later evolved. Many of these standards include DFS and transmit power control (TPC) for the purpose of facilitating spectrum sharing. They are designed to detect the presence of other systems, dynamically modify their use of the spectrum to protect primary users, and to allow sharing between systems using diverse protocol sets. They are almost identical in function to DSA systems and can be found within several IEEE 802 standards.

The Standards Coordinating Committee (SCC) 41 is focused on DSA networks and has several standards currently in development. They are well-known for their CR activities and have a broader scope than the previous co-existence oriented activities that have been or are being conducted in IEEE 802. Finally IEEE 802 activities related to CR technology comprises of IEEE 802.22 [59], IEEE 802.19, IEEE 802.16h, IEEE 802.16m and IEEE 802.11y. The IEEE 802.22 working group is the flagship IEEE 802 standard defining CR and DSA. IEEE 802.22 will be the first CR standard with tangible frequencies of operation. While SCC 41 and IEEE 802.22 are the primary cognitive standards efforts today, many completed IEEE 802 standards already include CR/DSA like capabilities or related building blocks. Most of these concepts have evolved out of co-existence activities. For example, IEEE 802.15 was one of the first standards groups to address co-existence issues since 802.15 protocols needed to share the same unlicensed band (2.4 GHz) used by IEEE 802.11.

Some other prior IEEE Standards work related to CR deals with DFS, dynamic channel selection (DCS) and TPC. These standards include IEEE 802.11h, IEEE 802.16-2004 and IEEE 802.15.4. These features deal with the fact that other systems (such as military radars) may operate in the Unlicensed National Information Infrastructure (UNII) bands and need protection. The DFS features developed for 802.11 allow for the detection of military radars and relocation of a potentially inter-

fering 802.11 basic service set (BSS) to another frequency. The techniques developed for 802.11h can be applied to other bands and other systems with similar issues, and be leveraged by CR/DSA systems. IEEE 802.16-2004 is another standard that includes DFS and TPC capabilities [43].

Standards Coordinating Committee 41 (SCC41) sponsors standards projects in the area of dynamic spectrum access networks (DySpaN). The SCC41 / P1900 activities are co-sponsored by the IEEE Communications and Electromagnetic Compatibility Societies. SCC41 addresses techniques and methods of DSA require managing interference, co-ordination of wireless technologies, and include network management and information sharing. SSC41 considers SDR to be a key enabler for CR/DSA [46]. It concentrates on developing architectural concepts and specifications for network management between incompatible wireless networks rather than specific mechanisms that can be added to the physical (PHY) or Media Access Control (MAC) protocol layers. SCC41 is developing policy-based network management for dynamic spectrum access among 3G/4G, WiFi, and WiMax networks. SCC41 has recently proposed two new working groups to address policy language (P1900.5) and radio frequency (RF) spectrum sensing (P1900.6). The goal of these groups is to develop the policy language framework using languages and address spectrum sensing functions that can be managed in the terminal radio managements.

The IEEE 802 LAN/ MAN Standards committee created the 802.22 working group (WG) on wireless regional area networks (WRAN) in response to the FCC Notice of Proposed Rule Making (NPRM) 04-113 [42] for the use of unlicensed wireless operation in the analog television (TV) bands. IEEE 802.22 defines air interface for use by license-exempt devices on a non-interfering basis in VHF and UHF (54-862 MHz) bands which are also referred to as the TV White Spaces.

IEEE 802.19 is a technical advisory group (TAG) within IEEE 802. IEEE 802.19

was created based on the successes of 802.15.2 to act as a co-existence advisory committee across all of IEEE 802. They have spearheaded the creation of special rules focused at fostering co-existence within IEEE 802 standards operating in unlicensed bands. This includes monitoring the creation of "co-existence assurance" documents for new IEEE 802 wireless standards that could rely on cognitive techniques. Currently, 802.19 is working on a recommended practice for methods of assessing co-existence of wireless networks. When completed, these methods may be of use for cognitive systems.

IEEE 802.16 is intended for use in licensed and unlicensed bands. Co-existence issues have been a concern almost from the beginning. However, in 2004, project 802.16h was started to consider 'Improved co-existence mechanisms for license-exempt operation'. The resulting standard likely will include cognitive capabilities and mechanisms that can be broadly applicable in many systems. As of this date, the current draft of this standard is 'D6' and it is still being balloted within the 802.16 WG.

1.5 Contributions of this Dissertation

In this work, we target the random variable which accounts for the fraction of available subcarriers for the secondary users in an OFDMA based CR system. The time and location dependency of the traffic is taken into account by a non-homogenous PPP. We derive the PMF of the fraction of available subcarriers under a few assumptions on the network topology and the distribution of the number of requested subcarriers from each primary user (requesting distribution). Based on two sufficient conditions, any arbitrary requesting distribution is categorized into either "greedy" or "non-greedy" distribution. It is shown that the knowledge of the mean (first moment) of the requesting distribution suffices to categorize. These conditions are critical in the system design when it is preferred that for a fixed traffic of pri-

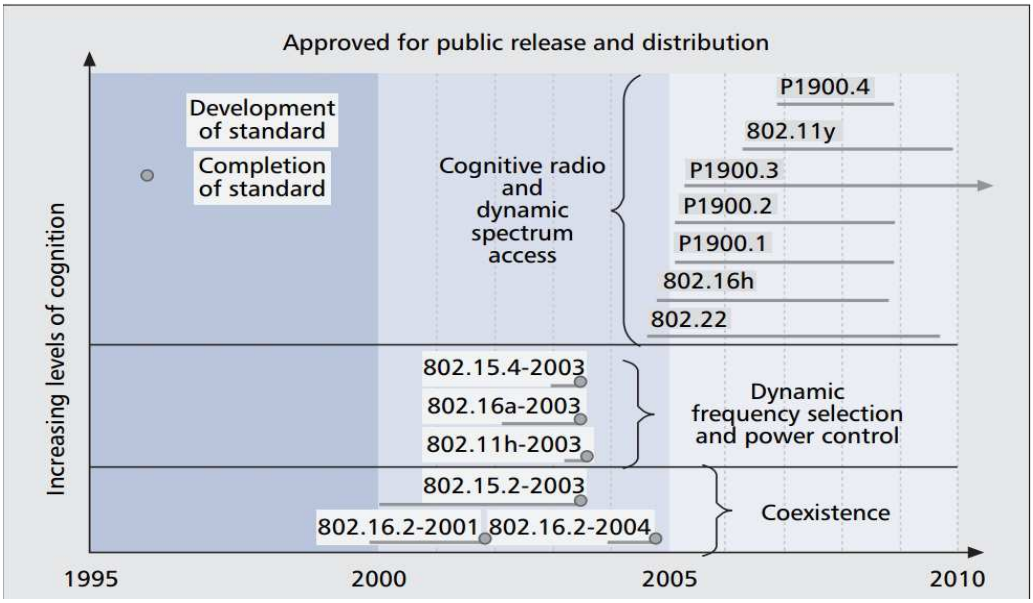

Figure 1.1: The evolution of IEEE standardization activities relating to dynamic spectrum access starting with coexistence standards, evolving toward DFS/PC, and finally encompassing true CR/DSA techniques [56].

mary users, the increase in the total number of subcarriers guarantees the increase in the spectrum availability. We show that for some "greedy" systems, providing more subcarriers will not increase the spectrum availability for a secondary network. The sustainable traffic of the system subject to a fixed spectrum outage probability is also investigated. It is shown that for a fixed spectrum outage probability, as long as the system is "greedy", providing more subcarriers does not help to support more primary users to successfully avoid spectrum outage. The asymptotic mean of the fraction of available subcarriers and corresponding upper and lower bounds are derived and analyzed as the total number of system subcarriers and primary network traffic go to infinity. It is shown that the mean of the subcarrier requesting distribution suffices to determine the asymptotic spectrum availability of the system.

Next, we propose a comprehensive statistical model for user activity, spectrum occupancy, and system throughput in the presence of mutual interference in an

OFDMA-based CR network which accounts for the sensing procedure of spectrum sensor, spectrum demand-model and spatial density of primary users, system objective for user satisfaction which is to support as many users as possible, and environment-dependent conditions such as propagation path loss, shadowing, and channel fading. We show that the number of active primary users is not a Poisson random variable (unlike previous works assumptions) under limited spectrum constraint. The proposed model is valid for any area at any time therefore it is independent of time and location. Our framework also allows us to derive the distribution of received signal power at the spectrum sensor from active primary users in a limited or finite region considering the shape of region and the position of the spectrum sensor. Next, to investigate deeper, the behavior of the mean number of active primary users and occupied subcarriers as a function of primary network traffic are studied. Two parameters *user activity rate* and *spectrum access rate* are defined. These parameters provide insight on the asymptotic behavior of requesting distributions as the primary network traffic goes to infinity. We demonstrate the use of our model in evaluating a system performance such as the probability of miss detection of an occupied subcarrier by the spectrum sensor. It is shown that this probability is a function of system traffic and the requesting distribution. It is also shown for extreme traffic of users, the applied requesting distribution and total number of provided subcarriers can not further improve the asymptotic sensing accuracy of the secondary user. Then, considering the spectrum sensor as a single sensing secondary user, we introduce a statistical model for the throughput of the primary network and the secondary user in the presence of mutual interference. The interference is the result of imperfect detection of the secondary user due to poor channel conditions and propagation path loss. It is shown that with increase in the primary network transmit power, the average throughput of both primary network

and secondary user increases. The SU throughput in the presence of mutual interference due to imperfect detection of the SU in an OFDMA-based cognitive radio system is investigated and its asymptotic behavior as the primary network traffic and PU transmit power go to infinity is analytically derived and compared to the simulation results. It is shown that with increase in the primary network transmit power, the average throughput of the SU increases and converges to a limit point. It is also proved that with increase in primary network traffic, SU throughput decreases and converges to a limit point. Numerical results verify the validity of our model in capturing the effects of system specifications such as the requesting distribution and the traffic of PUs.

Finally, in the last section, unlike previous sections that the modeling is theoretical and based on limiting assumptions, the spectrum usage modeling is based on real data collected from an extensive measurement. The spectrum usage is modeled by estimating the Probability Mass Function (PMF) of the number of occupied channels. Note that this also gives an insight regarding the spectrum availability. To do this, the data collected from a spectrum occupancy measurement campaign conducted in the State of Qatar is used. The measurements are performed over three consecutive days considering 700-3000 MHz frequency band at four different locations concurrently. We show that after applying the Chi square test, the Log-Normal distribution fits the best among other candidates to the empirical PMF independent of location and the threshold used to define a channel as occupied.

2. A PROBABILISTIC MODEL FOR USER DEMANDS AND SPECTRUM AVAILABILITY

2.1 Introduction

In this section, we target the random variable which accounts for the fraction of available subcarriers for the secondary users in an OFDMA based CR system. The time and location dependency of the traffic is taken into account by a non-homogenous Poisson Point Process (PPP). A good model for the fraction of available subcarriers is important for CR system design and analysis as it can provide, among other things, an analysis of the demand for spectrum by primary users and an estimate of the fraction of bandwidth that may be available to secondary users. We derive the Probability Mass Function (PMF) of the fraction of available subcarriers under a few assumptions on the network topology and the distribution of the number of requested subcarriers from each primary user (requesting distribution). Based on two sufficient conditions, any arbitrary requesting distribution is categorized into either "greedy" or "non-greedy" distribution. The sustainable traffic of the system subject to a fixed spectrum outage probability is also investigated. The asymptotic mean of the fraction of available subcarriers and corresponding upper and lower bounds are derived and analyzed as the total number of system subcarriers and primary network traffic go to infinity.

We consider demands made by a set of spatially Poisson distributed users on available channels in their proximity and assess their effect on channel availability for secondary users under various channel requesting distributions. We show that for some "greedy" systems, providing more subcarriers will not increase the spectrum availability for a secondary network. The sustainable traffic of the system subject

to a fixed spectrum outage probability is also investigated. It is shown that for a fixed spectrum outage probability, as long as the system is "greedy", providing more subcarriers does not help to support more primary users to successfully avoid spectrum outage. The asymptotic mean of the fraction of available subcarriers and corresponding upper and lower bounds are derived and analyzed as the total number of system subcarriers and primary network traffic go to infinity. It is shown that the mean of the subcarrier requesting distribution suffices to determine the asymptotic spectrum availability of the system.

2.1.1 Organization

In Section 2.2 we introduce the underlying primary user demand model and derive upper and lower bounds on the mean-fraction of available channels. Existence conditions of such bands are derived in Section 2.3. The asymptotic mean of the fraction of available subcarriers as the total number of system subcarriers and primary network traffic go to infinity is studied in Section 2.4. Here, it is shown that the mean of the subcarrier requesting distribution suffices to determine the asymptotic spectrum availability of the system. In Section 2.5 we study the effect of a given outage probability on the average number of users that can be sustained by the system and in Section 2.6 we present numerical results. Finally Section 2.7 concludes.

2.2 System Model and Problem Statement

It is assumed that an ideal spectrum sensor (SS) is used to sense the spectrum activity. Note that there is an analogy between the SS and the secondary user since they both constantly sense the spectrum for available holes. There exist M number of spectrum bands with different bandwidths BW_i $i = 1, 2, ..., M$ and power spectral densities (PSD). Fig. 2.1 depicts the mentioned spectrum bands. Instead of considering the whole spectrum, we take one step back and first study only one of the

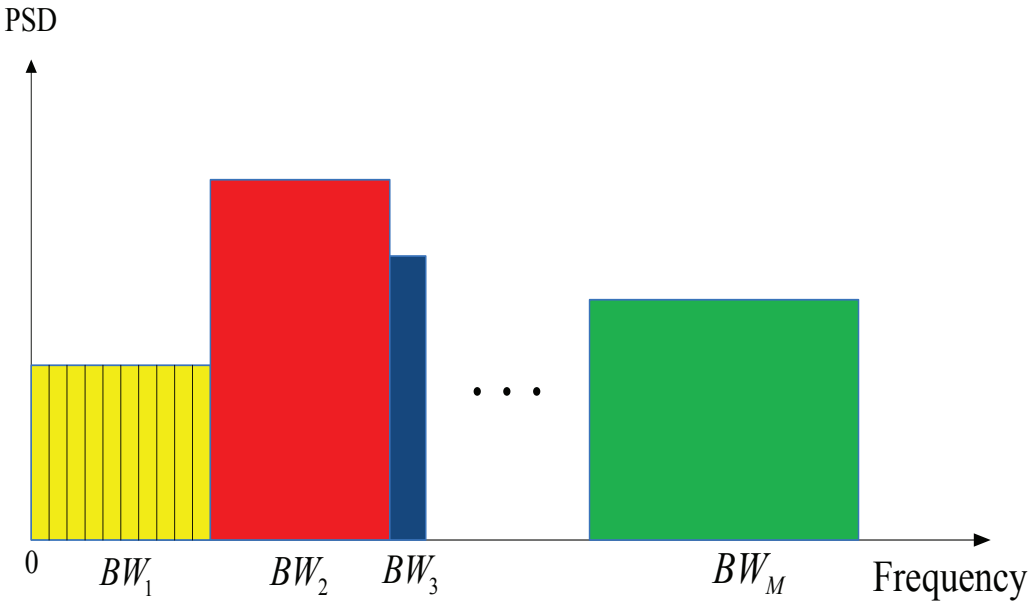

Figure 2.1: Illustration of spectrum bands where multiuser-OFDM is used for the first band as the multiple access method.

spectrum bands. The problem of modeling the whole spectrum is the generalization of modeling one band conditioned all the other bands use the same multiple access method. Without loss of generality we consider spectrum band 1 with bandwidth BW_1. Excluding the effect of fading and shadowing and only considering the power attenuation, the radius of sensing of the spectrum sensor is a function of path loss exponent (α), transmit power of the primary users assuming all users transmit at the same constant power level, (P_T), and the noise level of the device (γ). Therefore, the corresponding radius of sensing of the spectrum sensor is:

$$r_s = f(\alpha, P_T, \gamma). \tag{2.1}$$

The number of users is denoted by k. We assume k is produced by a non-homogeneous PPP with intensity of $\lambda(\vec{x}, t)$ where $\vec{x} \subset V \subset R^2$ and V is the entire area that the process takes place in. The rate is a function of both time and space. At any given

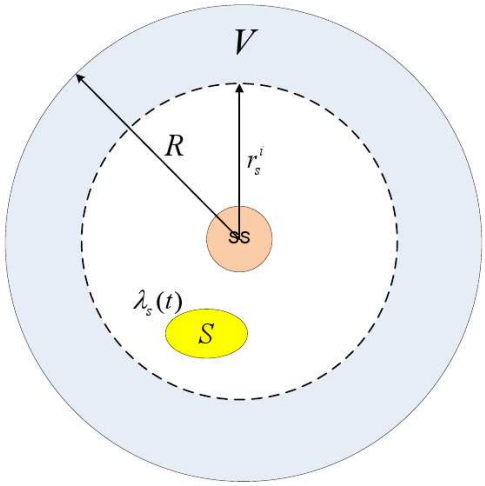

Figure 2.2: Illustration of the spectrum sensor location, radius of non-fading sensing, r_s, and the entire area, V, that the process takes place in.

time instant (t_0), for any set $S_1 \subset V$ (e.g. a spatial region), the number of users inside this region can be modeled as a Poisson random variable with the associated rate function of [33]:

$$\lambda_{S_1}(t_0) = \int_{S_1} \lambda(\vec{x}, t_0) d\vec{x}. \tag{2.2}$$

We assume that the whole region under study, V, is a large circular area with radius R and the spectrum sensor is located at the center with the coordinates of $(0, 0)$ in the plane. The rate is a function of time and space since in practice the number of users varies by time like day/night or rush hour/regular hours (non-homogeneous in time) and location like downtown/rural areas (non-homogeneous in space). Fig. 2.2 depicts the spectrum sensor location, radius of non-fading sensing r_s, and the entire area V that the process takes place in.

We assume primary users sharing the spectrum band use OFDMA as the multiple access method and the system operating in the spectrum band under study provides N subcarriers where N is usually a power of two. It is also assumed that the primary users are operating under a centralized system such that they send their

requests to access the spectrum to a central system. Since not all the primary users may transmit, we assume a user sends its request to transmit with the probability p_{tr}. In this case, "requesting users" are distributed in the area of study based on a non-homogenous PPP of intensity $\lambda_{tr}(\vec{x}, t) = p_{tr}\lambda(\vec{x}, t)$. It is also assumed that each requesting user may require several subcarriers to communicate. The number of required subcarriers is determined such that it satisfies the user minimum requirements for communication. These requirements are based on different user needs such as minimum quality of service, data rate, bit error rate and etc.

Since the intensity of the PPP of the requesting users is also a function of location, the Poisson random variable showing the number of requesting users inside two regions with the same area but different locations may have different parameters. Therefore, we label a region with its area and the corresponding coordinates of its center from the spectrum sensor. We study the system at any time instant but we may apply the results to obtain the average performance of the network with dynamically changing topology over a time interval. For any given time instant t_0, the number of requesting users inside a region of area S_1 with the coordinates of (a, b) from the spectrum sensor, $U_{S1,(a,b)}(t_0)$, has a Poisson distribution with the rate of:

$$\Lambda_{S1,(a,b)}(t_0) = \int_{x \in S_1} \lambda_{tr}(\vec{x}, t_0) d\vec{x}. \tag{2.3}$$

From now, we assume S_1 as the region of non-fading sensing of the spectrum sensor and $(a, b) = (0, 0)$. Note that the results hold for any arbitrary region and coordinates but we drop the notations regarding the area and coordinates for the sake of brevity. Moreover, since the results are derived at any given time instant, we eliminate the notation t_0. When the number of requesting users in an area is less than N, there will be available subcarriers. We introduce random variable M as the number of

subcarriers that a requesting user requires. M has PMF of $P_M(m),\ m = 1, 2, ..., N$, where $P_M(m)$ is the "requesting distribution". We also define the random variable W as:

$$W = \sum_{k=0}^{U} M_k, \tag{2.4}$$

where U is the number of requesting users inside the area of perfect sensing of the spectrum sensor, $M_0 = 0$, and $M_k,\ k = 1, 2, ..., U$ are independent and identically distributed. W represents the total number of requested subcarriers. Since U is a Poisson random variable, W has a *compound Poisson* distribution and can take values in $\{0, 1, 2, ..., \infty\}$. Clearly, all requests $W \geq N$ will not be satisfied and some will result in outage. Next, the effect of subcarrier requests on the mean fraction of remaining subcarriers is studied.

The random variable Z is defined as the fraction of available (remaining) subcarriers:

$$Z = \begin{cases} 1 - \frac{W}{N} & W < N \\ 0 & W \geq N. \end{cases} \tag{2.5}$$

Z takes $(N+1)$ values in $\left\{0, 1 - \frac{N-1}{N}, ..., 1 - \frac{2}{N}, 1 - \frac{1}{N}, 1\right\}$. Authors are interested in particular in quantifying the mean value of Z, i.e. the mean fraction of available subcarriers, as a function of the requesting distribution $P_M(m)$, the number of available subcarriers N, and the mean number of primary requesting users Λ. We have:

$$E[Z] = \sum_{w=0}^{N-1} \left(1 - \frac{w}{N}\right) \Pr\left(W = w\right). \tag{2.6}$$

In what follows, a system is defined to be "greedy" if:

$$\lim_{N \to \infty} E\left[Z\right] < 1. \tag{2.7}$$

In simple terms, a system is "greedy" when as the number of subcarriers N goes to infinity the fraction of available subcarriers does not go to 1.

There appears to be no simple expression for (2.6), so we resort to upper and lower bounds. Since $1 - \frac{W}{N} \leq 1 \quad for \quad W = 0, 1, 2, ..., \infty$, we have:

$$E\left[Z\right] \leq \sum_{w=0}^{N-1} Pr\left(W = w\right) = Pr(W \leq N-1). \tag{2.8}$$

Applying the *Chernoff* bound [41], we find an upper bound for the above left tail probability:

$$Pr(W \leq N-1) \leq \min_{u \leq 0} \quad e^{-u(N-1)} M_W(u), \tag{2.9}$$

where $M_W(u) = E\left[e^{uW}\right]$ is the *moment generating function* of the random variable W. Since W has compound Poisson distribution, its moment generating function is:

$$M_W(u) = \exp(\Lambda(M_M(u) - 1)). \tag{2.10}$$

The minimizing u which results to the tightest upper bound is the negative solution of:

$$M'_M\left(u\right) - \frac{N-1}{\Lambda} = 0. \tag{2.11}$$

If we call this desired solution as u^*, the tightest upper bound is:

$$\begin{aligned} E\left[Z\right] &\leq Pr\left(W \leq N-1\right) \\ &\leq e^{-u^*(N-1)} \exp(\Lambda(M_M(u^*) - 1)). \end{aligned} \tag{2.12}$$

In the case that there exists no negative u, the upper bound "1" is trivial.

It is shown in the numerical results that the Chernoff bound is not tight enough for some values of Λ. Therefore, another upper bound can be derived by bounding

the function $1-\frac{W}{N}$ by an exponential function $e^{-\alpha W}$ such that:

$$1-\frac{W}{N} \leq e^{-\alpha W} \ ; \ W \geq 0. \tag{2.13}$$

We choose α such that the above constraint is satisfied for all $W \geq 0$. For this purpose, we should have $\alpha \leq \frac{1}{N}$. $\alpha = \frac{1}{N}$ results to the tightest upper bound:

$$\begin{aligned} E[Z] &\leq \sum_{w=0}^{\infty} e^{-\frac{w}{N}} Pr(W=w) = E\left[e^{-\frac{w}{N}}\right] \\ &= M_W(u)\Big|_{u=-\frac{1}{N}} = \exp(\Lambda(M_M(-\frac{1}{N})-1)). \end{aligned} \tag{2.14}$$

Note that, for $\alpha = 0$ we have $1-\frac{W}{N} \leq e^0 = 1$ and the upper bound is the same as the Chernoff bound. The proposed upper bound can be used as a replacement for the Chernoff bound for values of Λ that Chernoff bound is loose. Moreover, it is always non-trivial (not equal to "1") and easy to evaluate since the upper bound is simply the realization of the moment generating function of W at $u = -\frac{1}{N}$. It is also useful in studying the asymptotic spectrum availability for secondary network as the total number of subcarriers, N, goes to infinity. Another advantage of this proposed upper bound is the simplicity of comparing the asymptotic spectrum availability for secondary users for different requesting distributions.

For the lower bound we have:

$$E\left[1-\frac{W}{N}\right] = \overbrace{\sum_{w=0}^{N-1}(1-\frac{w}{N})Pr(W=w)}^{\text{E[Z]}} + \underbrace{\sum_{w=N}^{\infty}(1-\frac{w}{N})Pr(W=w)}_{\text{Non-Positive terms}} \Rightarrow E\left[1-\frac{W}{N}\right] = 1-\frac{\Lambda E\left[M\right]}{N} < E\left[Z\right]. \tag{2.15}$$

Therefore, in the worst case scenario the mean of the fraction of available subcarriers for the secondary users is $1-\frac{\Lambda E[M]}{N}$. For the case of $N < \Lambda E\left[M\right]$, this lower bound turns out to be negative, therefore the lower bound "0" is trivial. Having upper and lower bounds provides information about the best and the worst spectrum availability for secondary network.

For the requesting PMF of *uniform* distribution:

$$P_M(m) = \frac{1}{N}; \quad m = 1, 2, ..., N, \tag{2.16}$$

we have $E\left[M\right] = \frac{N+1}{2}$. and for the modified binomial requesting distribution (which starts from 1 instead of 0)

$$P_M(m) = \binom{N-1}{m-1} p^{m-1}\left(1-p\right)^{N-m}, \quad m = 1, 2, ..., N, \tag{2.17}$$

we have $E\left[M\right] = (N-1)p + 1$. For uniform distribution, each requesting user may request a number of subcarriers between 1 and N with equal probability.

The lower bounds become in these cases respectively:

$$E\left[Z\right] \geq 1 - \frac{\Lambda\left(N+1\right)}{2N} \rightarrow 1 - \frac{\Lambda}{2}, \tag{2.18}$$

$$E\left[Z\right] \geq 1 - \Lambda\frac{(N-1)p+1}{N} \rightarrow 1 - \Lambda p, \tag{2.19}$$

where the limits on the right are as $N \rightarrow \infty$. Of course, if any of these lower bounds become negative, the lower bound 0 is trivially used instead.

In order to find the distribution and exact mean of Z it is enough to find the distribution of W due to the relationship between Z and W in Eq.(2.5). For this purpose, we use the characteristic function method. We know that for the random variable M with PMF of $P_M(m)$ and the characteristic function of $\Phi_M(\omega) = E\left[e^{j\omega M}\right]$ we will have:

$$P_M(m) \stackrel{F}{\rightarrow} \Phi_M(-\omega), \tag{2.20}$$

where F notes for the Fourier transform of a discrete time aperiodic signal. Since W has compound Poisson distribution its characteristic function is:

$$\Phi_W(\omega) = \exp(\Lambda(\Phi_M(\omega) - 1)). \tag{2.21}$$

For the uniform distribution in (3.10) the characteristic function is:

$$\Phi_M(\omega) = \frac{e^{j\omega} - e^{j\omega(N+1)}}{N(1 - e^{j\omega})}, \tag{2.22}$$

and for the modified binomial distribution in (2.17):

$$\Phi_M\left(\omega\right) = e^{j\omega}\left(1 - p + pe^{j\omega}\right)^{N-1}. \tag{2.23}$$

Finally we take the inverse Fourier transform of $\Phi_W(-\omega)$ to find $P_W(w)$:

$$P_W(k) = \frac{1}{2\pi}\int_{-\pi}^{\pi} \Phi_W(-\omega)e^{j\omega k}d\omega; k = 0, 1, 2, ..., \infty. \tag{2.24}$$

An interesting property of the characteristic function of W is that its cumulants are proportional with the central moments of M with the coefficient $\Lambda_{S1,(a,b)}$. For the nth cumulant of W we have:

$$\kappa_{n,W} = \frac{1}{j^n}\frac{d^n \ln \Phi_W(\omega)}{d\omega^n}\bigg|_{\omega=0} = \Lambda E\left[M^n\right]. \tag{2.25}$$

In cases that it is complicated to find the exact closed form distribution of W, the distribution can be approximated by the use of its cumulants. In [19, 51] the cumulants are used to approximate the distribution of the interference caused by the secondary users on a licensed user as a *shifted log normal* distribution and *truncated stable distribution* [53] respectively. However, in this contribution we use numerical analysis using Eq.(2.24) to find the PMF of W.

2.3 Existence Conditions of the Non-Trivial Bounds

A non-trivial upper bound (lower bound) is a bound which is not equal to "1"("0"). Note that the upper bound derived from the Chernoff bound technique can be sometimes trivial.

2.3.1 Non-Trivial Upper Bounds

In order to find the condition on the existence of a non-trivial upper bound, we first study the behavior of the moment generating function of a positive random variable.

Proposition 1: *For the* strictly positive *random variable M (taking values greater*

than zero) with the moment generating function $M_M(u) = E\left[e^{uM}\right]$*, the moment generating function and all its derivatives are* strictly positive *for all* u*.*

Proof: Since M only takes positive values and the function e^{uM} is always positive, we have:

$$\forall\ u,\ M_M(u) = E\left[e^{uM}\right] = \sum_m e^{um} Pr(M = m) > 0. \tag{2.26}$$

$$\begin{aligned} \forall\ u,\ M_M^{(n)}(u) &= \frac{d^n M_M(u)}{du^n} = E\left[M^n e^{uM}\right] \\ &= \sum_m m^n e^{um} Pr(M = m) > 0. \end{aligned} \tag{2.27}$$

$$\begin{aligned} \lim_{u\to\infty} M_M(u) &= \lim_{u\to\infty} M_M^{(n)}(u) = \infty \\ \lim_{u\to-\infty} M_M(u) &= \lim_{u\to-\infty} M_M^{(n)}(u) = 0. \end{aligned} \tag{2.28}$$

In the previous section it was shown that in order to find the u that leads to the tightest upper bound we have to solve (2.11). If we have:

$$G(u) = M'_M(u) = \frac{dM_M(u)}{du} = E\left[Me^{uM}\right], \tag{2.29}$$

then (2.11) changes to:

$$G\left(u\right) - \frac{N-1}{\Lambda} = 0. \tag{2.30}$$

Therefore, based on the behavior of the moment generating function of strictly positive random variables, we have:

$$\begin{aligned} &\forall\ u, G(u) > 0,\ G'(u) > 0,\ G''(u) > 0 \\ &\lim_{u\to-\infty} G(u) = 0\ ,\ \lim_{u\to\infty} G(u) = \infty. \end{aligned} \tag{2.31}$$

So $G(u)$ is a positive, monotonically increasing convex function. Note that $G(0) = M'_M(0) = E\left[M\right]$.

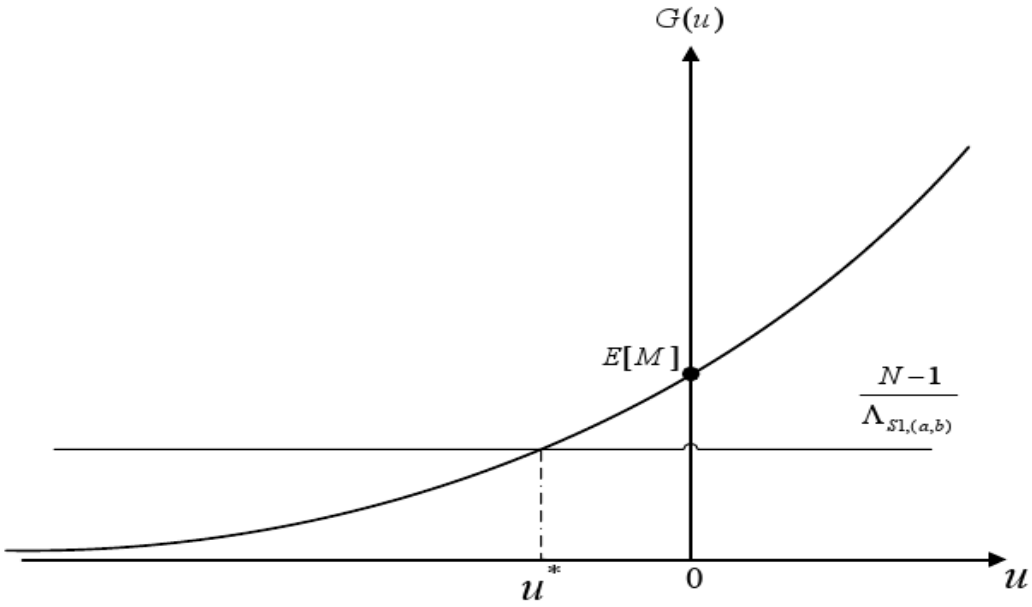

Figure 2.3: The graphical method of finding the root of Eq.(2.30).

As it was explained in the previous section, the negative roots of (2.30) result in the non-trivial tightest upper bound. Since $G(u)$ is a monotonically increasing function and according to (2.28), Eq.(2.30) always has a root and this root is *unique*. Fig.2.3 depicts the graphical method of finding the root of (2.30). In this figure it is obvious that in order to have a negative root we should have:

$$\frac{N-1}{\Lambda} < E\left[M\right]. \tag{2.32}$$

2.3.2 Non-Trivial Lower Bounds

In order to find the condition on the existence of a non-trivial lower bound, we use Eq.(2.15). It can be seen that in order to have a non-trivial lower bound the left hand of the inequality in this equation should be positive. Therefore the condition

is:

$$\frac{N}{\Lambda} > E\left[M\right]. \tag{2.33}$$

To summarize the conditions for both bounds:

$$\begin{cases} \frac{N-1}{\Lambda} < E\left[M\right] & \text{Non-trivial upper bound} \\ \frac{N-1}{\Lambda} \geq E\left[M\right] & \text{Upper bound “1”} \\ \frac{N}{\Lambda} > E\left[M\right] & \text{Non-trivial lower bound} \\ \frac{N}{\Lambda} \leq E\left[M\right] & \text{Lower bound “0”}. \end{cases} \tag{2.34}$$

2.4 Asymptotic Limits

In this section, we study the asymptotic behavior of the system by obtaining the limit points for both upper bounds, lower bound, and $E\left[Z\right]$ as N goes to infinity. The knowledge of these limit points provides insight on the best and the worst asymptotic spectrum availability for the secondary users corresponding to the upper and lower bounds, respectively. They can be used as a simple rule of thumb giving the asymptotic mean of the fraction of available spectrum conditioned on the knowledge of Λ. Moreover, having the limit points makes the comparison among different bounds for different requesting distributions possible.

2.4.1 The Limit Point of Upper Bounds

To find the tightest Chernoff bound we must solve (2.11). Plugging the moment generating function of the uniform distribution into (2.11), the bound in (2.9) as $N \to \infty$ becomes:

$$E[Z] \leq \exp\left[\sqrt{\Lambda}\left(2 - \sqrt{\Lambda} - e^{-\sqrt{\Lambda}}\right)\right]. \tag{2.35}$$

the proof is in Appendix A.

The proposed upper bound is obtained from the Eq.(2.14). For the uniform distribution with the moment generating function of (A.1), the proposed upper bound in Eq.(2.14) turns to:

$$\exp\left(\Lambda\left(\frac{e^{\frac{-1}{N}}-e^{\frac{-(N+1)}{N}}}{N\left(1-e^{\frac{-1}{N}}\right)}-1\right)\right). \tag{2.36}$$

Finally the proposed upper bound as N goes to infinity has the limit of:

$$\exp\left(-\Lambda e^{-1}\right). \tag{2.37}$$

It is insightful to compare the limit points of the Chernoff bound and the proposed upper bound and find the range of values of Λ in which one outperforms the other in the sense of accuracy. In order to find the values of Λ in which the Chernoff bound is more accurate than the proposed bound, we should have:

$$\begin{aligned}
&\exp\left(\sqrt{\Lambda}\left(2-\sqrt{\Lambda}-e^{-\sqrt{\Lambda}}\right)\right)\leq\exp\left(-\Lambda\ e^{-1}\right)\\
&\Rightarrow 2-\sqrt{\Lambda}\left(1-e^{-1}\right)-e^{-\sqrt{\Lambda}}\leq 0\\
&\Rightarrow \Lambda\geq 9.56.
\end{aligned} \tag{2.38}$$

Therefore for large N and rate of greater than 9.56 Chernoff bound is more accurate.

For the modified binomial distribution with the moment generating function of:

$$\Phi_M(u)=e^u\left(1-p+pe^u\right)^{N-1}. \tag{2.39}$$

the proposed upper bound in Eq.(2.14) turns to:

$$\exp\left(\Lambda\left(e^{-\frac{1}{N}}\left(1-p+pe^{-\frac{1}{N}}\right)^{N-1}-1\right)\right). \tag{2.40}$$

Finally the proposed upper bound as N goes to infinity has the limit of:

$$\exp\left(\Lambda\left(e^{-p}-1\right)\right). \tag{2.41}$$

Comparing the limits of the proposed upper bound for both uniform and modified binomial distribution in (2.37) and (2.41) respectively, we see that in order for the modified binomial upper bound outperform uniform upper bound we should have $p \leq 0.458$:

$$\exp\left(\Lambda\left(e^{-p}-1\right)\right) \geq \exp\left(-\Lambda e^{-1}\right) \quad \Rightarrow p \leq 0.458. \tag{2.42}$$

2.4.2 The Limit Point of $Pr\left(W \leq N-1\right)$

In order to find this limit point we need the PMF of W, $P_W(w)$. Although we managed to find this PMF numerically using (2.24), we need it in the closed form. For the case of M_k having the uniform distribution, the problem of finding the PMF of W for the set of values of $w \in \{0, 1, 2, \cdots, N+1\}$ is tractable. Fortunately in order to find the limit point we only need the PMF for these values.

Proposition 2: *The closed form PMF of W for the uniform distribution is:*

$$Pr\left(W \leq N-1\right) = \sum_{m=0}^{N-1} PU_m \left(\frac{1}{N}\right)^m \binom{N-1}{m}, \tag{2.43}$$

where $P(U=k) = PU_k$. The proof is in Appendix B.

For large N, the dominant term in $\binom{N-1}{m}$ is $\frac{N^m}{m!}$. Therefore the limit point of

$Pr\left(W \leq N-1\right)$ is:

$$\begin{aligned} Pr\left(W \leq N-1\right) &\approx \sum_{m=0}^{\infty} \frac{PU_m}{m!} = \sum_{m=0}^{\infty} \frac{e^{-\Lambda}\Lambda^m}{\left(m!\right)^2} \\ &= E\left[\frac{1}{U!}\right]. \end{aligned} \tag{2.44}$$

2.4.3 The Limit Point of $E\left[Z\right]$

For $E\left[Z\right]$ we have:

$$\begin{aligned} E\left[Z\right] &= PU_0 + \sum_{k=1}^{N-1}\left(1-\frac{k}{N}\right)P\left(w=k\right) \\ &= PU_0 + \sum_{k=1}^{N-1}\sum_{m=1}^{k}\left(1-\frac{k}{N}\right)PU_m\left(\frac{1}{N}\right)^m\binom{k-1}{m-1} \\ &= PU_0 + \sum_{m=1}^{N-1}\left(PU_m\left(\frac{1}{N}\right)^m\sum_{k=m}^{N-1}\left(1-\frac{k}{N}\right)\binom{k-1}{m-1}\right) \\ &= PU_0 + \sum_{m=1}^{N-1}\left(PU_m\left(\frac{1}{N}\right)^m\sum_{k=1}^{N-1}\left(1-\frac{k}{N}\right)\binom{k-1}{m-1}\right) \\ &= PU_0 + \sum_{m=1}^{N-1}\left(PU_m\left(\frac{1}{N}\right)^m\sum_{j=0}^{N-2}\left(1-\frac{j+1}{N}\right)\binom{j}{m-1}\right) \\ &= PU_0 + \sum_{m=1}^{N-1}\left(PU_m\left(\frac{1}{N}\right)^m\left[\sum_{j=0}^{N-2}\binom{j}{m-1} - \frac{1}{N}\sum_{j=0}^{N-2}\binom{j}{m-1}\right.\right. \\ &\left.\left. -\frac{1}{N}\sum_{j=0}^{N-2} j\binom{j}{m-1}\right]\right). \end{aligned} \tag{2.45}$$

Applying the formula $\sum_{k=0}^{n}\binom{k}{b}\binom{n-k}{q-b}=\binom{n+1}{q+1}$ which applies for any integers b, q, and n satisfying $0\leq b\leq q\leq n$ and by choosing $q=b+1$ we have:

$$\begin{aligned}\sum_{k=0}^{n}\binom{k}{b}\binom{n-k}{q-b}&=\sum_{k=0}^{n}\binom{k}{b}\binom{n-k}{1}\\&=n\sum_{k=0}^{n}\binom{k}{b}-\sum_{k=0}^{n}k\binom{k}{b}=\binom{n+1}{b+2}\\&\Rightarrow\sum_{k=0}^{n}k\binom{k}{b}=n\binom{n+1}{b+1}-\binom{n+1}{b+2}.\end{aligned}\tag{2.46}$$

Therefore for $E[Z]$ we have:

$$\begin{aligned}E[Z]=PU_0+\sum_{m=1}^{N-1}\Bigg(PU_m\left(\frac{1}{N}\right)^m\Bigg(\binom{N-1}{m}-\frac{1}{N}\binom{N-1}{m}\\-\frac{1}{N}\left((N-2)\binom{N-1}{m}-\binom{N-1}{m+1}\right)\Bigg).\end{aligned}\tag{2.47}$$

Now in order to find the limit point as N goes to infinity we should determine the terms of N with the highest exponent. The dominant terms in $\binom{N-1}{m}$ and $\binom{N-1}{m+1}$ are $\frac{N^m}{m!}$ and $\frac{N^{m+1}}{(m+1)!}$, respectively. Hence the limit point of $E[Z]$ will be:

$$E[Z]\approx\sum_{m=0}^{\infty}\frac{PU_m}{(m+1)!}=\sum_{m=0}^{\infty}\frac{e^{-\Lambda}\Lambda^m}{(m+1)!m!}=E\left[\frac{1}{(U+1)!}\right].\tag{2.48}$$

It is seen that for both uniform and modified binomial distributions, both upper bounds, lower bound, and $E[Z]$ converge to a limit less than "1". This is an undesired phenomenon for systems with the goal to increase the spectrum availability by providing more subcarriers while the primary network traffic is fixed.

2.5 Effect of Requesting Distribution and Spectrum Outage Probability

For a system with an arbitrary requesting distribution, in order for (2.7) to hold, it is enough that the Chernoff bound converges to a limit point less than "1". This condition is mentioned in (2.32). Therefore, a sufficient condition for a system to be "greedy" is:

$$\lim_{N\to\infty} \frac{\Lambda E[M]}{N-1} > 1. \tag{2.49}$$

Both uniform and modified binomial distributions belong to the class of distributions with the mean of $aN+b$ where $a, b \in \mathbb{R}$ $a > 0$, $b \geq 0$. In this case, for the values of $\Lambda > \frac{1}{a}$, we have a "greedy" system.

For a "non greedy" system with an arbitrary requesting distribution we have:

$$\lim_{N\to\infty} E\left[Z\right] = 1. \tag{2.50}$$

It is sufficient that the lower bound converges to "1". This condition is mentioned in (2.15). Therefore, the sufficient condition for a system to be "non greedy" is:

$$\lim_{N\to\infty} \frac{E[M]}{N} = 0. \tag{2.51}$$

Distributions with fixed mean satisfy the above condition. These distributions result in "non greedy" systems and provide hope for spectrum availability for the secondary users with increase in N. It is seen that in the last condition, the knowledge of the mean (first moment) of the requesting distribution is sufficient to determine if a system is "non greedy". However, in order to determine a "greedy" system, the knowledge of both $E[M]$ and Λ is required.

Next, we study the sustainable traffic of the system for uniform distribution. The

system is sustainable as long as W is not greater than N; otherwise it is in *spectrum outage* which is an undesired phenomenon in practice. For a probability of spectrum outage α, we have:

$$P_{outage} = \alpha = Pr(Z = 0) = 1 - \sum_{m=0}^{N-1} PU_m \left(\frac{1}{N}\right)^m \binom{N-1}{m}. \tag{2.52}$$

Hence, the corresponding Λ for a fixed N is the positive solution of the following nonlinear equation:

$$\sum_{m=0}^{N-1} PU_m \left(\frac{1}{N}\right)^m \binom{N-1}{m} + \alpha - 1 = 0. \tag{2.53}$$

2.6 Numerical Results and Discussions

Using (2.21), (2.22), (2.23), and (2.24), the PMF of W is evaluated for both distributions and is shown in Fig. 2.4. For modified binomial distribution, there are oscillations around integer values $((N-1)p+1)k;\ k = 1, 2, \cdots$; However, as k gets larger than Λ the PMF decays.

Applying (2.5) and (2.24), the PMF of Z is shown in Fig. 2.5 for both distributions. It is seen that for small values of Λ the probability of having *none* or *all* of the subcarriers available is significantly larger compared to the probability of having a fraction of subcarriers available. This is an indication of binary state spectrum availability. However, with increase in Λ, the PMF tends to the dirac delta function at "0" which indicates the transition from random to deterministic behavior.

Fig. 2.6 shows the behavior of bounds as N increases at a fixed rate of Λ for both distributions. Since for both distributions and the given Λ ($\Lambda = 5$) system is "greedy", with increase in N the curves converge to a limit point less than 1.

Fig. 2.7 shows the bounds as Λ increases up to 15 for a fixed number of subcarriers

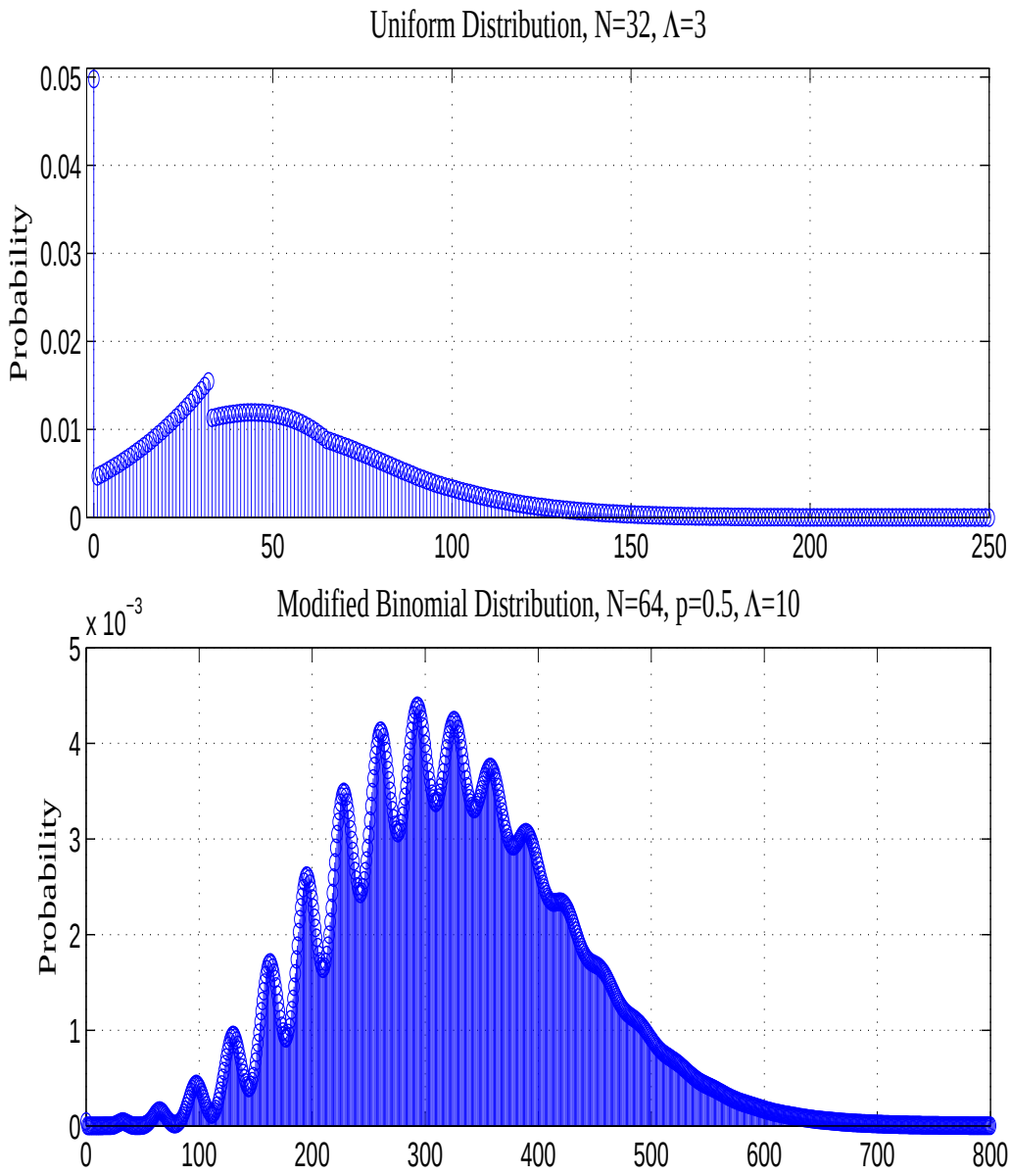

Figure 2.4: PMF of W for both distributions.

($N = 32$) for the uniform distribution. It can be seen that with increase in Λ which represents the traffic of the requesting users, all the curves decrease. We see that the Chernoff bound is loose for small Λ whereas it rapidly gets tighter as Λ increases but the proposed upper bound is more accurate for $\Lambda \leq 9.56$. It is seen in Fig.2.7 that for small values of Λ the proposed upper bound is the most accurate. However, as

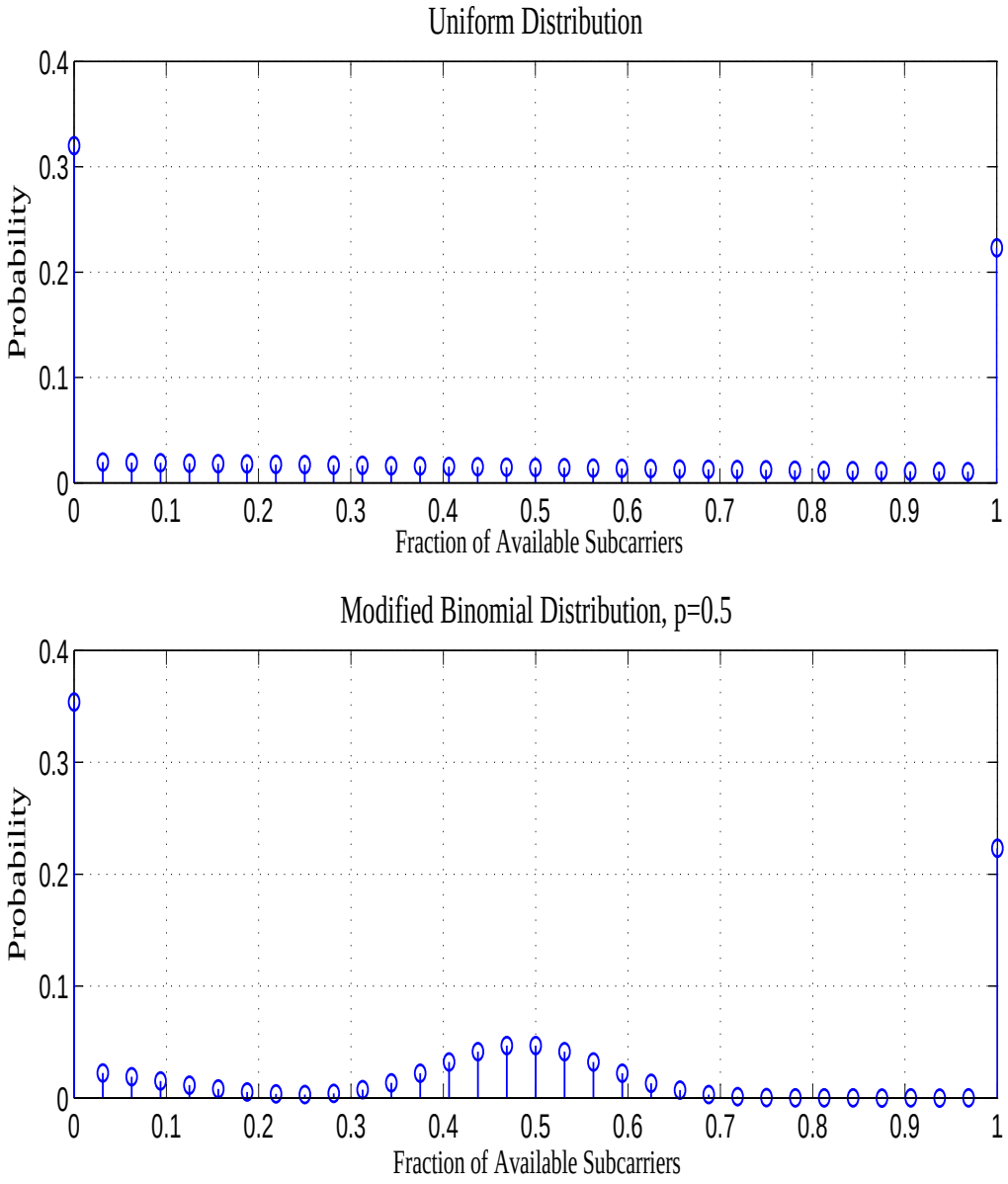

Figure 2.5: PMF of Z for both distributions, $N = 32$, $\Lambda = 1.5$.

Λ increases, the lower bound tends to be the most accurate bound. Hence for the case of heavy traffic of requesting users, the lower bound can be used instead of $E[Z]$ with good approximation.

Therefore, it is seen that for both distributions, increase in N does not result to the increase of $E[Z]$ due to the saturation of the curves whereas with increase

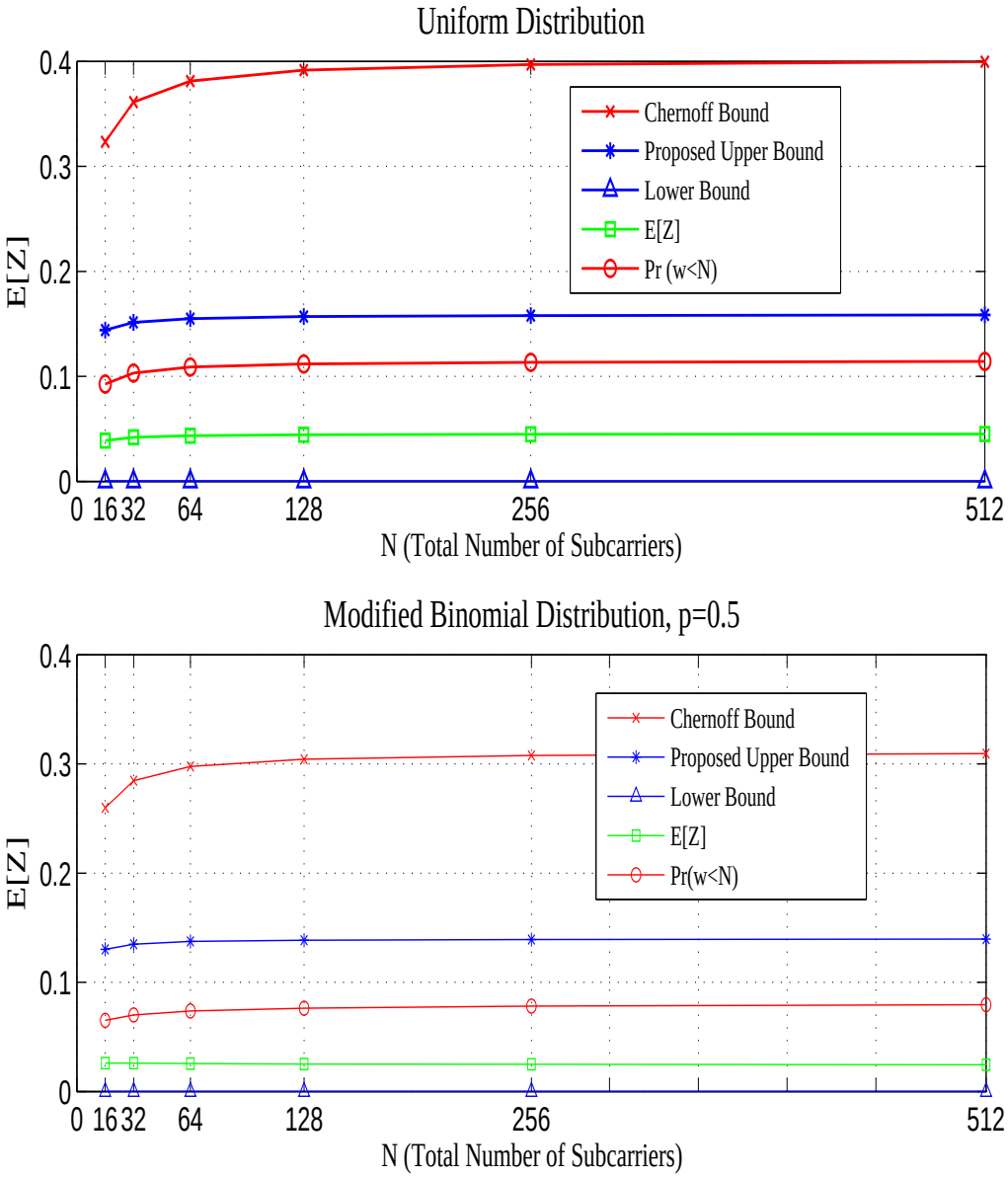

Figure 2.6: Effect of large N on the bounds for both distributions, $\Lambda = 5$.

in Λ, $E[Z]$ and all other bounds decrease. Hence, the spectrum availability for the secondary network is very sensitive to traffic. On the other hand, the spectrum availability is not responsive to the increase of N as it was shown by the saturated curves.

Fig.2.8 shows the maximum values of Λ as a function of N such that $P_{Outage} \leq$

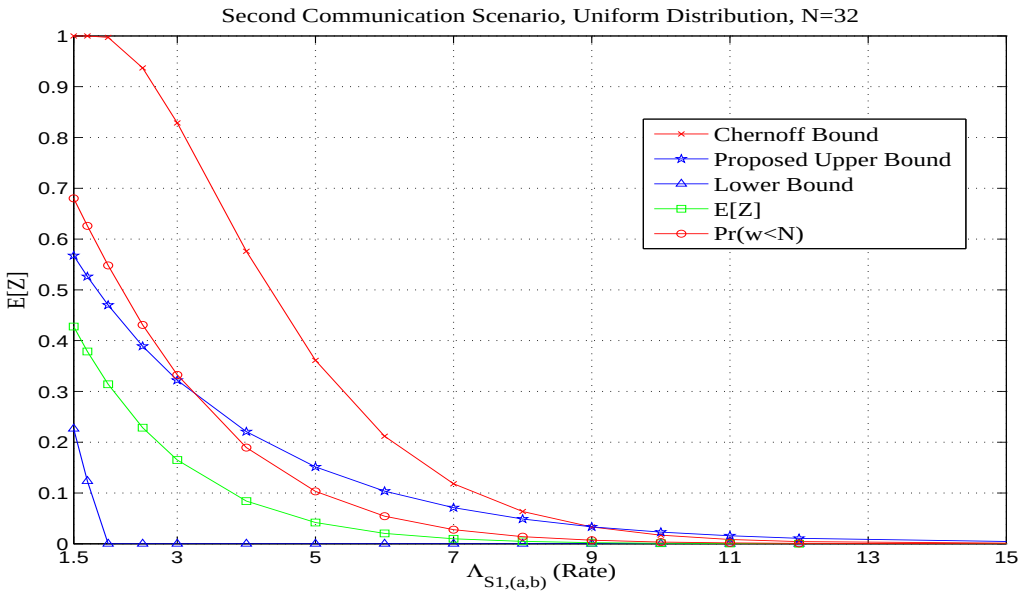

Figure 2.7: Effect of Λ on the bounds for uniform distribution, $N = 32$.

0.01. It is seen that in order to keep the outage probability less than 0.01 the rate values are pretty small. In Fig.2.9 the maximum rates are shown when the constraint on the outage probability has loosen a bit such that $P_{Outage} \leq 0.1$. Consequently the rates can be larger compared to the previous case. Fig.2.10 depicts the minimum values of Λ such that the system will be in outage with probability more than 0.99. Therefore for any of the indicated values of Λ in this figure, there will be no available subcarriers with the probability of 0.99 for the corresponding N. For all figures it is seen that the curve gets saturated and the rate does not increase with the increase in N. This is an indication of the limited performance capability of the system. For instance, for the uniform distribution in order to have $P_{Outage} \leq 0.01$, Λ can not be more than 0.2.

2.7 Summary

We mathematically derived the PMF of the fraction of available subcarriers for the secondary users in an OFDMA based CR radio system. The derivation was

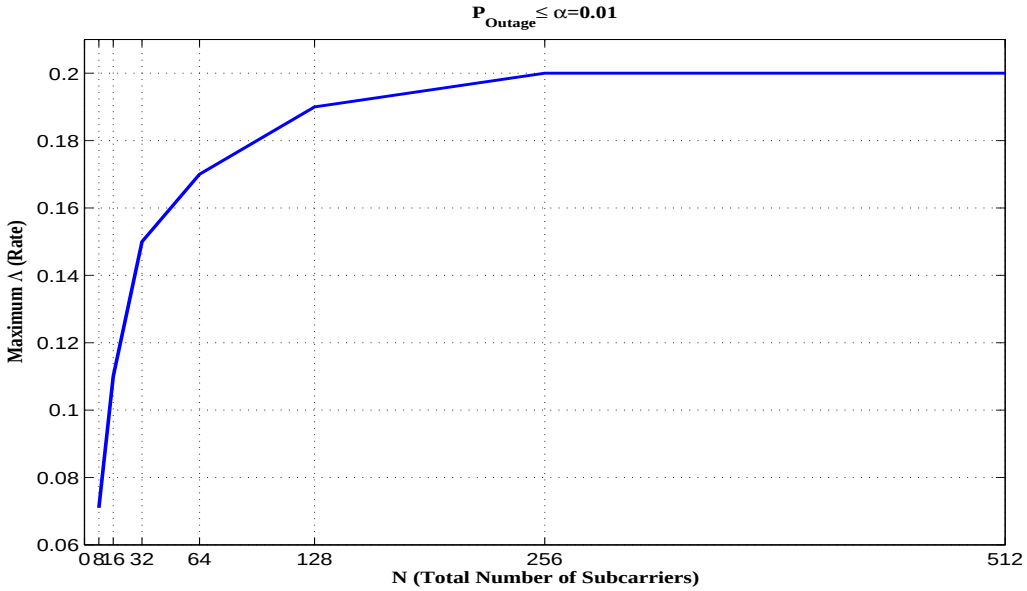

Figure 2.8: Maximum values of Λ as a function of N for $P_{Outage} \leq 0.01$.

based on a few assumptions on the network topology and the requesting distribution. Two classical uniform and binomial distributions were considered as the requesting distribution and the asymptotic mean of the fraction of available subcarriers and its corresponding upper and lower bounds were both analytically and numerically derived as the total number of subcarriers provided by the system and the primary network traffic go to infinity. The drawback of using the uniform and binomial distributions as the requesting distribution was shown which resulted to the limited spectrum availability. Next, two sufficient conditions were proposed to determine whether a distribution results in a "greedy" or "non greedy" system. It was shown that for a "greedy" system, providing more subcarriers will not increase the spectrum availability. It was also shown that the knowledge of the mean (first moment) of the requesting distribution suffices to determine whether a system is "greedy" or not. Moreover, the PMF of the total number of requested subcarriers from all primary users was analytically derived for the uniform distribution. Finally, the sustainable

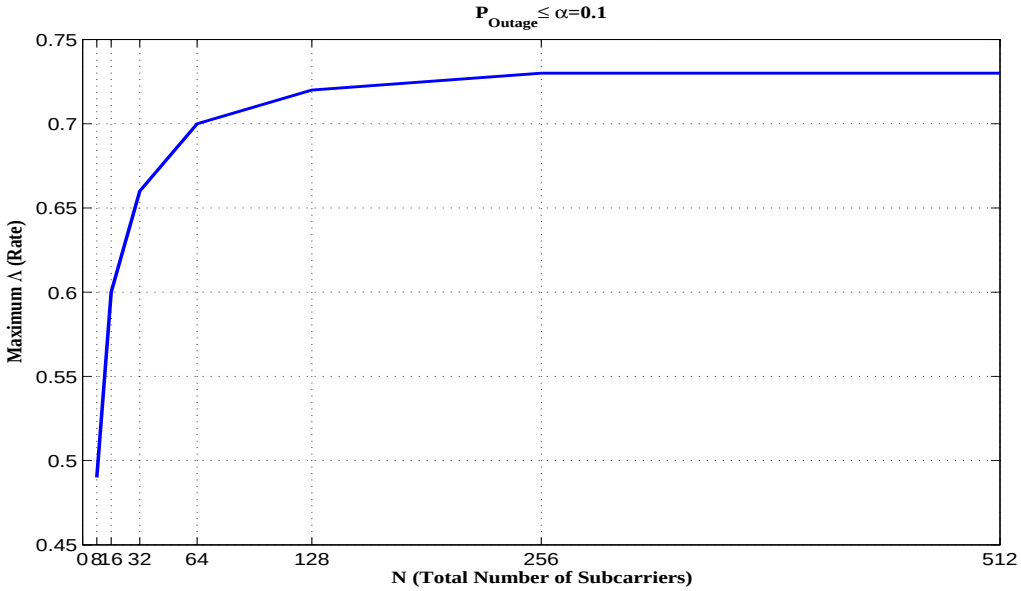

Figure 2.9: Maximum values of Λ as a function of N for $P_{Outage} \leq 0.1$.

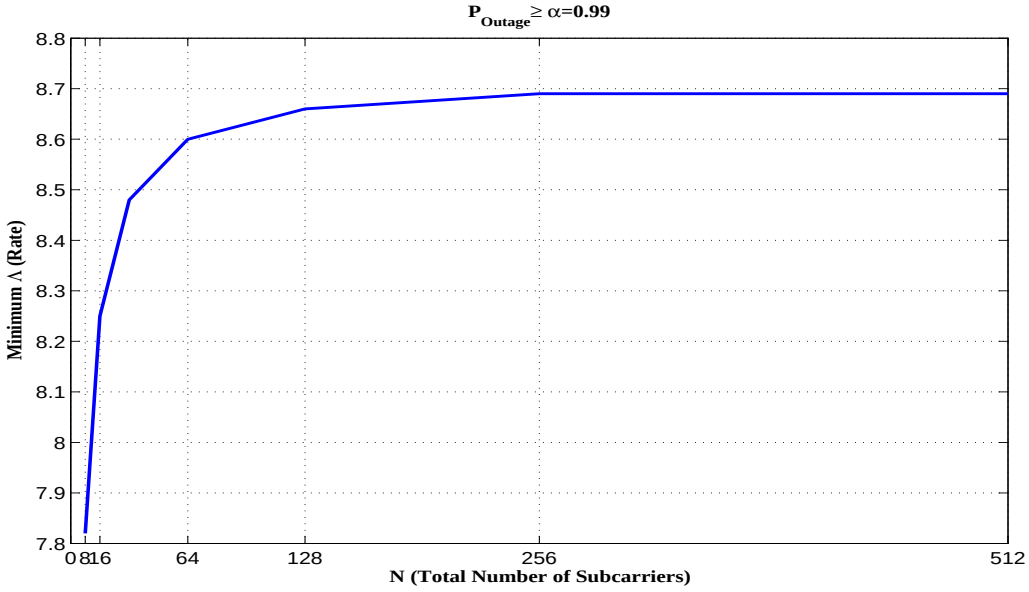

Figure 2.10: Minimum values of Λ as a function of N for $P_{Outage} \geq 0.99$.

traffic of the system subject to a fixed spectrum outage probability was studied. We showed that for a fixed spectrum outage probability, as long as the requesting

distribution is undesired, adding more subcarriers to the system will not help to support more primary users to successfully avoid the spectrum outage.

3. A PROBABILISTIC MODEL FOR USER ACTIVITY, SPECTRUM OCCUPANCY, AND SYSTEM THROUGHPUT

3.1 Introduction

Cognitive radio systems are a promising solution to the spectrum scarcity problem. Accurate modeling of user activity, spectrum utilization, and system throughput is vital to achieve a better quantitative understanding of such systems. In this section, we consider a set of primary users that are spatially distributed based on Poisson point process and make demand on available channels in their proximity and assess the effect of these demands on user activity, spectrum occupancy, and total system throughput under various channel requesting distributions and fading environments. The asymptotic mean number of active primary users and occupied subcarriers are evaluated considering the primary network traffic. The probability of miss detection of an occupied subcarrier by a single sensing secondary user is analytically derived. It is shown that this probability is a function of system traffic and the requesting distribution. It is also shown for extreme traffic of users, the applied requesting distribution and total number of provided subcarriers can not further improve the asymptotic sensing accuracy of the secondary user. Finally, the primary network and the secondary user throughputs in the presence of mutual interference due to imperfect detection of the secondary user are investigated and their asymptotic values as the primary network traffic, primary user transmit power, and secondary user transmit power go to infinity are analytically derived. It is shown that with increase in the primary network transmit power, the average throughput of both primary network and secondary user increases.

3.1.1 Organization

The section is organized as follows. Section 3.2 presents the system model. Section 3.3 derives the probability of miss detection of an occupied subcarrier by the spectrum sensor and also studies the asymptotic performance of the spectrum sensor at large primary network traffic. In Section 3.4 a statistical model for primary and secondary throughput in the presence of mutual interference in an OFMA based CR network is proposed. Both throughputs are largely affected by the probability of miss detection of an occupied subcarrier by the sensing secondary user. Asymptotic throughput of both primary network and secondary user considering the primary network traffic, and both primary and secondary transmit powers are obtained. Section 3.5 provides numerical results to illustrate the effectiveness of our framework for characterizing the user activity, spectrum occupancy, spectrum sensor performance, and system throughput in terms of various system parameters. Section 4.4 brings the conclusion.

3.2 System Model and Problem Statement

It is assumed that the primary users are spatially scattered in a two dimensional region V according to a homogeneous PPP with spatial density λ (in primary users per unit area). Each user makes request according to its communication needs to use one or more of N available subcarriers.

Let U be the number of primary users in a region $\Re \subset V$ with the total area $A_{\Re}$. Then U is a Poisson random variable with parameter $\Lambda = \lambda A_{\Re}$ [33]. Λ is the mean number of primary users in region $\Re$ and represents the primary network traffic in that region. Authors in most spectrum modeling contributions assume that each primary user requires a fixed number of channels which, is somewhat limiting. In fact, users have different rate requirements, which means they may request varying

numbers of the N available subcarriers. We model this by assuming that the k-th primary user requests M_k of the N subcarriers, where $M_k,\ k = 1, 2, \cdots, U$, are independent, identically distributed (i.i.d.) random variables taking values in $\{1, 2, \cdots, N\}$ and having a common distribution $P_M(m),\ m = 1, 2, \cdots, N$. In what follows, $P_M(m)$ will be referred as the *requesting distribution*. Thus, at any given time and in the area $\Re$, the number of subcarrier requests, W is

$$W = \sum_{k=1}^{U} M_k, \tag{3.1}$$

where it is understood that $W = 0$ if $U = 0$. W has *compound Poisson* distribution and can take values in $\{0, 1, 2, ..., \infty\}$. Obviously due to limited number of subcarriers, all requests $W \geq N$ will not be able to be satisfied and will result in outage. Hence, the number of active users primary is less than or equal to the number of requesting primary users.

We classify the requesting primary users into N class based on the number of subcarriers that they require. The number of requesting users that require i subcarriers to transmit, U_i, is a Poisson random variable with parameter $\Lambda P_M(i)$. Note that $U_i,\ \ i = 1, 2, \cdots, N$ are independent Poisson random variables [33]. We show them as a vector with their corresponding parameters:

$$\overline{U} = [U_1, \cdots, U_N] \sim Poisson\left(\overline{\Lambda} = [\Lambda p_1, \cdots, \Lambda p_N]\right), \tag{3.2}$$

where $p_i = P_M(i)$. $\overline{\Lambda}$ is a vector which shows the mean of requesting users of each class. We show the number of active primary users that occupy i subcarriers by X_i. Due to the following constraint, $X_i,\ i = 1, 2, \cdots, N$ are neither independent nor

Poisson:

$$\sum_{i=1}^{N} i \cdot X_i \leq N. \tag{3.3}$$

The above constraint indicates that the number of occupied subcarriers can not exceed the total number of subcarriers. Therefore, the possible values that X_i can take is $\left\{0, 1, 2, \cdots, \left\lfloor \frac{N}{i} \right\rfloor\right\}$ which shows it can't be Poisson where $\lfloor N \rfloor$ is the greatest integer smaller than N. An active primary user of class i, occupies i subcarriers. The total number of active users is:

$$Y = \sum_{i=1}^{N} X_i. \tag{3.4}$$

Y takes values between 0 to N. This value depends on the criteria that the central system applies to assign the available subcarriers to the requesting users based on a predetermined priority and fairness. Here we assume this criteria is to support as many users as possible. Therefore, requesting users asking for only one subcarrier are in top priority and requesting users asking for all N subcarriers are in the least priority. Since $X_i, \quad i = 1, 2, \cdots, N$ are dependent, in order to find the PMF of Y we should first find the joint PMF of $X_i's$. In Fig.3.1 the flowchart which depicts the algorithm to find the joint PMF of $X_i's$ is shown. This flowchart receives the joint PMF of several dependent random variables as the input and provides the equivalent PMF in terms of the marginal PMFs of several independent random variables as the output. The first step of the algorithm requires to find the possible solutions of a Diophantine inequality [35,62]. This can be practically implemented by integer linear programming [1, 55]. Due to the independency of the number of requesting users, we have:

$$Pr\left(U_1 = m_1, \cdots, U_k = m_k\right) = \prod_{i=1}^{k} Pr\left(U_i = m_i\right). \tag{3.5}$$

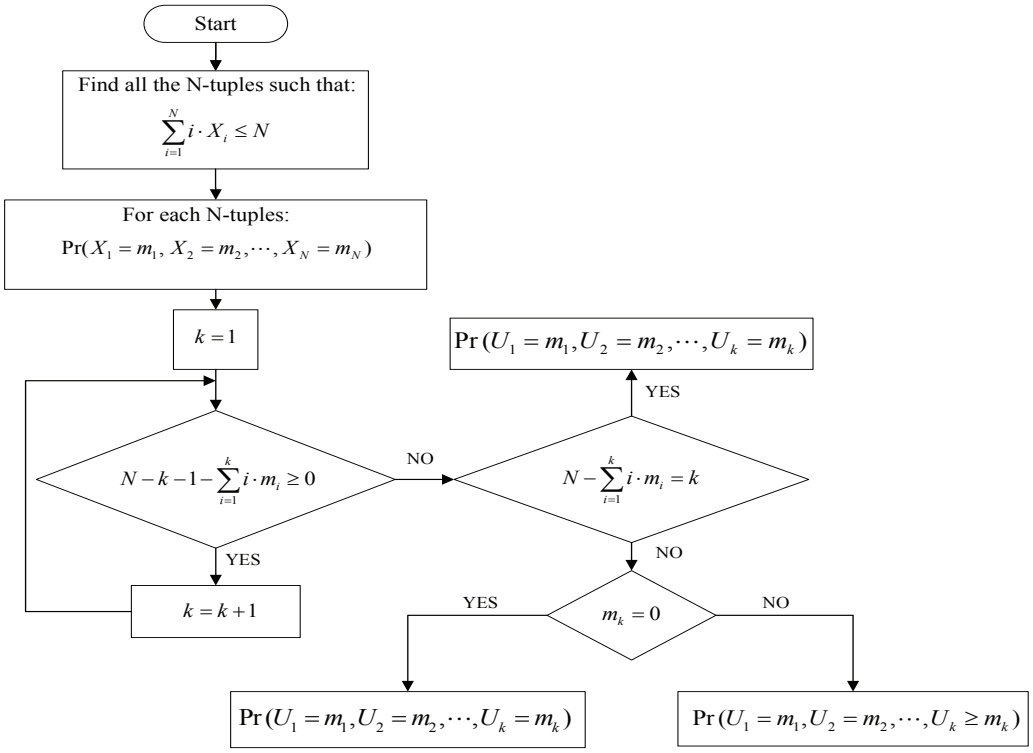

Figure 3.1: Flowchart to find the joint PMF of $X_i's$.

Once the joint PMF of $X_i's$ is obtained, evaluating the PMF of Y is straightforward. We define the set "A_k" as the collection of all N-tuples such that:

$$A_k = \left\{ \overline{m} = (m_1, \cdots, m_N) \mid \sum_{i=1}^{N} m_i = k, \sum_{i=1}^{N} i \cdot m_i \le N \right\}. \tag{3.6}$$

then we have:

$$P_Y(Y = k) = \sum_{\overline{m} \in A_k} Pr\left(\overline{X} = \overline{m}\right);\ k \in \{0, 1, \cdots, N\}, \tag{3.7}$$

where $\overline{X} = [X_1, \cdots, X_N]$. Having the joint PMF of $X_i's$, we can also find the marginal PMF $Pr\,(X_j = k)$. We define the set "$B_{j,k}$" as the collection of all N-tuples such

that:

$$B_{j,k} = \left\{ \overline{m} = (m_1, \cdots, m_j = k, \cdots, m_N) \mid \sum_{i=1}^{N} i \cdot m_i \leq N \right\}. \tag{3.8}$$

then we have:

$$P_{X_j}(X_j = k) = \sum_{\overline{m} \in B_{j,k}} Pr\left(\overline{X} = \overline{m}\right);\ k \in \left\{0, 1, \cdots, \left\lfloor \frac{N}{j} \right\rfloor\right\}. \tag{3.9}$$

According to Eq.(3.2), the mean of the requesting users is determined by the PMF of random variable M, $P_M(m)$. We consider four different distributions for random variable M. Uniform and modified binomial distribution (which starts from 1 despite of the binomial distribution that starts from 0) with the following PMFs, respectively:

$$P_M(m) = \frac{1}{N}; \quad m = 1, 2, ..., N. \tag{3.10}$$

$$P_M(m) = \binom{N-1}{m-1} p^{m-1} (1-p)^{N-m}; \quad m = 1, 2, ..., N. \tag{3.11}$$

We also consider two more distributions which are *linearly ascending* and *linearly descending* distributions due to their extreme practical interpretation. At linearly ascending distribution, top priority requesting users (class 1) have the smallest mean and the least priority users (class N) have the largest mean:

$$P_M(m) = \frac{m}{\sum_{i=1}^{N} i} = \frac{2m}{N(N+1)}; \quad m = 1, 2, \cdots, N. \tag{3.12}$$

Linearly descending distribution, is the opposite of the previous one:

$$P_M(m) = \frac{N+1-m}{\sum_{i=1}^{N} i} = \frac{2N+2-2m}{N(N+1)}; \quad m = 1, 2, \cdots, N. \tag{3.13}$$

We define the user activity rate (ζ), as the ratio of the mean number of active

users to the mean number of total requesting users:

$$\zeta = \frac{E[Y]}{\Lambda}. \tag{3.14}$$

This parameter represents the activation rate of requesting users.

Another important random variable is the total number of occupied subcarriers:

$$OCC = \sum_{i=1}^{N} i \cdot X_i. \tag{3.15}$$

Once the joint PMF of $X_i's$ is obtained, evaluating the PMF of OCC is straightforward. We define the set "C_k" as the collection of all N-tuples such that:

$$C_k = \left\{ \overline{m} = (m_1, \cdots, m_N) \mid \sum_{i=1}^{N} i \cdot m_i = k \right\}. \tag{3.16}$$

then we have:

$$P_{OCC}(OCC = k) = \sum_{\overline{m} \in C_k} Pr\left(\overline{X} = \overline{m}\right);\ k \in \{0, 1, \cdots, N\}. \tag{3.17}$$

We also define the spectrum access rate (η), as the ratio of the mean number of occupied subcarriers to the mean number of requested subcarriers:

$$\eta = \frac{E[OCC]}{E[W]} = \frac{E[OCC]}{\Lambda E[M]}. \tag{3.18}$$

This parameter represents the satisfaction rate of demands for spectrum. In Section 3.5 both parameters ζ and η are plotted for all four requesting distributions as a function of primary network traffic (Λ).

At relatively large Λ, due to the effect of prioritization there will be N active

users of class 1. Therefore, $E\left[OCC\right] \rightarrow N$. For the under study requesting distributions (3.10)-(3.13), since $E[M]$ is a function of N, we can investigate the asymptotic spectrum access rate as $N \rightarrow \infty$. For uniform, modified binomial, linearly ascending, and linearly descending distributions we have $\eta \rightarrow \frac{2}{\Lambda}, \frac{1}{p\Lambda}, \frac{3}{2\Lambda}$, and $\frac{3}{\Lambda}$ as the number of provided subcarriers goes to infinity, respectively. This shows the impact of requesting distribution on the asymptotic spectrum availability for users. Therefore, in order to increase the spectrum access by adding subcarriers to the system, appropriate requesting distributions must be applied. Distributions in which $\Lambda E[M] = o(N)$ $\left(\lim_{N\rightarrow\infty} \frac{\Lambda E[M]}{N} = 0\right)$ are appropriate requesting distributions and providing more subcarriers would increase the spectrum access rate. Note that for system design purposes, the first moment of the distribution is sufficient to determine whether this distribution can fully utilize the spectrum.

3.3 Spectrum Sensor Point of View

It is assumed that a spectrum sensor is used to sense the activity of the spectrum band. There is an analogy between the spectrum sensor and the secondary user, since they both constantly sense the spectrum for available holes. We assume that the entire region under study, V, is a large square area with edge length R and the spectrum sensor is located at the center with the coordinates of $(0, 0)$ in the plane. We take the effects of fading and non perfect detection of the spectrum sensor into consideration. Since our perception of the spectrum occupancy is the output of spectrum sensor, having a mathematical model of the dynamic behavior of the spectrum from the spectrum sensor point of view is essential. Therefore, we study the more realistic scenario when active users are not detected by the spectrum sensor due to deep fading and propagation path loss.

We assume all active primary users transmit at the same power level P_T and there

is no channel side information at the primary user transmitter. Hence, their total power is evenly divided among their corresponding subcarriers. It is also assumed that the nth subcarrier, $n = 1, \cdots, N$ between the yth active user, $y = 1, \cdots, Y$ and the spectrum sensor has the gain of χ_n^y. $\chi_n^y \in R^+$ is a unit-mean random variable representing the frequency-flat fading effects. We assume all gains to be independent and identically distributed (i.i.d.) across different users and different subcarriers with $f_\chi(.)$ and $F_\chi(.)$ denoting its probability density function (PDF) and cumulative distribution function (CDF), respectively. Although the i.i.d. channel gains do not exactly reflect practical scenarios, but this assumption makes the problem more tractable. We model the propagation power loss at a distance r from the transmitter by $g(r)$ where $g(r)$ is the distance-dependent path-loss. The path-loss is usually modeled as $g(r) = Cr^{-\alpha}$ where $\alpha > 2$ is the path-loss exponent and C is a constant [50]. However, such model has a singularity at $r = 0$ and is not valid for $r < 1$ as the wireless channel can not amplify the transmitted signal. To circumvent this issue we assume that the primary users can not be located closer than a distance r_0 to the spectrum sensor ($r_0 \geq 1$). For ease of exposition, we will consider $r_0 = 1$. Note that in practice $R >> r_0$ and this assumption becomes more valid.

The received signal to noise ratio (SNR) of a subcarrier occupied by the active user of class i at the spectrum sensor is given by:

$$\gamma_i(r, h) = \frac{P_T}{i} \frac{g(r)h}{N_0}, \tag{3.19}$$

where r is the distance between the active user and spectrum sensor, i is the number of occupied subcarriers by the active user of class i, $h = \chi^2$ represents the fading effects on the received power with the PDF $f_h(h) = \frac{f_\chi(\sqrt{h})}{2\sqrt{h}}$, and N_0 denotes the power of the background additive white Gaussian noise (AWGN).

The probability of successfully declaring a subcarrier as occupied denoted by $P_d(\gamma)$, improves with increasing SNR of the received signal. For the case of energy detector, probability of detecting an unknown deterministic signal in white Gaussian noise is given by [58]:

$$P_d(\gamma) = Q\left(\frac{Q^{-1}(P_f) - \sqrt{\nu}\gamma}{\sqrt{1+2\gamma}}\right), \tag{3.20}$$

where $Q(y) = \left(1/\sqrt{2\pi}\right)\int_y^\infty e^{-t^2/2}dt$ is the normal Q-function, ν is the product of the energy detectors integration time and channel bandwidth, and P_f is the probability of false alarm. For small P_f, $P_d(\gamma)$ can be approximated as [3]:

$$P_d(\gamma_i(r,h)) = \begin{cases} 0, & \gamma_i < \gamma_0 \\ 1, & \gamma_i \geq \gamma_0, \end{cases} \tag{3.21}$$

where γ_0 is a certain threshold which is a measure of the spectrum sensor detection sensitivity. γ_0 is chosen as the SNR at which the probability of detection in (3.20) turns out to be 0.5 [3]. Therefore, $\gamma_0 = Q^{-1}(P_f)/\sqrt{\nu}$.

We show $Pr\left(r^{-\alpha}h < \frac{i}{\overline{SNR}}\right)$ by $P_{miss,i}$ as the probability of miss detection of an occupied subcarrier belonging to an active user of class i, where $\overline{SNR} = \frac{P_T C}{\gamma_0 N_0}$ and form the vector $\overline{P}_{miss} = [P_{miss,1}, \cdots, P_{miss,N}]^T$.

The distance between an active primary user and the spectrum sensor r has the following distribution:

$$f_r(r) = \begin{cases} \frac{2\pi r}{R^2}, & 0 \leq r \leq R/2 \\ \frac{4r}{R^2}\left(\frac{\pi}{2} - 2\cos^{-1}\frac{R}{2r}\right), & \frac{R}{2} \leq r \leq b \\ 0, & r < 0, r > b, \end{cases} \tag{3.22}$$

where $b = \frac{R}{\sqrt{2}}$. We define the random variable ρ as $\rho = r^{-\alpha}, 1 < r < b$. Thus, for the PDF of ρ we have:

$$f_\rho(\rho) = \frac{f_{r|1<r<b}\left(\rho^{-\frac{1}{\alpha}}\right)}{\alpha\rho^{1+\frac{1}{\alpha}}}; b^{-\alpha} < \rho < 1, \tag{3.23}$$

where:

$$f_{r|1<r<b}(r) = \begin{cases} \frac{f_r(r)}{1-\frac{\pi}{R^2}}, & 1 < r < b \\ 0, & otherwise. \end{cases} \tag{3.24}$$

and $f_{r|A}(r)$ is the conditional PDF of r given an event A. Hence, defining $z = \rho h$ and assuming ρ and h being independent, we have:

$$\begin{aligned} P_{miss,i} = F_z\left(\frac{i}{\overline{SNR}}\right) = &\int_{h=0}^{\frac{i}{\overline{SNR}}} \int_{\rho=b^{-\alpha}}^{1} f_h(h) f_\rho(\rho) dh d\rho \\ &+ \int_{h=\frac{i}{\overline{SNR}}}^{\frac{i}{\overline{SNR}}b^\alpha} \int_{\rho=b^{-\alpha}}^{\frac{i}{h\overline{SNR}}} f_h(h) f_\rho(\rho) dh d\rho. \end{aligned} \tag{3.25}$$

Considering the area of an annulus with $1 < r < \frac{R}{2}$, since PDF of r is linear in this area, (3.25) will be further simplified. In this case we have:

$$f_\rho(\rho) = \frac{\rho^{-\frac{2}{\alpha}-1}}{K\alpha}; \left(\frac{R}{2}\right)^{-\alpha} < \rho < 1, \tag{3.26}$$

where $K = \frac{R^2}{8} - \frac{1}{2}$, and:

$$\begin{aligned} P_{miss,i} = F_z\left(\frac{i}{\overline{SNR}}\right) = &\int_{h=0}^{\frac{i}{\overline{SNR}}} f_h(h) dh \\ &+ \frac{1}{2K} \int_{h=\frac{i}{\overline{SNR}}}^{\frac{i}{\overline{SNR}}(R/2)^\alpha} \left(\frac{R^2}{4} - \left(\frac{h\overline{SNR}}{i}\right)^{\frac{2}{\alpha}}\right) f_h(h) dh. \end{aligned} \tag{3.27}$$

Recalling set "A_k" in (3.6) and assuming a fixed number of active users and without any prior knowledge on their class, the occupied subcarrier may belong to

any of the active users with equal probability, the probability of miss detection of an occupied subcarrier conditioned on having $k(k \neq 0)$ active users is:

$$Pr\left(miss|Y=k\right)=\frac{1}{k}\left(\sum_{\overline{m}\in A_k} P_{\overline{m}|Y=k}\cdot\overline{m}\right)\cdot\overline{P}_{miss}, \tag{3.28}$$

where:

$$P_{\overline{m}|Y=k}=Pr\left(\overline{X}=\overline{m}\mid Y=k\right)=\frac{Pr\left(\overline{X}=\overline{m}\right)}{P_Y\left(Y=k\right)}. \tag{3.29}$$

Note that $Pr\left(miss|Y=0\right)=0$. Therefore, the probability of miss detection of an occupied subcarrier is:

$$Pr(miss)=\sum_{k=0}^{N} Pr\left(miss|Y=k\right)P_Y\left(Y=k\right). \tag{3.30}$$

Hence, the probability of miss detection is a function of path-loss exponent, edge length of the area under study, user transmit power, decision threshold of the spectrum sensor, traffic of users, requesting distribution, and type of fading.

We can study the asymptotic performance of the spectrum sensor as $\Lambda=\lambda R^2$ goes to infinity.

Theorem 1: Regardless of requesting distribution and N, as $\Lambda\rightarrow\infty$ the probability of miss detection of an occupied subcarrier by the spectrum sensor decreases and converges to

$$Pr\left(miss\right)\rightarrow P_{miss,1}. \tag{3.31}$$

Proof: The proof is given in Appendix C.

For large values of Λ that primary users are assigned spectrum according to their priority, with increase in Λ, $Pr\left(miss\right)$ decreases since active primary users with higher probability are among lower class users and such users result in smaller

$Pr\,(miss)$ due to their larger subcarrier power. Therefore, for extreme traffic of users, the designed requesting distribution and total number of provided subcarriers can not further improve the asymptotic performance of the spectrum sensor.

In Section 3.5 the effects of these parameters on the spectrum sensor performance are numerically investigated.

3.4 Primary and Secondary Throughput in the Presence of Mutual Interference

In this Section, we consider the spectrum sensor as a sensing secondary user which opportunistically accesses the spectrum once an empty subcarrier is detected. It is assumed the secondary user only requires one empty subcarrier to carry out its communication. We assume there exists one primary receiver (uplink scenario) and both the secondary and primary receivers are located within in a close range to the secondary user at the origin. Therefore, the effects of propagation path loss on the secondary transmit power at the secondary and primary receivers are negligible and the distance from an active primary user to the primary and secondary receivers will approximately follow the PDF of (3.22). It is also assumed that once the secondary user detects multiple idle subcarriers, it *randomly* chooses one of them and starts its transmission. Therefore, only one of the active primary users will be the victim of the interference. Future extensions can study the arbitrary location of the primary and secondary receivers, multiple secondary users, and also the scenario in which the secondary user requires a random number of subcarriers due to its varying communication requirements. The additive thermal noise is assumed to be zero mean mutually independent, circularly symmetric, complex Gaussian random variable with unit variance. The nth subcarrier power gains from the yth primary transmitter to the primary and secondary receivers are denoted by $g^y_{p,n}$ and $g^y_{s,n}$, respectively. Similarly, $\beta_{p,n}$ and $\beta_{s,n}$ are the nth subcarrier power gains from the secondary transmitter

to the primary and secondary receivers, respectively. All gains are assumed to be i.i.d. variables across different users and different subcarriers with PDF $f_h(\cdot)$.

3.4.1 Throughput of the Primary Transmitter

If all transmitted signals from primary and secondary users follow i.i.d. zero mean, circularly symmetric complex Gaussian distribution, the achievable throughput of a primary transmitter of class i and receiver pair based on the sum rate capacity of parallel channels is given by [63]:

$$C_{P,i} = \sum_{k=1}^{i} \log_2 \left(1 + r^{-\alpha} g_{p,k} \frac{P_T}{i}\right), \tag{3.32}$$

and:

$$C_{P,i}^{int} = \sum_{k=1,k\neq q}^{i} \log_2 \left(1 + r^{-\alpha} g_{p,k} \frac{P_T}{i}\right) + \log_2 \left(1 + \frac{r^{-\alpha} g_{p,q} P_T}{i\left(1 + \beta_{p,q} P_S\right)}\right), \tag{3.33}$$

where (3.32) and (3.33) represent the achievable throughput when there is no interference from the secondary user and when the secondary user interferes with the primary user due to missed detection of the qth subcarrier, respectively. P_S is the secondary transmit power.

In order to find the probability of interference from the secondary user on a class i primary user, obtaining the probability of miss detection of exactly k subcarriers conditioned on having *occ* occupied subcarriers and x_i class i primary users is helpful:

$$\begin{aligned} Pr\left(\text{num of miss} = k | OCC, X_i\right) = & \binom{occ}{k} Pr\left(miss | OCC, X_i\right)^k \\ & \left(1 - Pr(miss | OCC, X_i)\right)^{occ-k}, \end{aligned} \tag{3.34}$$

where:

$$Pr\left(miss|OCC, X_i\right) = \left(\sum_{\overline{m} \in \left\{ C_{occ} \cap B_{i,x_i} \right\}} \frac{1}{\sum_{n=1}^{N} m_n} \frac{Pr\left(\overline{X} = \overline{m}\right)}{Pr\left(OCC, X_i\right)} \cdot \overline{m} \right) \cdot \overline{P}_{miss}, \quad (3.35)$$

where it is again assumed that the miss detected subcarrier may belong to any of active users with equal probability for any user configuration.

Note that $Pr\left(miss|OCC = 0, X_i = 0\right) = 0$ then $Pr\left(\text{num of miss} = k|0, 0\right) = \delta\left(k\right)$ where $\delta\left(k\right)$ is the Dirac delta function. For the case of $C_{occ} \cap B_{i,x_i} = \varnothing$, $Pr\left(\text{num of miss} = k|OCC, X_i\right)$ is not defined.

Similarly, The probability of correctly declaring exactly k out of $N - occ$ unoccupied subcarriers as empty, $(Pr(\text{CDE}))$ is:

$$Pr\left(\text{CDE} = k|OCC = occ\right) = \binom{N - occ}{k} \left(1 - P_f\right)^k P_f^{N-occ-k}. \quad (3.36)$$

Note that this probability only depends on occ.

Interference occurs when the secondary user miss detects at least one of i subcarriers of the primary user of class i and then selects that subcarrier for transmission. The probability that the secondary user detects $l + k$ idle subcarriers out of N subcarriers where l is the number of subcarriers that are miss detected and k is the number of subcarriers that are correctly declared empty conditioned on knowing the number of occupied subcarriers, number of class i primary users, and using (3.34) and (3.36) is:

$$\begin{aligned} &Pr\left(l \text{ among } occ, k \text{ among } N - occ|OCC = occ, X_i = x_i\right) = \\ &Pr\left(\text{num of miss} = l|OCC, X_i\right) Pr\left(\text{CDE} = k|OCC\right) = f\left(l\right) g\left(k\right), \end{aligned} \quad (3.37)$$

where $J = l + k$ is the number of idle subcarriers ($0 \leq J \leq N$) that the secondary user has detected. Note that for $l > occ$ and $k > N - occ$, $f(l)$ and $g(k)$ are equal to zero, respectively. The probability of interference on one of x_i primary users of class i conditioned on $OCC = occ$, $X_i = x_i$, and $J = j \neq 0$ is:

$$Pr\left(Int_{class\ i} | J, OCC, X_i\right) = \sum_{l=1}^{j} \left(f(l)\, g(j-l)\, \frac{l}{j} \sum_{n=1}^{ix_i} \frac{n}{l} \frac{\binom{ix_i}{n}\binom{occ-ix_i}{l-n}}{\binom{occ}{l}} \right). \tag{3.38}$$

When there are x_i primary users of class i, there will be ix_i subcarriers that choosing any of them will result to interference on a primary user of class i. The second summation in (3.38) is the probability that at least one of ix_i subcarriers is miss detected and then one of them is chosen for transmission by the secondary user. Note that j is the number of idle subcarriers from the secondary user point of view. Therefore, (3.38) is the probability that the secondary user chooses one of l miss detected subcarriers for its transmission while that subcarrier belongs to any of x_i primary users. It is obvious that $Pr\left(Int_{class\ i} | l = 0\right) = Pr\left(Int_{class\ i} | j = 0\right) = Pr\left(Int_{class\ i} | occ = 0\right) = Pr\left(Int_{class\ i} | x_i = 0\right) = 0$. Assuming a fixed number of occupied subcarriers (occ), idle subcarriers (j), and class i primary users ($x_i, x_i \neq 0$) the interference may occur on any of active primary users of class i with equal probability. Therefore, the probability of interference on a specific primary user of class i is:

$$\begin{aligned} Pr\left(Int_i\right) = \sum_{j=1}^{N} \sum_{occ=1}^{N} \sum_{x_i=1}^{\left\lfloor \frac{occ}{i} \right\rfloor} \frac{1}{x_i} Pr\left(Int_{class\ i} | J, OCC, X_i\right) \\ P\left(J | OCC, X_i\right) P\left(X_i | OCC\right) P_{OCC}(occ), \end{aligned} \tag{3.39}$$

where:

$$P\left(J|OCC, X_i\right) = \sum_{l=0}^{j} f\left(l\right) g\left(j-l\right). \tag{3.40}$$

Note that for the case of $C_{occ} \cap B_{i,x_i} = \varnothing$, (3.38) and (3.40) are not defined. Obtaining $P\left(X_i|OCC\right)$ is also straightforward. Hence, the throughput of a primary user of class i in the presence of secondary user interference is given by:

$$\tau_{P,i} = Pr\left(Int_i\right) C_{P,i}^{int} + \left(1 - Pr\left(Int_i\right)\right) C_{P,i}. \tag{3.41}$$

The total throughput of the whole primary network in the presence of secondary user interference is:

$$T_P = \sum_{k=0}^{N} T_{P|OCC=k} P_{OCC}\left(OCC = k\right), \tag{3.42}$$

where:

$$T_{P|OCC=k} = \left(\sum_{\overline{m} \in C_k} \frac{Pr\left(\overline{X} = \overline{m}\right)}{P_{OCC}\left(k\right)} \cdot \overline{m} \right) \cdot \overline{\tau}_{P|OCC=k}, \tag{3.43}$$

$$\tau_{P,i|OCC=k} = \begin{cases} P\left(Int_i|OCC = k\right) C_{P,i}^{int} + \left(1 - P\left(Int_i|OCC = k\right)\right) C_{P,i}, & i \leq k \\ 0, & i > k, \end{cases} \tag{3.44}$$

and $\overline{\tau}_{P|OCC=k} = \left[\tau_{P,1|OCC=k}, \cdots, \tau_{P,N|OCC=k}\right]^T$. For the second condition in (3.44), it is obvious that the throughput of a primary user of class i is 0 if the number of occupied subcarriers is less than i. To obtain $Pr\left(Int_i\middle|OCC\right)$ we have:

$$\begin{aligned} Pr\left(Int_i\middle|OCC\right) = \sum_{j=1}^{N} \sum_{x_i=1}^{\left\lfloor \frac{occ}{i} \right\rfloor} \frac{1}{x_i} Pr\left(Int_{class\ i}|J, OCC, X_i\right) \\ P\left(J|OCC, X_i\right) P\left(X_i|OCC\right). \end{aligned} \tag{3.45}$$

In order to evaluate the average throughput of the whole primary network or a single primary user of class i, first we need to find the mean of (3.32) and (3.33). Here we assume the fading is Rayleigh and the area under study is an annulus with $1 < r < \frac{R}{2}$. All the subcarriers power gains are assumed to be i.i.d. exponential random variables with unit mean. For mean of (3.32) we have:

$$\begin{aligned} E\left[C_{P,i}\middle|r^{-\alpha}=\rho\right] &= \sum_{k=1}^{i} E\left[\log_2\left(1+r^{-\alpha}g_{p,k}\frac{P_T}{i}\right)\middle|r^{-\alpha}=\rho\right] \\ &= \sum_{k=1}^{i}\log_2 e\int_{g_p=0}^{\infty}\ln\left(1+\rho g_p\frac{P_T}{i}\right)e^{-g_p}dg_p \\ &= i\exp\left(\frac{1}{\rho\frac{P_T}{i}}\right)E_1\left(\frac{1}{\rho\frac{P_T}{i}}\right)\log_2 e, \end{aligned} \tag{3.46}$$

where $E_1(x)=\int_x^{\infty}\frac{e^{-u}}{u}du$. Therefore, we have:

$$E\left[C_{P,i}\right] = i\frac{\log_2 e}{K\alpha}\int_{\rho=\left(\frac{R}{2}\right)^{-\alpha}}^{1}\rho^{-\frac{2}{\alpha}-1}\exp\left(\frac{1}{\rho\frac{P_T}{i}}\right)E_1\left(\frac{1}{\rho\frac{P_T}{i}}\right)d\rho. \tag{3.47}$$

The second term in (3.33) represents the effect of secondary user interference on the throughput of a class i primary user. To obtain the mean of this term we first introduce a lemma from [26].

Lemma 1: Let $x_1,\cdots,x_N,y_1,\cdots,y_M$ be arbitrary non negative random variables. Then:

$$E\left[\ln\left(1+\frac{\sum_{n=1}^{N}x_n}{1+\sum_{m=1}^{M}y_m}\right)\right] = \int_0^{\infty}\frac{M_y(z)-M_{x,y}(z)}{z}e^{-z}dz, \tag{3.48}$$

where $M_y(z)=E\left[e^{-z\sum_{m=1}^{M}y_m}\right]$ and $M_{x,y}(z)=E\left[e^{-z\left(\sum_{n=1}^{N}x_n+\sum_{m=1}^{M}y_m\right)}\right]$. The proof is in [26].

Therefore, for the mean of second term in (3.33) we have:

$$E\left[\log_2\left(1+r^{-\alpha}\frac{g_pP_T}{i\left(1+\beta_pP_S\right)}\right)=C_{P,i,second}^{int}|r^{-\alpha}=\rho\right]=$$
$$\log_2 e\int_{z=0}^{\infty}\frac{\rho P_T}{i\left(1+zP_S\right)\left(1+z\rho\frac{P_T}{i}\right)}e^{-z}dz, \tag{3.49}$$
$$E\left[C_{P,i,second}^{int}|r^{-\alpha}=\rho\right]=\log_2 e\frac{\rho\frac{P_T}{i}}{\rho\frac{P_T}{i}-P_S}\left[e^{\frac{i}{\rho P_T}}E_1\left(\frac{i}{\rho P_T}\right)-e^{\frac{1}{P_S}}E_1\left(\frac{1}{P_S}\right)\right].$$

Hence, for the mean of (3.33):

$$E\left[C_{P,i}^{int}\right]=\frac{i-1}{i}E\left[C_{P,i}\right]+\frac{1}{K\alpha}\int_{\rho=\left(\frac{R}{2}\right)^{-\alpha}}^{1}\rho^{-\frac{2}{\alpha}-1}E\left[C_{P,i,second}^{int}|r^{-\alpha}=\rho\right]d\rho. \tag{3.50}$$

For fixed P_T, as the secondary user transmit power (P_S) goes to infinity, the second term of (3.33) goes to zero. This term is very small compared (3.32) and the first term of (3.33). Moreover, $Pr\left(Int_i|OCC=k\right)$ in (3.44) is not a function of P_S. Therefore, the throughput of the primary network is robust to the increase of secondary user power. This is true since the interference from the secondary user occurs only on one of multiple occupied subcarriers of the primary network.

We can find the asymptotic primary network throughput as $\Lambda=\lambda R^2$ goes to infinity. The convergence point is derived in the following theorem:

Theorem 2: Regardless of requesting distribution, as $\Lambda\to\infty$ the throughput of primary network increases and converges to

$$T_p\to\sum_{j=1}^{N}f\left(j\right)^2C_{P,1}^{int}+\left(N-\sum_{j=1}^{N}f\left(j\right)^2\right)C_{P,1}. \tag{3.51}$$

Proof: The proof is given in Appendix D.

For large values of Λ, with increase in Λ, the number of occupied subcarriers increases which is equivalent to the increase in primary network throughput.

3.4.2 Throughput of the Secondary Transmitter

Assuming all transmitted signals from primary and secondary users follow i.i.d. zero mean, circularly symmetric complex Gaussian distribution, the achievable throughput of the secondary transmitter and receiver pair is given by [63]:

$$C_S = \log_2 \left(1 + \beta_S P_S\right), \tag{3.52}$$

and:

$$C_{S,i}^{int} = \log_2 \left(1 + \frac{\beta_S P_S}{1 + r^{-\alpha} g_s P_T / i}\right), \tag{3.53}$$

where (3.52) and (3.53) represent the achievable throughput when there is no interference from any of primary users and when a class i primary user causes interference on the secondary user due to missed detection of one of its subcarriers by the secondary user, respectively.

The throughput of the secondary user can be expressed in two terms which represent the throughput when there exists interference from the primary network and the throughput when there is no interference on the secondary user. The first term showing the contribution of interference is:

$$T_{S|OCC=k}^{int} = \left(\sum_{\overline{m} \in C_k} \frac{Pr\left(\overline{X} = \overline{m}\right)}{P_{OCC}\left(k\right)} \cdot \overline{m}\right) \cdot \overline{\tau}_{S|OCC=k}^{int}, \tag{3.54}$$

where $\tau_{S,i|OCC=k}^{int} = Pr\left(Int_i \middle| OCC = k\right) C_{S,i}^{int}$ and $\overline{\tau}_{S|OCC}^{int} = \left[\tau_{S,1|OCC}^{int}, \cdots, \tau_{S,N|OCC}^{int}\right]^T$.

The second term for the secondary user throughput when there is no interference can be written as:

$$T_{S|OCC=k}^{no\ int} = \sum_{j=1}^{N} \sum_{l=0}^{j} v\left(l\right) g\left(j-l\right) \frac{j-l}{j} C_S, \tag{3.55}$$

where:

$$
\begin{aligned}
& v\left(l\right) g\left(k\right) = Pr\left(\text{num of miss} = l|OCC\right) Pr\left(\text{CDE} = k|OCC\right) \\
& Pr\left(\text{num of miss} = l|OCC\right) = \binom{occ}{l} Pr\left(miss|OCC\right)^{l} \\
& \left(1 - Pr(miss|OCC)\right)^{occ-l} \\
& Pr\left(miss|OCC\right) = \left(\sum_{\overline{m} \in C_{occ}} \frac{1}{\sum_{n=1}^{N} m_n} \frac{Pr\left(\overline{X} = \overline{m}\right)}{Pr\left(OCC = occ\right)} \cdot \overline{m} \right) \cdot \overline{P}_{miss}.
\end{aligned}
\tag{3.56}
$$

Note that (3.55) shows the probability that the secondary user chooses an empty subcarrier for transmission among the detected idle subcarriers. Finally for the throughput of the secondary user we have:

$$
T_S = \sum_{k=0}^{N} \left(T_{S|OCC=k}^{int} + T_{S|OCC=k}^{no\ int} \right) P_{OCC}\left(OCC = k\right). \tag{3.57}
$$

Similar to the previous Section, In order to evaluate the average throughput of the secondary user, we obtain the mean of (3.52) and (3.53). Using the same method in the last Section and applying *Lemma1*:

$$
\begin{aligned}
& E\left[C_S\right] = \exp\left(1/P_S\right) E_1\left(1/P_S\right) \log_2 e \\
& E\left[C_{S,i}^{int}\right] = \frac{1}{K\alpha} \int_{\rho=\left(\frac{R}{2}\right)^{-\alpha}}^{1} \rho^{-\frac{2}{\alpha}-1} E\left[C_{S,i}^{int} \middle| r^{-\alpha} = \rho\right] d\rho,
\end{aligned}
\tag{3.58}
$$

where:

$$
E\left[C_{S,i}^{int} \middle| r^{-\alpha} = \rho\right] = \log_2 e \frac{P_S}{P_S - \rho P_T / i} \left[e^{1/P_S} E_1\left(1/P_S\right) - e^{i/\rho P_T} E_1\left(i/\rho P_T\right) \right]. \tag{3.59}
$$

We propose a theorem regarding the asymptotic throughput of the secondary user as primary user power P_T goes to infinity.

Theorem 3: As $P_T \to \infty$ the throughput of the secondary user increases and converges to

$$T_S \to C_S \left(1 - \sum_{k=0}^{N} P_f^{N-k} P_{OCC}\left(OCC = k\right)\right). \tag{3.60}$$

Proof: The proof is given in Appendix E.

Since the secondary user transmits in only one subcarrier, unlike the primary network, it is extremely vulnerable to interference. Hence, the main contribution on the throughput is the scenario when the secondary user transmits in an empty subcarrier. At large primary user transmit power regime, the throughput of the secondary user while there is interference from an active primary network is very small. (3.45) and (3.53) are small and $T^{int}_{S|OCC=k}$ is negligible compared to $T^{no\ int}_{S|OCC=k}$. With increase in P_T, although $T^{int}_{S|OCC=k}$ decreases, due to the decrease in probability of miss detection $T^{no\ int}_{S|OCC=k}$ increases which causes the total secondary throughput (3.57) to increase.

The asymptotic throughput of the secondary user as $\Lambda = \lambda R^2$ goes to infinity is derived next.

Theorem 4: Regardless of requesting distribution, as $\Lambda \to \infty$ the throughput of the secondary user decreases and converges to

$$T_S \to \sum_{j=1}^{N} f\left(j\right)^2 C^{int}_{S,1}. \tag{3.61}$$

Proof: The proof is given in Appendix F.

Due to vulnerability of the secondary user to interference, the dominating term in determining the throughput is $T^{no\ int}_{S|OCC=k}$. For large values of Λ, with increase in Λ, the number of occupied subcarriers increases. Therefore, $T^{no\ int}_{S|OCC=k}$ decreases causing

the average throughput to decrease. Note that as $\Lambda \to \infty$ and $P_T \to \infty$, $T_S \to 0$. At large values of Λ all N subcarriers are occupied and since probability of miss detection goes to zero as $P_T \to \infty$, no idle subcarrier is detected by the secondary user and it can not initiate its transmission.

3.5 Numerical Results and Discussions

Fig. 3.2 shows $E[Y]$ as a function of Λ for all four distributions for $N = 16$. With increase in Λ the probability of having higher number of active primary users increases. As Λ goes to infinity the probability of having N active primary users goes to 1 since the mean of top priority primary users (class 1) goes to infinity and all N subcarriers will be assigned to N primary users of class 1. The number of active primary users is highly determined by the number of active users of class 1 (X_1) due to their top priority. It can be seen that for same values of Λ, the distribution with smaller $p_1 = P_M(1)$ has smaller $E[Y]$. Therefore, modified binomial distribution has the smallest mean and linearly descending distribution has the largest mean. All curves converge to N as Λ increases but as it is expected the distribution with larger p_1 saturates faster. Hence, modified binomial distribution is the least sensitive to the increase of Λ.

Figs. 3.3-3.5 show the mean number of active primary users of classes 1, 2, and 5 as a function of Λ for $N = 16$, respectively. In Fig. 3.3, It can be seen that the value of Λ which the curves for linearly descending and uniform distributions go to N is the same value which their corresponding $E[Y]$ in Fig. 3.2 goes to N. This again shows the dominant effect of primary users of class 1 on the mean number of active primary users. It is also seen that except class 1, the curve for the mean of other classes for all four distributions reaches a maximum and then goes to zero as Λ increases. This happens since for small values of Λ, there are available subcarriers for all classes.

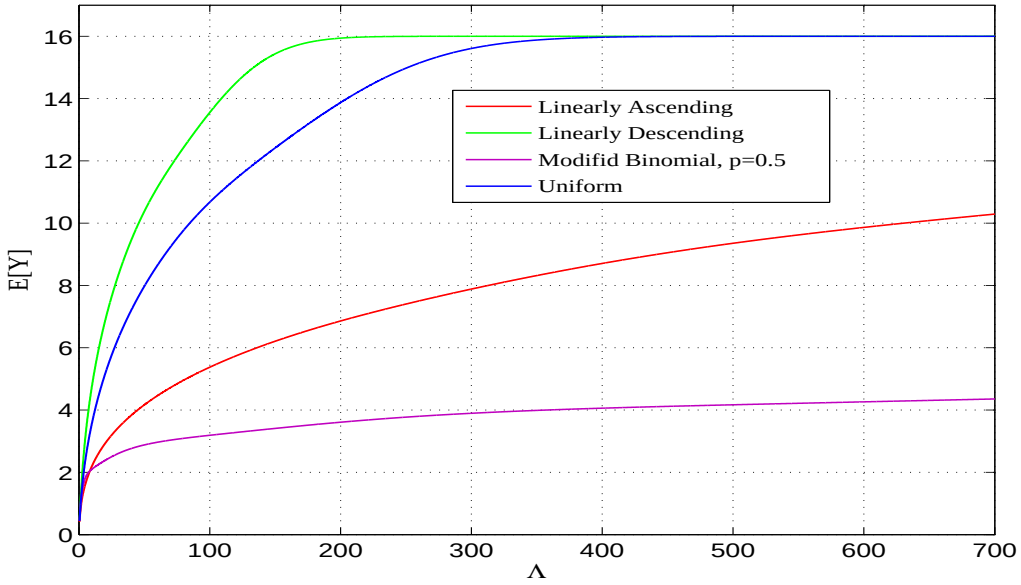

Figure 3.2: $E[Y]$ as a function of Λ for all four distributions, $N = 16$.

Thus, with increase in Λ, the mean of requesting primary users and subsequently the mean number of active primary users increases. As Λ (traffic) gets larger, the mean of class 1 primary users gets large enough such that in order to access the spectrum, other classes must be prevented from accessing the spectrum. Hence, the mean number of active primary users of other classes starts to decrease. As another observation, the maximum gets smaller and also occurs at smaller values of Λ for all four distributions as the class increases which is another effect of prioritization.

Priority and mean number of requesting primary users are two important factors in determining the mean number of active primary users of a class. For the linearly descending distribution, the class with higher priority has a larger mean as well. Therefore, as it is seen in Figs. 3.3-3.5 for all classes for the same value of Λ, the class with higher priority has a larger mean. For the uniform distribution all classes have the same mean so the priority is the only factor affecting the mean. Therefore, for all classes at the same Λ, the class with higher priority has a larger mean. But for

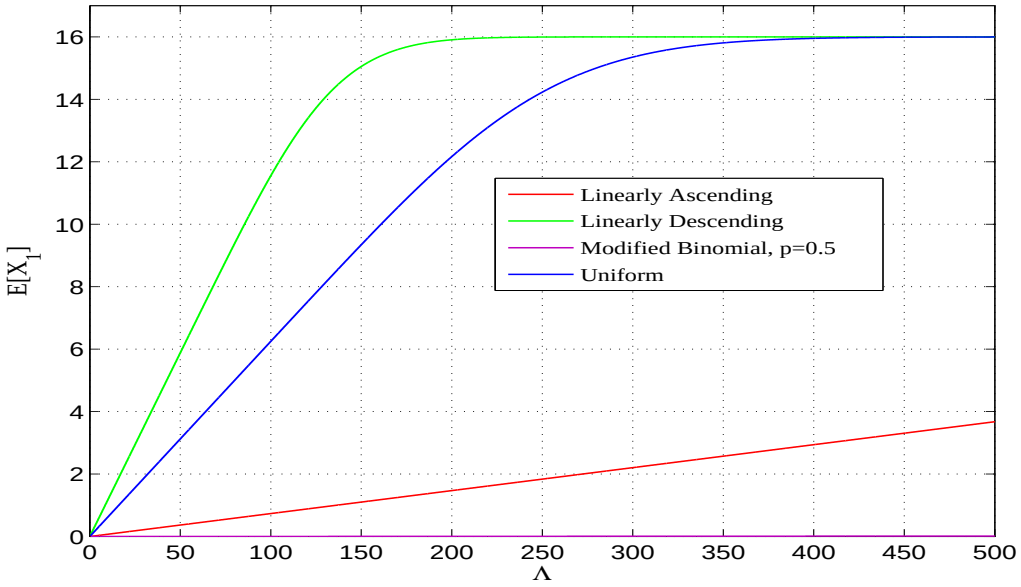

Figure 3.3: $E[X_1]$ as a function of Λ for all four distributions, $N = 16$.

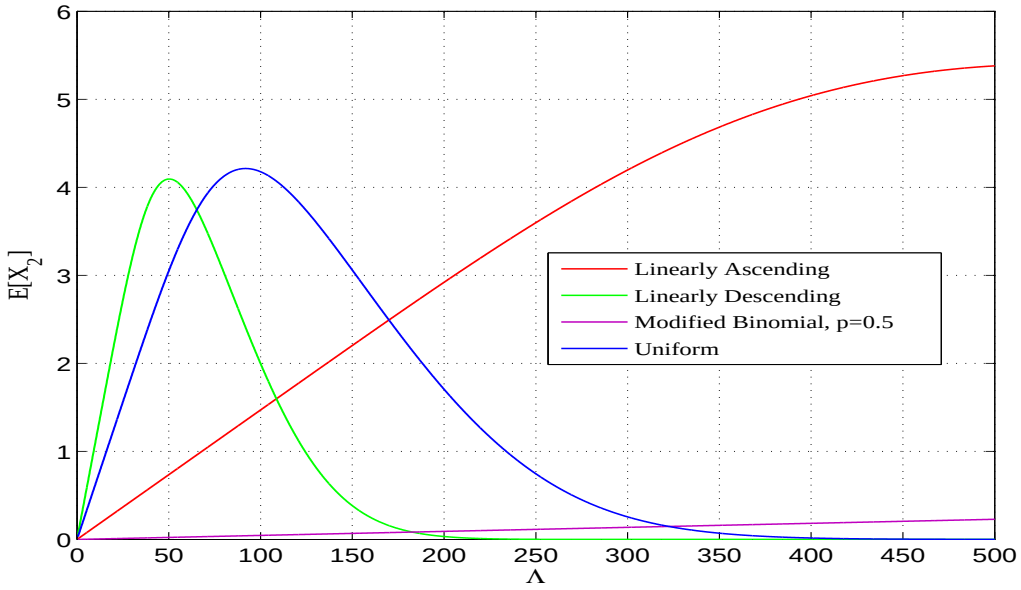

Figure 3.4: $E[X_2]$ as a function of Λ for all four distributions, $N = 16$.

modified binomial and linearly ascending distributions, the class with higher priority does not necessarily have a larger mean. This leads to some cases in which a primary

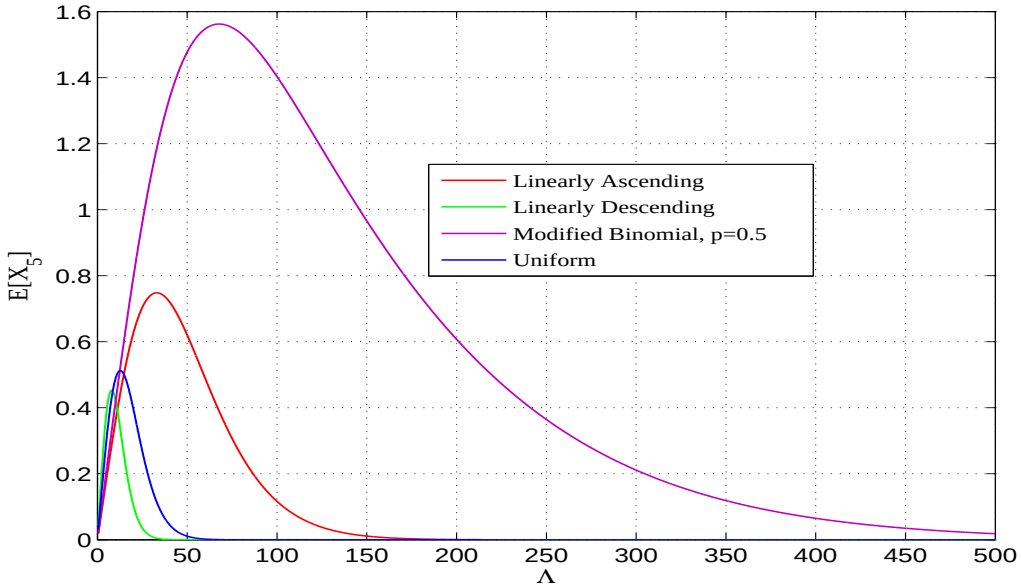

Figure 3.5: $E[X_5]$ as a function of Λ for all four distributions, $N = 16$.

user with less priority has a larger mean compared to a primary user with higher priority at the same value of Λ. The examples can be seen in Figs. 3.3 and 3.4 for the linearly ascending distribution where mean of class 2 is larger than of class 1, and in Figs. 3.3, 3.4, and 3.5 for the modified binomial distribution where mean of class 5 is larger than of class 2 and mean of class 2 is larger than of class 1.

Fig. 3.6 shows the user activity rate for four distributions as a function of traffic. It is seen that although the modified binomial distribution has smaller mean of requesting primary users of class 1 compared to the linearly ascending distribution, for small values of Λ the former has larger user activity rate. This is due to the fact that at low traffic, primary users with larger mean number have more effect on determining $E[Y]$ compared to top priority requesting primary users. However, with increase in traffic the priority of primary users comes first.

Fig. 3.7 shows $E[OCC]$ as a function of Λ for all four distributions for $N = 16$. With increase in Λ, $E[OCC]$ converges to N. This indicates that the majority of

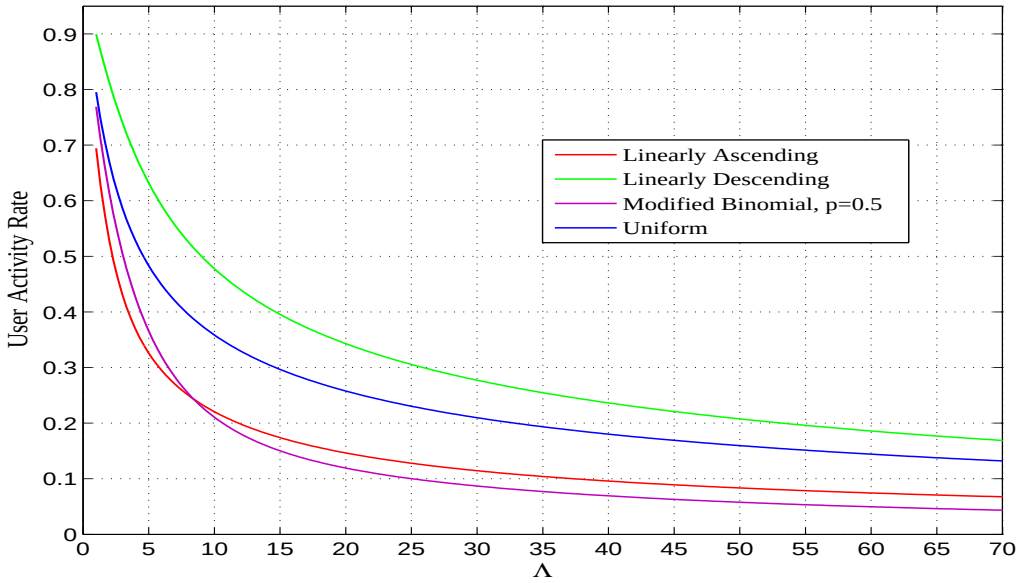

Figure 3.6: ζ as a function of Λ for all four distributions, $N = 16$.

active primary users belong to class 1. The curve for the linearly descending distribution is first to reach the maximum ($N = 16$), since class 1 requesting primary users have the largest mean compared to other distributions. It is also seen that all distributions except the modified binomial which has a non-linear distribution, have monotonically increasing curves. The fluctuations of the curve for the modified binomial distribution is the result of trade off between the primary users with larger mean and primary users with higher priority. All curves increase rapidly for small values of Λ and then slowly converge to N for larger values of Λ. This is the result of preventing higher class primary users from accessing the spectrum. The increase in the mean number of subcarriers is equivalent to the increase in the number of top priority primary users, which indicates the system sensitivity to the mean of such primary users. It is also seen that at low traffic that priority is not of significant importance, primary users with larger mean have more impact on determining $E[OCC]$. Thus, it is seen that at low traffics the order of all curves is reverse compared to higher

traffics when priority is more effective.

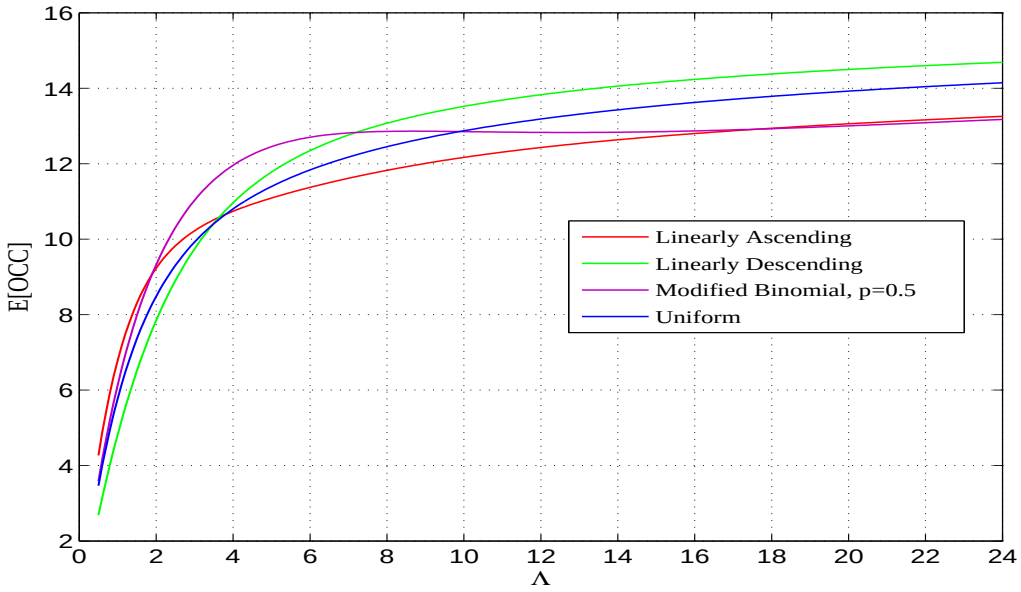

Figure 3.7: $E[OCC]$ as a function of Λ for all four distributions, $N = 16$.

Fig. 3.8 shows the spectrum access rate for four distributions as a function of traffic. It is seen that at low traffic, since users with larger mean have more effect on determining $E[OCC]$, modified binomial distribution has larger access rate compared to uniform distribution although both distributions have the same $E[M]$. However, with increase in Λ that priority gets more effective, uniform distribution has larger access rate. Note that as it was mentioned in Section 3.2, for large Λ and N, both distributions have the same spectrum access rate of $\frac{2}{\Lambda}$.

Fig. 3.9 shows $\overline{P}_{miss}$ for different fadings, it is seen that with increase in class of users, $\overline{P}_{miss}$ increases since the subcarrier power decreases. We also observe that for Log-normal fading, higher dB-spread results in larger $\overline{P}_{miss}$. Therefore, in order to have smaller miss detection probability, more sensitive detectors are required at higher dB-spreads.

In Fig. 3.10, the probability of miss detection of an occupied subcarrier by the

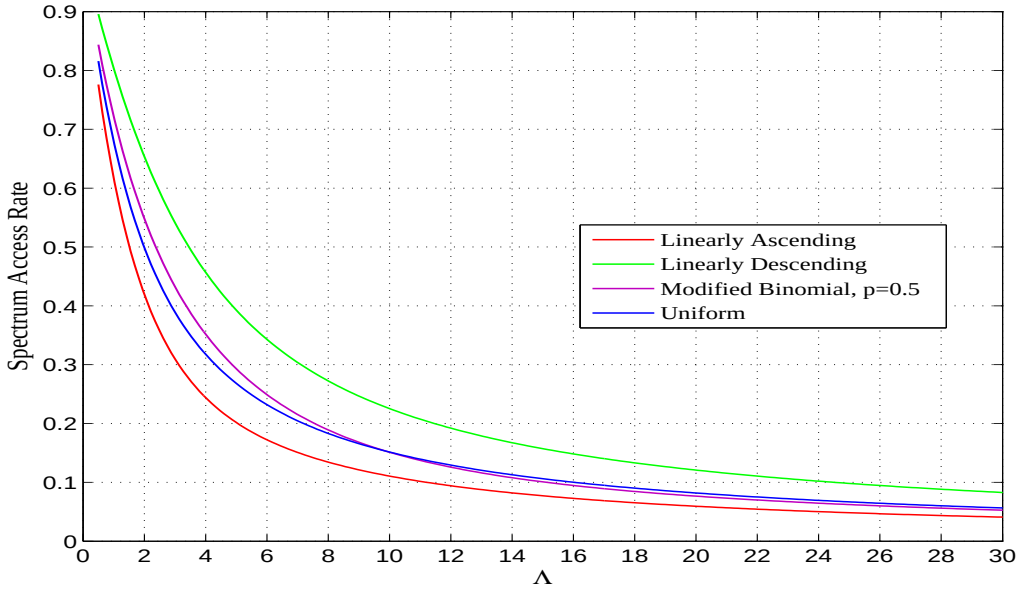

Figure 3.8: η as a function of Λ for all four distributions, $N = 16$.

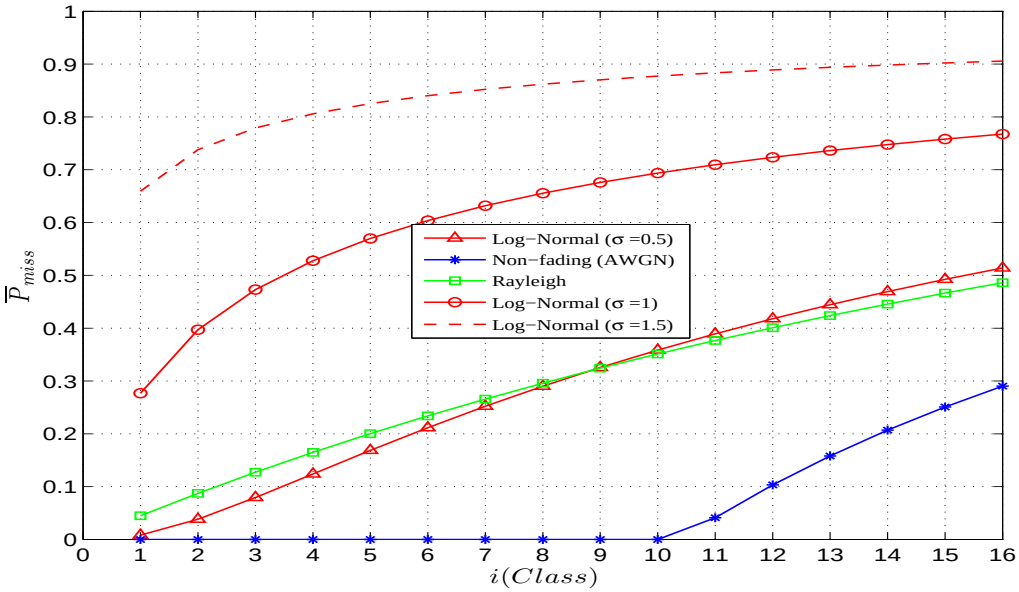

Figure 3.9: $\overline{P}_{miss}$ for different fadings, $N = 16, \alpha = 2, R = 3, \overline{SNR} = -2dB$.

spectrum sensor is plotted as a function of traffic under Rayleigh fading. It is seen that the performance of the spectrum sensor is a function of primary network traffic

and the applied requesting distribution. Due to their larger subcarrier power, lower class active primary users subcarriers are miss detected with smaller probability. Therefore, among several sets with the same number of active primary users, the set that includes a larger number of lower class active primary users results in smaller $Pr(miss)$. Hence, it is observed that for large Λ that priority is more effective, the distribution with larger mean of class 1 requesting primary users has smaller $Pr(miss)$ (linearly descending). It is also seen for small values of Λ that mean number of a class is more effective compared to its priority, the distribution that its largest mean of requesting primary users belong to a lower class has smaller $Pr(miss)$ (modified binomial outperforms linearly ascending). It can be seen that in agreement with *Theorem 1*, as $\Lambda \to \infty$ all curves decrease and eventually converge to $P_{miss,1}$. It is also observed that all curves have a maximum at low values of Λ. This happens since for small values of Λ, there are available subcarriers for all classes. So, with increase in Λ, primary users of all classes including higher class primary users with larger probability of miss detection become active which results to the increase in $Pr(miss)$. However, as Λ gets larger, the mean of class 1 primary users gets large enough such that other class users are not allowed to be active. Hence, $Pr(miss)$ begins to decrease.

In Fig. 3.11, $Pr(miss)$ is plotted as a function of $\overline{SNR}$ for different types of fading for uniform and linearly descending distributions. It is seen that with increase in $\overline{SNR}$, $Pr(miss)$ decreases for all types of fading and distributions. The effect of higher dB-spread on the increase of $Pr(miss)$ is obvious. It is also observed that linearly descending distribution has a better performance compared to the uniform distribution due to the larger mean of top priority primary users.

Fig. 3.12 shows average T_P as a function of Λ for all four distributions for $N = 16$ and fixed P_T and P_S. The curves in this figure have similar behavior to the curves

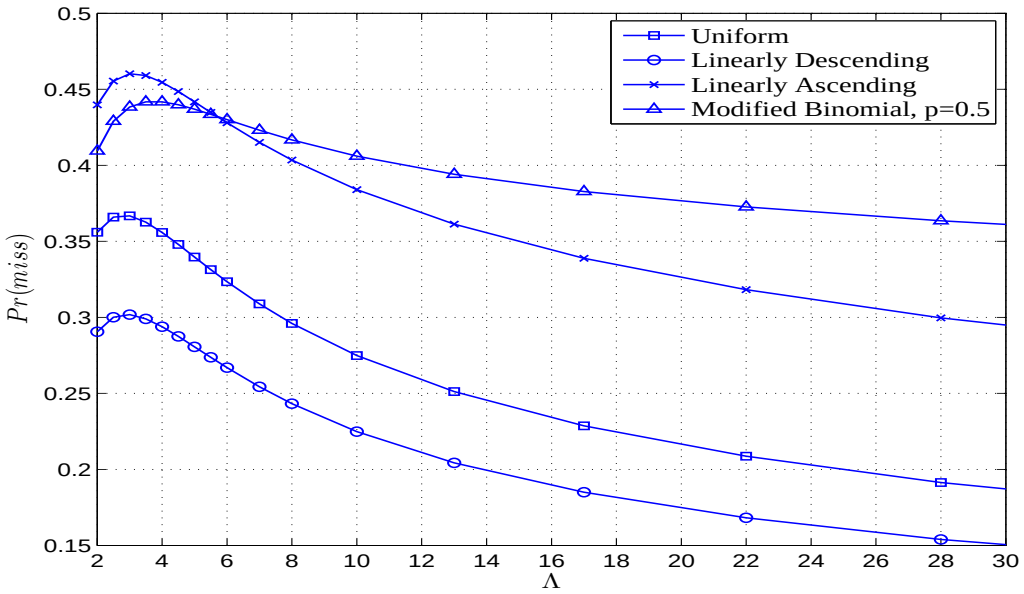

Figure 3.10: $Pr(miss)$ for Rayleigh fading as a function of Λ for all four distributions, $N = 16, \alpha = 2, R = 3, \overline{SNR} = -5dB$.

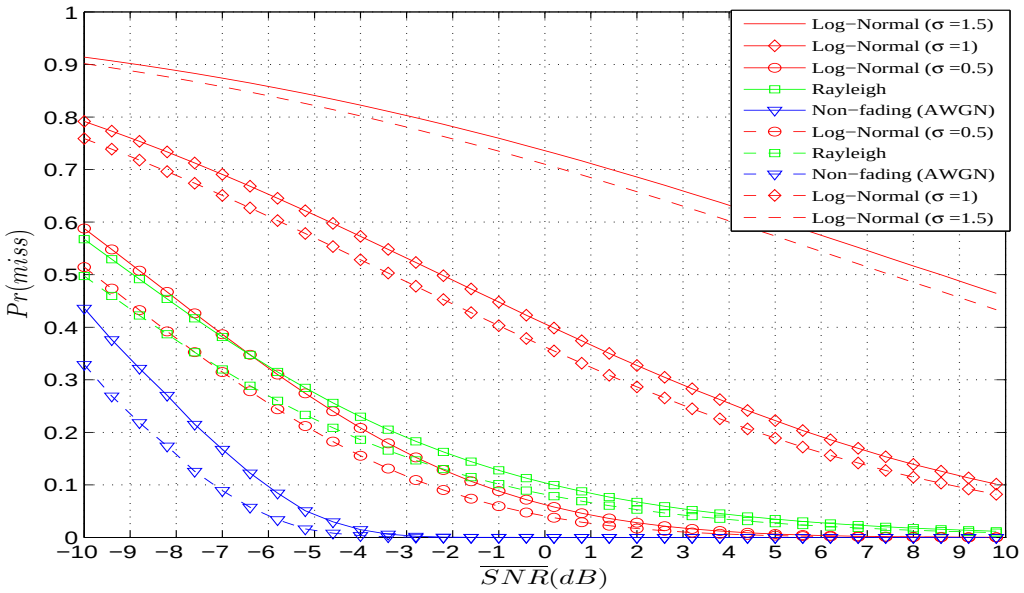

Figure 3.11: $Pr(miss)$ as a function of $\overline{SNR}$ for different fadings and linearly descending (dashed) and uniform (solid) distributions, $N = 16, \alpha = 2, R = 3, \Lambda = 10$.

in Fig. 3.7 since more occupied subcarriers is equivalent to larger average primary throughput. With increase in Λ, average T_P increases and converges to a limit point which is the result of *Theorem 2*. The curve for the linearly descending distribution is the first to converge to (3.51), since all N subcarriers get occupied faster. All curves increase rapidly for small values of Λ and then slowly converge to (3.51) for larger values of Λ. This is the result of preventing higher class primary users that have larger average throughput from being active. With a similar argument regarding Fig. 3.7, It is seen that at low traffic primary users with larger mean have more impact on determining T_P. Hence, modified binomial distribution average throughput is larger than other distributions. However, with increase in traffic, priority of primary users effects the throughput.

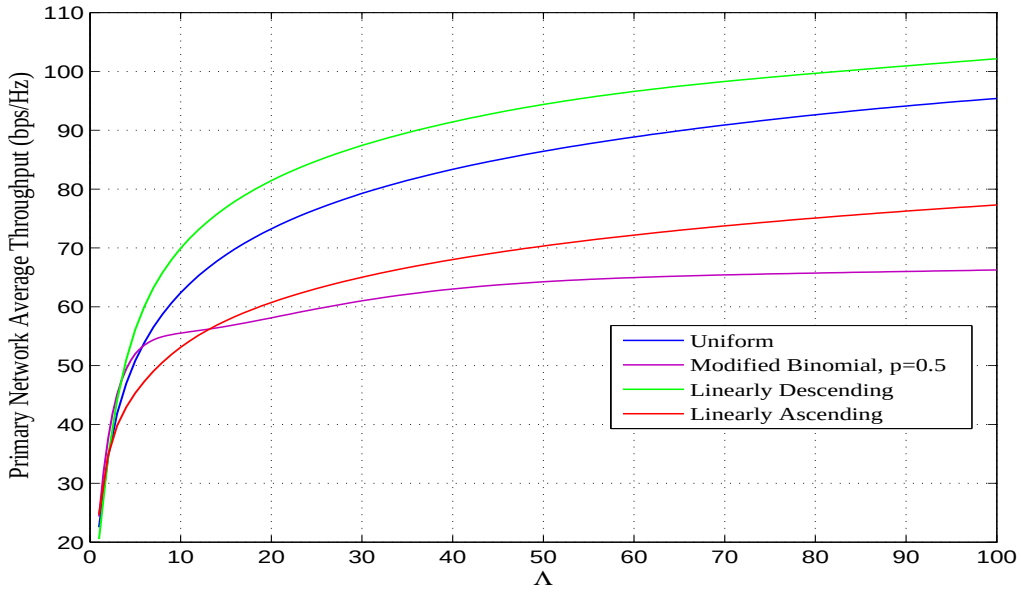

Figure 3.12: Average T_P as a function of Λ for all four distributions, $N = 16, \alpha = 2, R = 3, P_S = 10dB, P_T = 20dB$.

Fig. 3.13 exhibits the insensitivity of average primary network throughput to the interfering secondary user transmit power at fixed P_T as it was explained in Section

3.4.1. The figure is plotted at $\Lambda = 10$. Therefore, the explanation for the order of curves is as same as previous figure at $\Lambda = 10$.

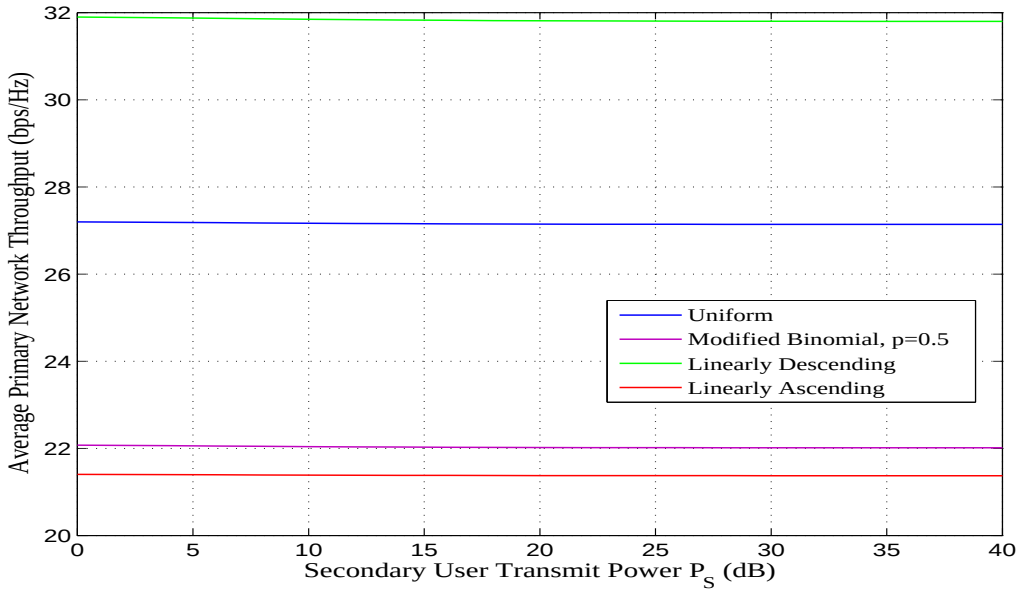

Figure 3.13: Average T_P as a function of P_S for all four distributions, $N = 16, \alpha = 2, R = 3, \Lambda = 10, P_T = 20dB$.

Fig. 3.14 depicts average T_P as a function of P_T for all four distributions for $N = 16$ and fixed P_S. With increase in primary transmit power, the average primary throughput increases since probabilities of miss detection and interference decrease and (3.32) increases. The figure is plotted at $\Lambda = 10$. Therefore, the explanation for the order of curves is as same as Fig. 3.12 at $\Lambda = 10$.

Fig. 3.15 depicts average T_S as a function of P_T for all four distributions at $\Lambda = 10$ and fixed P_S. It is observed that with increase in P_T all curves increase and converge to a limit point. This behavior is in agreement with *Theorem 3*.

In Fig. 3.16 average T_S as a function of Λ for all four distributions for $N = 16$ and fixed P_T and P_S is shown. It is seen that with increase in Λ all curves decrease and converge to a limit point. This behavior is in agreement with *Theorem 4*. It

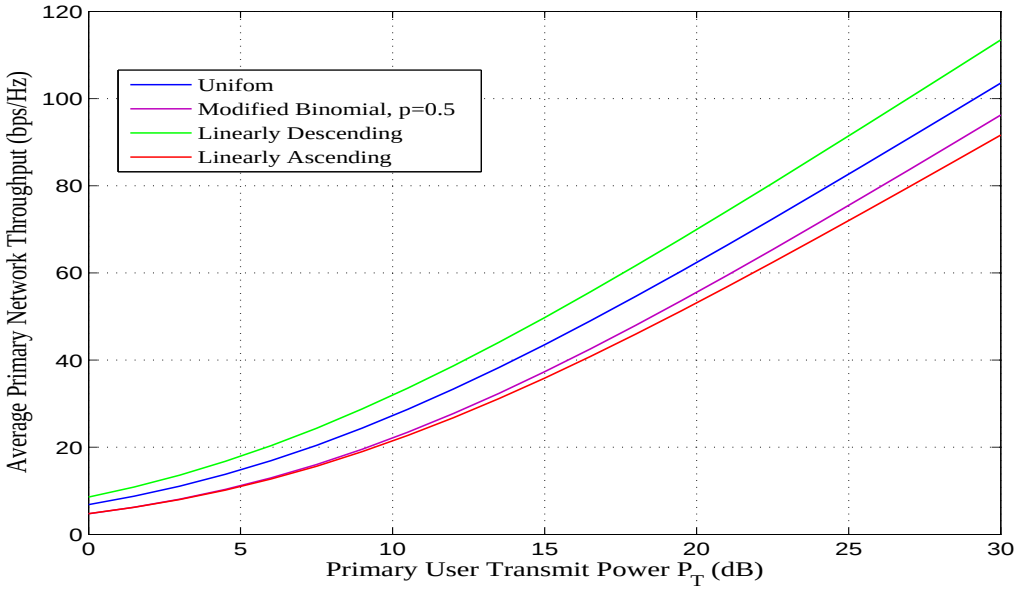

Figure 3.14: Average T_P as a function of P_T for all four distributions, $N = 16, \alpha = 2, R = 3, \Lambda = 10, P_S = 10dB$.

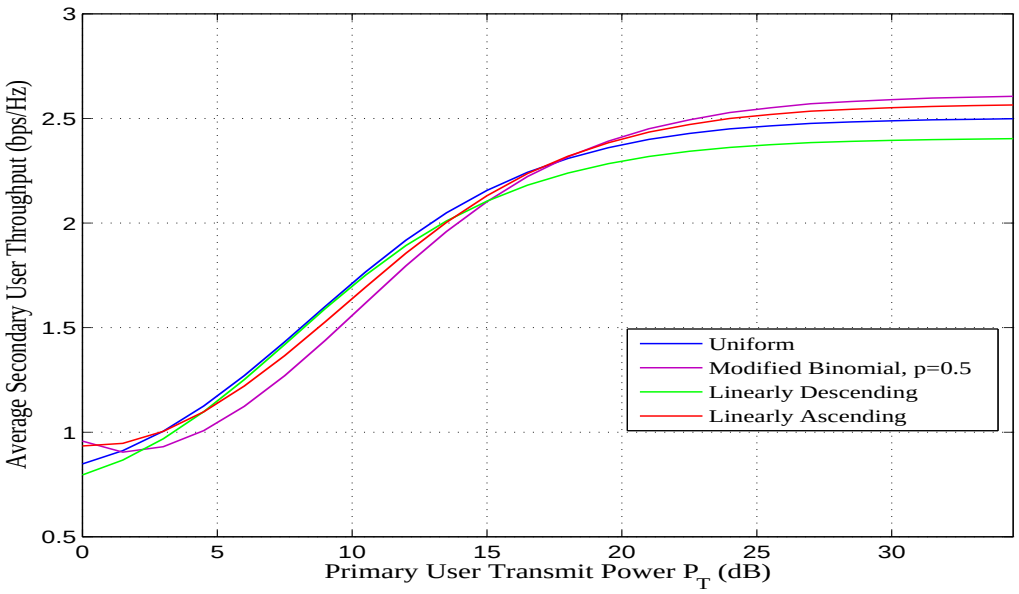

Figure 3.15: Average T_S as a function of P_T for all four distributions, $N = 16, \alpha = 2, R = 3, \Lambda = 10, P_S = 10dB$.

can also be seen that a distribution that its mean number of occupied subcarriers is more sensitive to the increase in Λ, decreases and converges faster.

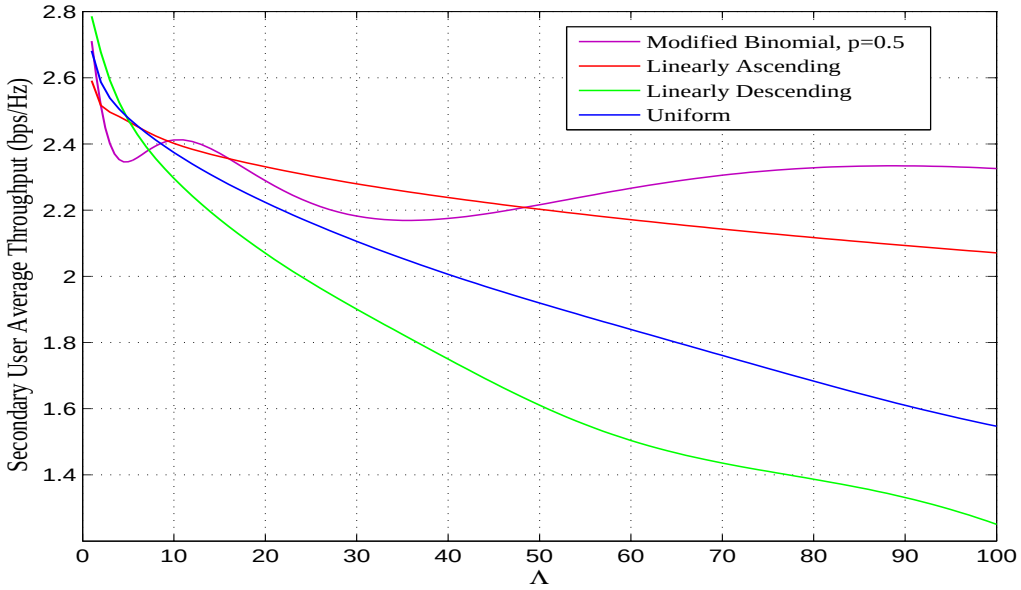

Figure 3.16: Average T_S as a function of Λ for all four distributions, $N = 16, \alpha = 2, R = 3, P_S = 10dB, P_T = 20dB$.

3.6 Summary

A comprehensive statistical model for user activity, spectrum occupancy, and system throughput in an OFDMA based CR network is proposed. The effects of sensing procedure of secondary user, spectrum demand-model and spatial density of primary users, system objective for user satisfaction, and environment-dependent conditions such as propagation path loss, shadowing, and channel fading are taken into account. Various channel requesting distributions are considered. The PMF of the number of active primary users and occupied subcarriers are obtained. It is shown that the number of active primary users can not follow a Poisson distribution under limited spectrum constraint. The probability of miss detection of an occupied subcarrier due to imperfect detection of the secondary user under various system

parameters is evaluated and its asymptotic behavior as the primary network traffic goes to infinity is studied. It is observed that this probability is a function of system traffic and requesting distribution. Lastly, the primary network and the secondary user throughputs in the presence of mutual interference are investigated and their asymptotic values at large primary network traffic, large primary user transmit power, and large secondary user transmit power are analytically derived.

4. SPATIO-TEMPORAL MEASUREMENT AND MODEL FOR NUMBER OF OCCUPIED CHANNELS

4.1 Introduction

Compact mathematical formulations that describe the realistic spectrum usage would improve the recent theoretical work to a large extent. The data generated from such models would also increase the quality of the simulation based research in the aspect of realism. Besides, in practice, measurement campaigns would prefer if they could characterize results with a few well known parameters instead of exchanging large amount of data. In previous sections, we theoretically characterized the dynamic nature of the spectrum based on some limiting assumptions. For example, we assumed users are scattered in the plane based on a Poisson point process. However, in practice users may have a particular spatial distribution which depends on the location and time. Therefore, in this section we try to come up with a mathematical model for the spectrum usage based on real data collected from an extensive measurement. The spectrum usage is modeled by estimating the Probability Mass Function (PMF) of the number of occupied channels. Note that this also gives an insight regarding the spectrum availability. To do this, the data collected from a spectrum occupancy measurement campaign conducted in the State of Qatar is used. The measurements are performed over three consecutive days considering 700-3000 MHz frequency band at four different locations concurrently. We show that after applying the Chi square test, the Log-Normal distribution fits the best among other candidates to the empirical PMF independent of location and the threshold used to define a channel as occupied. The measurement data are collected from these different locations concurrently considering 700 - 3000 MHz RF spectrum over three

successive days. Note that these spectrum measurement data are used to study the average power spectral density and bandwidth utilization at four different outdoor locations [6], at indoor vs. outdoor locations [47], and the effects of threshold and interference on the performance of practical spectrum sensing methods [7].

4.1.1 Organization

This section is organized as follows; in Section 4.2, measurement setup and geographical locations are described. The procedure to find the empirical distribution of the number of occupied channels and the best distribution candidate is explained in Section 4.3. Finally the conclusions are drawn in Section 4.4.

4.2 Measurement Setups and Locations

Data are collected from a wideband spectrum ranging from 700 MHz to 3 GHz at four different outdoor locations simultaneously in the City of Doha (the capital city) in the State of Qatar for three successive days. Location 1 is located in the west of Doha, and comprises a number of education campuses surrounded by vast open and generally flat spaces with some construction work going on in the campus and its immediate surroundings. There are no commercial and residential buildings or areas in the vicinity. In this area, the measurement data is collected on the roof of Texas A&M University at Qatar (TAMUQ) Engineering building. Location 2 is in the south east of Doha and is a busy commercial area that is close to the City of Doha international airport. Different radar and communications systems are deployed and as such it is an electromagnetically rich environment. Location 3 is closer to what is considered the downtown of City of Doha and consists of high towers (average 30 floors +) and large commercial centers in addition to a hospital and a police station. Location 4 is in the south of Doha and consists of factories and workshops.

The spectrum sensor measurement setup and settings used for all locations are

identical. In the spectrum sensor setup, a Rohde & Schwarz FSH6 portable spectrum analyzer is connected to a laptop computer via a USB-optical cable as shown in Fig. 4.1. The spectrum analyzer is also connected to a very high performance discone antenna (AOR DA5000) optimized for 700-3000 MHz frequency range and it has omni-directional horizontal receive capability. The following are the spectrum analyzer settings that are used for all the measurements: Center frequency is 1.85 GHz, frequency span is 2.3 GHz, resolution bandwidth is 300 kHz, video bandwidth is 300 kHz, sweep time is 128 ms, and detector type is auto peak (this detector type provides raw data). The sweep time value is selected as an optimum period considering the rise and fall times of sweeping band-pass filter and frequency resolution requirements. However, the rate of data recording is set to minimum value, which is one reading per minute. During a recording time, the entire spectrum of the 700-3000 MHz band is swept at once with this sweep and- dump rate and recorded in the computer memory. For each location, 4322 different readings of the 700-3000 MHz spectrum are collected during the measurement campaign. This was done for three consecutive days covering both weekdays and weekend which covers high as well as low population activity that can be reflected in spectrum utilization. The internal clock of each spectrum sensor setup is synchronized prior to placing them in their respective measurement locations. In addition, the measurement at all locations is started and stopped synchronously at the same time. Several software packages are used for data post processing. The Rohde & Schwarz FSH view is used to automatically save the measurement data obtained by the spectrum analyzer in the laptop computer.

4.3 Distribution of the Number of Occupied Channels

For each location there are 301 frequency samples from 700 MHz to 3 GHz observed for 4322 time instants. Therefore, there are 4322 snapshots of the observed frequency from 700 MHz to 3 GHz. Each sample in frequency represents a spectrum band with the bandwidth of 7.64 MHz. To define a frequency sample as "occupied", first we define a threshold γ. If the measured power spectral density of the considered sample is above the threshold it is defined as "occupied" otherwise it is "empty". Each occupied frequency sample is mapped to "1" and each vacant sample is mapped to "0". While counting the number of occupied channels at each time instant, an occupied channel is defined as a group of frequency samples successively mapped to "1". This group may consist of only one sample. In Fig. 4.2. a sample realization of the whole spectrum at an arbitrary time instant is shown; there are 6 occupied channels which are numbered by markers. Each occupied channel is actually a chunk of spectrum with random bandwidth. It should be noted that both the number and bandwidth of channels are random. In this section, we focus on the number of occupied channels and try to find the statistical characteristics such as the PMF of the number of used channels. Determining the distribution of the bandwidth of the occupied channels will remain as a future work.

Averaging over all the time instants, the empirical PMF is obtained and its mean and variance is evaluated. In order to properly model the statistical behavior, distribution fit is required. In general, the Chi square test and the Kolmogorov-Smirnov (K-S) test are the two well known tests to measure the *goodness of fit*. Despite the Chi square test that applies to both continuous and discrete distributions, the K-S test only applies to continuous distributions. Since the list of candidates we want to study consists of both continuous and discrete distributions, the Chi

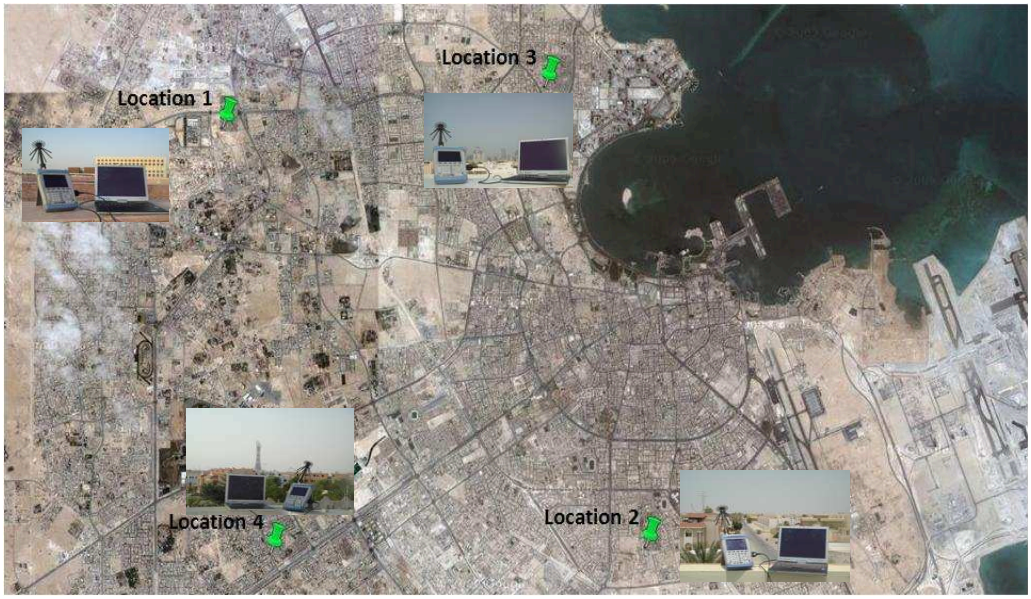

Figure 4.1: Aerial map showing the spectrum sensor setup locations (Courtesy of Google Inc.).

square goodness of fit test is more convenient to work. Besides, since we have a sufficient sample size, the Chi square approximation is valid. Therefore, for the distribution fit, the Chi square test is applied. Test statistics are obtained for several candidate theoretical distributions such as Log-Normal, Gamma, Nakagami, Weibull, and Poisson. Note that the Erlang distribution is a special case of the Gamma distribution where the shape parameter is an integer. In the Gamma distribution, this parameter is not restricted to the integers. Hence, with the study of Gamma distribution we also study the Erlang distribution. It should be noted that since the empirical PMF only takes non-negative integer values, some distributions that take negative values are removed from the list of candidates. Since the list of candidates is not extensive due to the lack of space, we only tried to study the distributions of interest in the communication context. The Chi square test is chosen to apply with [68]:

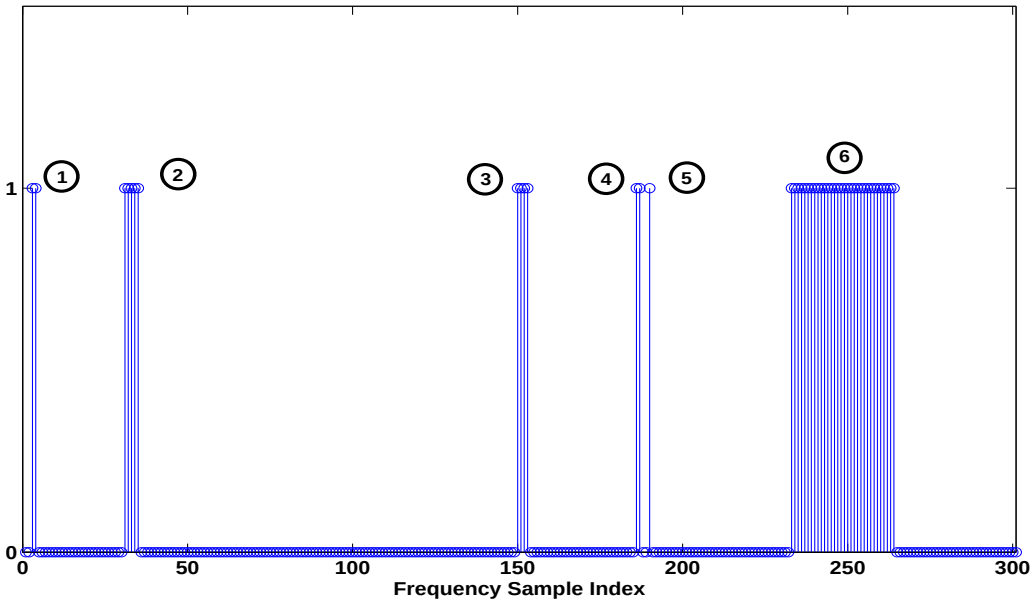

Figure 4.2: A sample realization of the whole spectrum at an arbitrary time instant. There are 6 occupied channels numbered by markers.

$$Q^2 = \sum_{r=1}^{R} \frac{(N_r - T_r)^2}{T_r} \tag{4.1}$$

where R is the number of non-empty bins, N_r is the observed frequency for r-th bin, T_r denotes the corresponding theoretical expected frequency in r-th bin. Prior to apply the Chi square test, degrees of freedom must be determined appropriately, since it is important in evaluating the significance level. In Chi square test, the number of degrees of freedom is $R - 1 - \varphi$, where φ is the number of estimated parameters (including location and scale parameters and shape parameters) for the distribution. Next, the test statistic obtained from (4.1) is compared to the right tail of $\chi^2_{R-1-\varphi}$ in case a significance level is considered.

Except Poisson distribution which is described by a single parameter PMF, other candidates have double parameter probability density function (PDF). We quantize the candidate PDFs to their corresponding PMFs on their integer values to have a

sensible comparison with the obtained empirical PMF while applying the Chi square test. In order to convert a PDF to its corresponding PMF, the following equation is used:

$$\Pr(x = k) = \int_{k}^{k+1} f(x)dx \tag{4.2}$$

where $f(x)$ is the PDF and $k \in \mathbb{Z}$.

Test statistics for all 4 locations with different thresholds $\gamma = -77, -75, -73, -71$ dBm were calculated. It is observed that independent of the threshold and location, in all the 16 cases the best candidate distribution is Log-Normal. Gamma and Nakagami are the second and the third best candidate distributions, respectively. Since the entire candidate theoretical PDFs have two parameters, their relative Chi square tests have identical degrees of freedom. Therefore, the candidate with the least test statistics is the most similar distribution. Note that for thresholds less than -77 dBm the results get too noisy due to the noise level constraint of the spectrum analyzer, hence are not reliable. The measured average noise level of the spectrum analyzers that we use for the given settings is -78 dBm. Since the noise varies with frequency, we use 3 dB margin in order to account this variation [67]. In addition, due to large number of possible cases (16 cases), we use -75 dBm as the threshold to present the results for all locations. Test statistics for four locations with $\gamma = -75$ dBm are tabulated in Tables 4.1-4.4.

It can be seen that for all the locations, the Log-Normal distribution has the least test statistics which indicates that among all the theoretical candidates, Log-normal distribution fits the best. Gamma and Nakagami are the next best candidates, respectively. Therefore we characterize the spectrum usage by choosing the Log-Normal distribution for the number of occupied channels. Note that this distribution

is completely defined by two parameters as $\ln\mathcal{N}(\mu, \sigma^2)$ where μ and σ^2 are the mean and variance of the variable's natural logarithm (by definition, the variable's logarithm is normally distributed). The empirical PMF along with other candidates for four locations at $\gamma = -75$ dBm are shown in Figs. 4.3-4.6. Table 4.5 shows the Log-Normal parameters for all four locations.

Table 4.1: Chi square test results at location 1

Theoretical Distribution	Test Statistics (Q^2)
Log-normal	0.1861
Gamma	0.1861
Nakagami	0.2070
Poisson	0.9786
Weibull	1.6699e+016

Table 4.2: Chi square test results at location 2

Theoretical Distribution	Test Statistics (Q^2)
Log-normal	0.0938
Gamma	0.1490
Nakagami	0.2946
Poisson	0.7078
Weibull	1.3879e+012

Table 4.3: Chi square test results at location 3

Theoretical Distribution	Test Statistics (Q^2)
Log-normal	0.1221
Gamma	0.1276
Nakagami	0.1770
Poisson	0.4852
Weibull	9.7249e+007

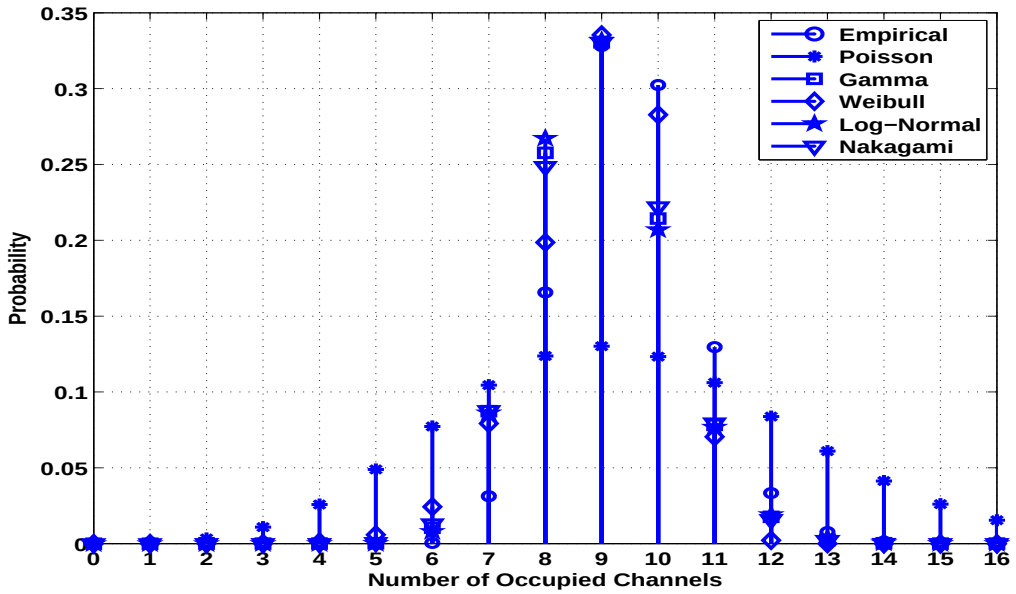

Figure 4.3: The empirical PMF and candidate distributions for location 1 at $\gamma = -75$ dBm.

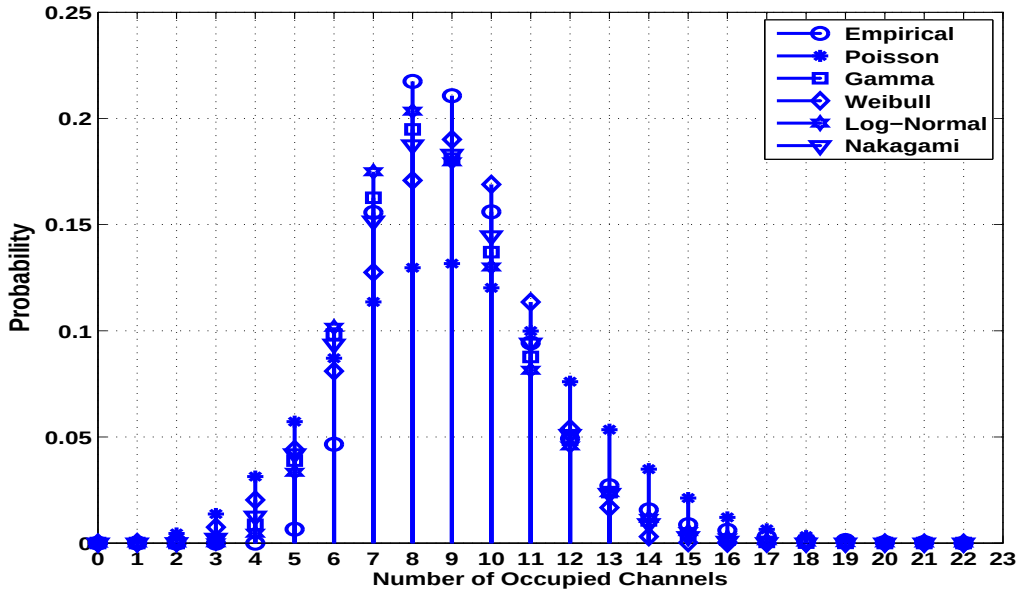

Figure 4.4: The empirical PMF and candidate distributions for location 2 at $\gamma = -75$ dBm.

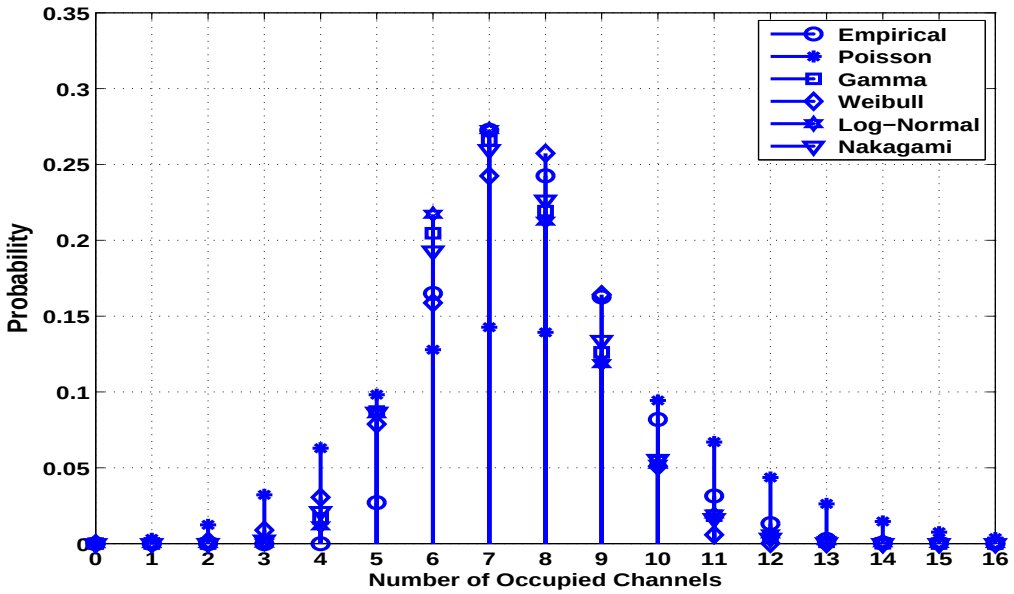

Figure 4.5: The empirical PMF and candidate distributions for location 3 at $\gamma = -75$ dBm.

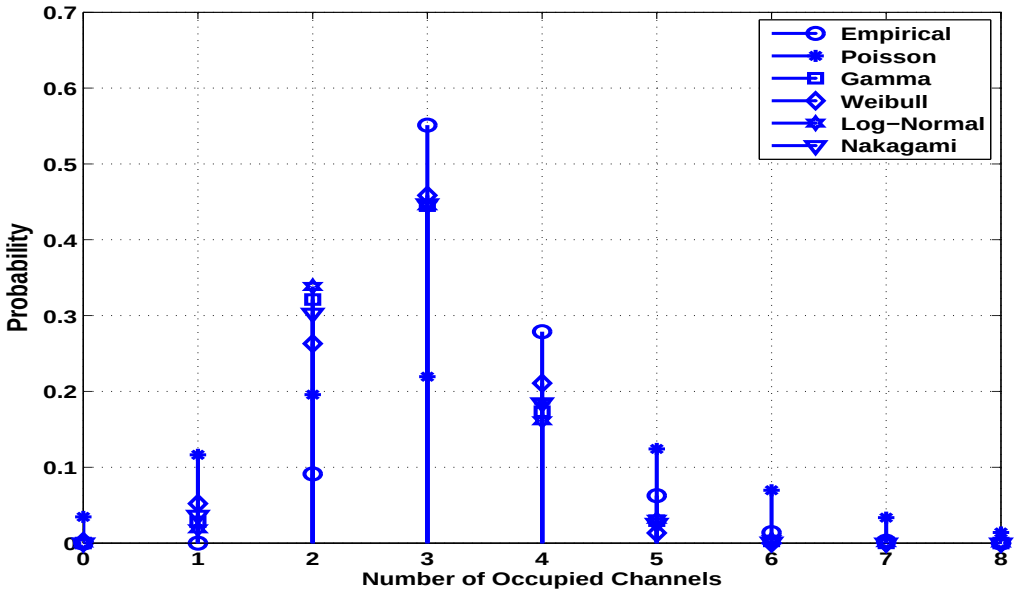

Figure 4.6: The empirical PMF and candidate distributions for location 4 at $\gamma = -75$ dBm.

Table 4.4: Chi square test results at location 4

Theoretical Distribution	Test Statistics (Q^2)
Log-normal	0.3825
Gamma	0.4079
Nakagami	0.6512
Poisson	0.8959
Weibull	1.1924e+004

Table 4.5: Log-Normal parameters for all four locations

Location	(μ, σ^2)
Location 1	(2.2407, 0.0150)
Location 2	(2.1344, 0.0822)
Location 3	(2.0374, 0.0360)
Location 4	(1.1852, 0.0561)

4.4 Summary

Reliable statistics and models have practical impact as they can be used to create spectrum utilization strategies and algorithms. In this section, we characterize the spectrum usage by evaluating the PMF of the number of occupied channels at four geographically different locations based on the extensive measurement conducted in the State of Qatar. Having the PMF can also provide valuable information about the spectrum usage. The PMF of each location can provide useful information about the spectrum utilization of that location. It is observed that the well known Log-Normal distribution fits the most to the empirical PMF independent of location and threshold. Since Log-Normal distribution is completely defined by two parameters, we can characterize the results for each location by providing those parameters instead of exchanging large amount of data.

5. CONCLUSIONS

5.1 Conclusions

In this section, we summarize all the contributions in this work. We showed that the number of active primary users is not a Poisson random variable (unlike previous works and it is valid for limited spectrum). The results of this work is used for standardization of IEEE 1900.7. As another benefit, this model is valid for any area at any time. By adding randomness to the number of requested subcarriers, our model considers different spectrum requests based on user communication needs (unlike most works on cognitive radio). Our model supports as many users as possible as well. We can design our system by only the knowledge of the first moment of the requesting distribution. Moreover, the proposed throughput model is more realistic since the spectrum is limited, sensing is imperfect, and there is fading, shadowing, and propagation path loss. We also studied the asymptotic behavior of performance metrics such as user activity rate, spectrum access rate, probability of miss detection, system throughput, and outage probability as the spectrum and traffic go to infinity.

We also proposed two comprehensive stochastic models. The first model captures the spectrum demand in an OFDMA based cognitive radio system. The second model is for user activity and spectrum occupancy. We also studied asymptotic spectrum availability as the network traffic and total number of subcarriers go to infinity. Another study on the sustainable traffic of the system subject to a fixed spectrum outage was also conducted. Effect of requesting distribution on the asymptotic spectrum availability of the system was investigated. Moreover, the effect of traffic of users, requesting distribution and type of fading on the miss detection probability of an occupied subcarrier was another subject of our analysis. We proposed a probabilis-

tic model from spectrum sensor point of view and studied the asymptotic spectrum sensor performance. Lastly, a probabilistic model for throughput of primary and secondary networks in the presence of mutual interference was mathematically proposed.

REFERENCES

[1] K. Aardal, C. Hurkens, and A. Lenstra. Solving a linear diophantine equation with lower and upper bounds on the variables. *Integer Programming and Combinatorial Optimization*, pages 229–242, 1998.

[2] I.F. Akyildiz, W.Y. Lee, M.C. Vuran, and S. Mohanty. Next generation/dynamic spectrum access/cognitive radio wireless networks: a survey. *Computer Networks*, 50(13):2127–2159, 2006.

[3] F.A. Andrews. Two 50% probabilities. *The Journal of the Acoustical Society of America*, 57:245, 1975.

[4] R. Bosisio and U. Spagnolini. Interference coordination vs. interference randomization in multicell 3gpp lte system. In *Wireless Communications and Networking Conference, 2008. WCNC 2008. IEEE*, pages 824–829. IEEE, 2008.

[5] D. Cabric, S.M. Mishra, and R.W. Brodersen. Implementation issues in spectrum sensing for cognitive radios. In *Signals, Systems and Computers, 2004. Conference Record of the Thirty-Eighth Asilomar Conference on*, volume 1, pages 772–776. Ieee, 2004.

[6] H. Celebi, A. Gorcin, K. A. Qaraqe, A. El-Saigh, H. Arslan, and M. S. Alouini. Empirical results for wideband multidimensional spectrum usage. In *IEEE International Symposium on Personal, Indoor and Mobile Radio Communications (PIMRC)*, Tokyo, Japan, September 2009.

[7] H. Celebi and K. A. Qaraqe. Measurement and challenges for practical spectrum sensing in cognitive radio systems. In *In Proc. IEEE 18th Signal Processing and Communications Applications Conference*, Diyarbakir, Turkey, April 2010.

[8] V. Chandrasekhar and J. Andrews. Uplink capacity and interference avoidance for two-tier femtocell networks. *IEEE Trans. Wireless Communications*, 8(7):3498–3509, 2009.

[9] R.R. Chen, K.H. Teo, and B. Farhang-Boroujeny. Random access protocols for collaborative spectrum sensing in multi-band cognitive radio networks. *Selected Topics in Signal Processing, IEEE Journal*, 5(1):124–136, 2011.

[10] R. I. C. Chiang, G. B. Rowe, and K. W. Sowerby. A quantitative analysis of spectral occupancy measurements for cognitive radio. In *Proc. IEEE Vehicular Technology Conference*, Dublin, Ireland, Apr. 2007.

[11] Federal Communications Commission et al. Facilitating opportunities for flexible, efficient, and reliable spectrum use employing cognitive radio technologies. *Et docket*, 3:108, 2003.

[12] J. Do, D.M. Akos, and P.K. Enge. L and S bands spectrum survey in the San Francisco bay area. In *Proc. Position Location and Navigation Symposium (PLANS 2004)*, 2004.

[13] O. Dousse, F. Baccelli, and P. Thiran. Impact of interferences on connectivity in ad hoc networks. *IEEE/ACM Trans. Networking*, 13(2):425–436, 2005.

[14] O. Dousse, M. Franceschetti, and P. Thiran. On the throughput scaling of wireless relay networks. *IEEE Trans. Information Theory*, 52(6):2756–2761, 2006.

[15] D. Duan, L. Yang, and J.C. Principe. Cooperative diversity of spectrum sensing for cognitive radio systems. *IEEE Trans. Signal Processing*, 58(6):3218–3227, 2010.

[16] S.E. Elayoubi, O. Ben Haddada, and B. Fourestie. Performance evaluation of frequency planning schemes in ofdma-based networks. *IEEE Trans. Wireless Communications*, 7(5):1623–1633, 2008.

[17] S. W. Ellingson. Spectral occupancy at vhf: Implications for frequency-agile cognitive radios. In *Proc. of IEEE Vehicular Technology Conference (VTC)*, pages 1379–1382, Dallas, USA, Sept. 2005.

[18] R.K. Ganti and M. Haenggi. Interference and outage in clustered wireless ad hoc networks. *IEEE Trans. Information Theory*, 55(9):4067–4086, 2009.

[19] A. Ghasemi. Statistical characterization of interference in cognitive radio networks. In *Personal, Indoor and Mobile Radio Communications, 2008. PIMRC 2008. IEEE 19th International Symposium on*, pages 1 –6, 2008.

[20] A. Ghasemi and E.S. Sousa. Collaborative spectrum sensing for opportunistic access in fading environments. In *New Frontiers in Dynamic Spectrum Access Networks, 2005. DySPAN 2005. 2005 First IEEE International Symposium on*, pages 131–136. IEEE, 2005.

[21] A. Ghasemi and E.S. Sousa. Fundamental limits of spectrum-sharing in fading environments. *IEEE Trans. Wireless Communications*, 6(2):649–658, 2007.

[22] A. Ghasemi and E.S. Sousa. Interference aggregation in spectrum-sensing cognitive wireless networks. *Selected Topics in Signal Processing, IEEE Journal*, 2(1):41–56, 2008.

[23] A. Ghasemi and E.S. Sousa. Spectrum sensing in cognitive radio networks: requirements, challenges and design trade-offs. *Communications Magazine, IEEE*, 46(4):32–39, 2008.

[24] C. Ghosh, S. Pagadarai, D. Agrawal, and A. Wyglinski. A framework for statistical wireless spectrum occupancy modeling. *IEEE Trans. Wireless Communications*, 9(1):38–44, 2010.

[25] A. Goldsmith. *Wireless communications*. Cambridge University Press, 2005.

[26] K.A. Hamdi. A useful lemma for capacity analysis of fading interference channels. *IEEE Trans. Communications*, 58(2):411–416, 2010.

[27] S. Haykin et al. Cognitive radio: brain-empowered wireless communications. *Selected Areas in Communications, IEEE Journal*, 23(2):201–220, 2005.

[28] J.P. Hong and W. Choi. Throughput characteristics by multiuser diversity in a cognitive radio system. *IEEE Trans. Signal Processing*, 59(8):3749–3763, 2011.

[29] H. Inaltekin, M. Chiang, H.V. Poor, and S. Wicker. The behavior of unbounded path-loss models and the effect of singularity on computed network characteristics. *IEEE J. Sel. Areas Commun*, 27(7):1078–1092, 2009.

[30] M. Islam, G. L. Tan, F. Chin, B. E. Toh, Y.-C. Liang, C. Wang, Y. Y. Lai, X. Qing, S. W. Oh, C. L. Koh, and W. Toh. Spectrum survey in singapore: Occupancy measurements and analyses. In *Proc. of International Conference on Cognitive Radio Oriented Wireless Networks and Communications (CROWNCOM)*, Singapore, May 2008.

[31] Y.U. Jang. Performance analysis of cognitive radio networks based on sensing and secondary-to-primary interference. *IEEE Trans. Signal Processing*, 59(11):5663–5668, 2011.

[32] X. Kang, Y.C. Liang, A. Nallanathan, H.K. Garg, and R. Zhang. Optimal power allocation for fading channels in cognitive radio networks: Ergodic capacity and outage capacity. *IEEE Trans. Wireless Communications*, 8(2):940–950, 2009.

[33] JFC Kingman. *Poisson processes*. Oxford University Press, 1993.

[34] M. Lopez-Benitez and F. Casadevall. Empirical time-dimension model of spectrum use based on a discrete-time markov chain with deterministic and stochastic duty cycle models. *IEEE Trans. Vehicular Technology*, 60(6):2519–2533, 2011.

[35] R. Mahmoudvand, H. Hassani, A. Farzaneh, and G. Howell. The exact number of nonnegative integer solutions for a linear diophantine inequality. *IAENG International Journal of Applied Mathematics*, 40:1–5, 2010.

[36] M. A. McHenry, P. A. Tenhula, D. McCloskey, D. A. Roberson, and C. S. Hood. Chicago spectrum occupancy measurements & analysis and a long-term studies proposal. In *Proc. of Workshop on Technology and Policy for Accessing Spectrum (TAPAS)*, Boston, USA, Aug. 2006.

[37] M.A. McHenry, P.A. Tenhula, D. McCloskey, D.A. Roberson, and C.S. Hood. Chicago spectrum occupancy measurements & analysis and a long-term studies proposal. In *Proceedings of the first international workshop on Technology and policy for accessing spectrum*, page 1. ACM, 2006.

[38] R. Menon, R. Buehrer, and J. Reed. On the impact of dynamic spectrum sharing techniques on legacy radio systems. *IEEE Trans. Wireless Communications*, 7(11):4198–4207, 2008.

[39] J. Mitola and G. Q. Maguire. Cognitive radio: Making software radios more personal. 6(4):13–18, August 1999.

[40] J. Mitola III and G.Q. Maguire Jr. Cognitive radio: making software radios more personal. *Personal Communications, IEEE*, 6(4):13–18, 1999.

[41] M. Mitzenmacher and E. Upfal. *Probability and computing: Randomized algorithms and probabilistic analysis*. Cambridge University Press, 2005.

[42] Apurva N Mody, Stephen R Blatt, Ned B Thammakhoune, Thomas P McElwain, Joshua D Niedzwiecki, Diane G Mills, Matthew J Sherman, and Cory S Myers. Machine learning based cognitive communications in white as well as the gray space. In *Military Communications Conference, 2007. MILCOM 2007. IEEE*, pages 1–7. IEEE, 2007.

[43] Apurva N Mody, Matthew J Sherman, Ralph Martinez, Ranga Reddy, and Thomas Kiernan. Survey of ieee standards supporting cognitive radio and dynamic spectrum access. In *Military Communications Conference, 2008. MILCOM 2008. IEEE*, pages 1–7. IEEE, 2008.

[44] L. Musavian and S. Aissa. Ergodic and outage capacities of spectrum-sharing systems in fading channels. In *Global Telecommunications Conference, 2007. GLOBECOM'07. IEEE*, pages 3327–3331. IEEE, 2007.

[45] A. Petrin and P. G. Steffes. Analysis and comparison of spectrum measurements performed in urban and rural areas to determine the total amount of spectrum

usages. In *Proc. of International Symposium on Advanced Radio Technologies*, pages 9–12, Boulder, USA, March 2005.

[46] R Venkatesha Prasad, Przemyslaw Pawelczak, James A Hoffmeyer, and H Steven Berger. Cognitive functionality in next generation wireless networks: standardization efforts. *Communications Magazine, IEEE*, 46(4):72–78, 2008.

[47] K. A. Qaraqe, H. Celebi, M. S. Alouini, L. Abuhantash, M. Al-Mulla, O. Al-Mulla, A. Jolo, A. Ahmad, and A. El-Saigh. A wideband spectrum occupancy measurement for indoor and outdoor environments. In *International Conference on Communications Technologies (ICCT)*, Riyadh, Saudi Arabia, January 2010.

[48] Khalid A. Qaraqe, Nariman Rahimian, Hasari Celebi, and Costas N. Gheorghiades. Spatio temporal measurement and model for number of occupied channels. In *Proc. 18th IEEE International Conference on Telecommunications (ICT 2011)*, Cyprus, May 2011.

[49] Z. Quan, S. Cui, and A.H. Sayed. An optimal strategy for cooperative spectrum sensing in cognitive radio networks. In *Global Telecommunications Conference, 2007. GLOBECOM'07. IEEE*, pages 2947–2951. IEEE, 2007.

[50] A. Rabbachin, T.Q.S. Quek, H. Shin, and M.Z. Win. Cognitive network interference. *Selected Areas in Communications, IEEE Journal*, 29(2):480–493, 2011.

[51] A. Rabbachin, T.Q.S. Quek, and M.Z. Win. Statistical modeling of cognitive network interference. In *GLOBECOM 2010, 2010 IEEE Global Telecommunications Conference*, pages 1 –6, 2010.

[52] E. Salbaroli and A. Zanella. Interference analysis in a poisson field of nodes of finite area. *IEEE Trans. Vehicular Technology*, 58(4):1776–1783, 2009.

[53] G. Samorodnitsky and M. S. Taqqu. *Stable Non-Gaussian Random Processes*. Chapman & Hall, 1994.

[54] F. H. Sanders. Broadband spectrum surveys in denver, co, san diego, ca, and los angeles, ca: Methodology, analysis, and comparative results. In *Proc. of IEEE Symposium on Electromagnetic Compatibility*, 1998.

[55] A. Schrijver. *Theory of Linear and Integer Programming*. John Wiley & Sons Inc, 1998.

[56] Matthew Sherman, Apurva N Mody, Ralph Martinez, Christian Rodriguez, and Ranga Reddy. Ieee standards supporting cognitive radio and networks, dynamic spectrum access, and coexistence. *Communications Magazine, IEEE*, 46(7):72–79, 2008.

[57] L. Song and D. Hatzinakos. Cooperative transmission in poisson distributed wireless sensor networks: protocol and outage probability. *IEEE Trans. Wireless Communications*, 5(10):2834–2843, 2006.

[58] A. Sonnenschein and P.M. Fishman. Radiometric detection of spread-spectrum signals in noise of uncertain power. *IEEE Trans. Aerospace and Electronic Systems*, 28(3):654–660, 1992.

[59] CR Stevenson et al. Tutorial on the p802. 22.2 par for: Recommended practice for the installation and deployment of ieee 802.22 systems.

[60] H.A. Suraweera, P.J. Smith, and M. Shafi. Capacity limits and performance analysis of cognitive radio with imperfect channel knowledge. *IEEE Trans. Vehicular Technology*, 59(4):1811–1822, 2010.

[61] Z. Tian and G.B. Giannakis. Compressed sensing for wideband cognitive radios. In *Acoustics, Speech and Signal Processing, 2007. ICASSP 2007. IEEE International Conference on*, volume 4, pages IV–1357. IEEE, 2007.

[62] A. Tripathi. On a linear diophantine problem of frobenius. *Integers: Electronic Journal of Combinatorial Number Theory*, 6(A14):A14, 2006.

[63] D. Tse and P. Viswanath. *Fundamentals of wireless communication*. Cambridge University Press, 2005.

[64] S.P. Weber, X. Yang, J.G. Andrews, and G. De Veciana. Transmission capacity of wireless ad hoc networks with outage constraints. *IEEE Trans. Information Theory*, 51(12):4091–4102, 2005.

[65] T.A. Weiss and F.K. Jondral. Spectrum pooling: an innovative strategy for the enhancement of spectrum efficiency. *Communications Magazine, IEEE*, 42(3):S8–14, 2004.

[66] M. Wellens, J. Riihijarvi, and P. Mahonen. Empirical time and frequency domain models of spectrum use. *Physical Communication*, 2(1-2):10–32, 2009.

[67] M. Wellens, J. Wu, and P. Mahonen. Evaluation of spectrum occupancy in indoor and outdoor scenario in the context of cognitive radio. In *Proc. of International Conference on Cognitive Radio Oriented Wireless Networks and Communications (CROWNCOM)*, Orlando, FL, USA, Aug. 2007.

[68] S. Yarkan and H. Arslan. Statistical Wireless Channel Propagation Characteristics in Underground Mines at 900MHz. In *IEEE Military Communications Conference, 2007. MILCOM 2007*, pages 1–7, 2007.

[69] H. Yin and S. Alamouti. Ofdma: A broadband wireless access technology. In *Sarnoff Symposium, 2006 IEEE*, pages 1–4. IEEE, 2006.

[70] T. Yucek and H. Arslan. A survey of spectrum sensing algorithms for cognitive radio applications. *Communications Surveys & Tutorials, IEEE*, 11(1):116–130, 2009.

[71] R. Zhang, S. Cui, and Y.C. Liang. On ergodic sum capacity of fading cognitive multiple-access and broadcast channels. *IEEE Trans. Information Theory,*, 55(11):5161–5178, 2009.

[72] Q. Zhao and B.M. Sadler. A survey of dynamic spectrum access. *IEEE Signal Processing Magazine*, 24(3):79–89, 2007.

APPENDIX A

As it was explained, in order to find the tightest Chernoff bound we have to solve Eq.(2.11). Since for the uniform distribution, the moment generating function is:

$$M_M(u) = \frac{e^u - e^{(N+1)u}}{N(1-e^u)}, \tag{A.1}$$

The Eq.(2.11) changes to:

$$\frac{\left[e^u - (N+1)\, e^{(N+1)u}\right] N\,(1-e^u) + e^u\left[e^u - e^{(N+1)u}\right]}{N^2\,(1-e^u)^2} - \frac{N-1}{\Lambda} = 0. \tag{A.2}$$

After some simplifications we have:

$$\begin{aligned} &\Lambda\left[e^u - (N+1)\, e^{(N+1)u} + Ne^{(N+2)u}\right] \\ &-(N-1)\, Ne^{2u} + 2(N-1)Ne^u - N(N-1) = 0. \end{aligned} \tag{A.3}$$

For large N we approximately have:

$$\begin{aligned} &Ne^{(N+2)u} - (N+1)e^{(N+1)u} \approx 0, \\ &N(N-1) \approx N^2. \end{aligned} \tag{A.4}$$

Therefore Eq.(A.3) turns into a quadratic equation:

$$N^2e^{2u} - \left[2N^2 + \Lambda\right] e^u + N^2 = 0. \tag{A.5}$$

With the roots of:

$$\begin{aligned} e^u &\approx \frac{2N^2 + \Lambda \pm \sqrt{\Lambda^2 + 4N^2\Lambda}}{2N^2} \\ &\approx 1 + \frac{\Lambda}{2N^2} \pm \frac{2N\sqrt{\Lambda}}{2N^2} \approx 1 \pm \frac{\sqrt{\Lambda}}{N}, \end{aligned} \tag{A.6}$$

Since the Chernoff bound is only valid for $u \leq 0$, the root which is less than one is the desired root:

$$e^{u^*} = 1 - \frac{\sqrt{\Lambda}}{N}. \tag{A.7}$$

Based on the Eq.(2.12), the Chernoff bound is:

$$\left(1 - \frac{\sqrt{\Lambda}}{N}\right)^{-(N-1)} \exp\left(\Lambda\left(\frac{1 - \frac{\sqrt{\Lambda}}{N} - \left(1 - \frac{\sqrt{\Lambda}}{N}\right)^{N+1}}{\sqrt{\Lambda}} - 1\right)\right). \tag{A.8}$$

As N goes to infinity, using the fact that $\lim_{n\to\infty}\left(1 + \frac{x}{n}\right)^n = e^x$, the above bound turns into the following:

$$\exp\left(\sqrt{\Lambda}\left(2 - \sqrt{\Lambda} - e^{-\sqrt{\Lambda}}\right)\right). \tag{A.9}$$

Note that the above limit is the approximate limit point using the simplifying assumptions on (A.4). For the desired root on (A.7), the first assumption on (A.4) for large N turns into:

$$\begin{aligned} & N\left(1 - \frac{\sqrt{\Lambda}}{N}\right)^{N+2} - (N+1)\left(1 - \frac{\sqrt{\Lambda}}{N}\right)^{N+1} \\ &= Ne^{-\sqrt{\Lambda}}\left(1 + \frac{\sqrt{\Lambda}}{N^2} - \frac{2\sqrt{\Lambda}}{N}\right) - (N+1)e^{-\sqrt{\Lambda}}\left(1 - \frac{\sqrt{\Lambda}}{N}\right) \\ &\approx e^{-\sqrt{\Lambda}}\left(-\sqrt{\Lambda} - 1\right). \end{aligned} \tag{A.10}$$

Therefore the limit point gets more accurate as Λ increases. In other word, our

assumption gets more valid as rate gets larger.

APPENDIX B

Recall that $W = \sum_{k=0}^{U} M_k$ with $M_0 = 0$ and $M_k \;\; k = 1, 2, ..., U$ are independent uniform random variables with PMF of (3.10). We know that for the equation of:

$$M_1 + M_2 + \cdots + M_u = k \; ; \quad M_i \in \mathbb{N} \tag{B.1}$$

where $\mathbb{N}$ is the set of natural numbers, the number of all the possible solutions is $\binom{k-1}{u-1}$. Since $1 \leq M_i \leq N$, this set of solutions is only valid for $1 \leq k \leq N+1$ because for $k \geq N+2$ there will be solutions that M_i is greater than N so not valid but they are among the $\binom{k-1}{u-1}$ solutions. Moreover, since $1 \leq M_i \leq N$, (B.1) has no solution for $u \leq \left\lfloor \frac{k-1}{N} \right\rfloor$ where $\lfloor m \rfloor$ is the greatest integer smaller than m. Therefore the range of values of u is $\left\lfloor \frac{k-1}{N} \right\rfloor + 1 \leq u \leq k$. Since the distribution is uniform, all solutions are equiprobable with probability of $\frac{1}{N}$. Therefore, for the PMF of W for the values of $w \in \{1, 2, \cdots, N+1\}$, we have:

$$\begin{aligned} P(W = k) &= PU_k \left(\frac{1}{N}\right)^k \binom{k-1}{k-1} + PU_{k-1} \left(\frac{1}{N}\right)^{k-1} \binom{k-1}{k-2} + \cdots \\ &\quad + PU_{\left\lfloor \frac{k-1}{N} \right\rfloor + 1} \left(\frac{1}{N}\right)^{\left\lfloor \frac{k-1}{N} \right\rfloor + 1} \binom{k-1}{\left\lfloor \frac{k-1}{N} \right\rfloor} \\ &= \sum_{m=\left\lfloor \frac{k-1}{N} \right\rfloor + 1}^{k} PU_m \left(\frac{1}{N}\right)^m \binom{k-1}{m-1} \; ; \quad k \in \{1, 2, \cdots, N+1\} . \end{aligned} \tag{B.2}$$

We also have:

$$P(W = 0) = PU_0 = e^{-\Lambda}. \tag{B.3}$$

For $Pr\left(W \leq N-1\right)$ since for $1 \leq k \leq N-1$, $\left\lfloor \frac{k-1}{N} \right\rfloor + 1 = 1$ we have:

$$\begin{aligned} Pr\left(W \leq N-1\right) &= PU_0 + \sum_{k=1}^{N-1} P\left(W=k\right) \\ &= PU_0 + \sum_{k=1}^{N-1} \sum_{m=1}^{k} PU_m \left(\frac{1}{N}\right)^m \binom{k-1}{m-1} \\ &= PU_0 + \sum_{m=1}^{N-1} \left(PU_m \left(\frac{1}{N}\right)^m \sum_{k=m}^{N-1} \binom{k-1}{m-1} \right) \\ &= PU_0 + \sum_{m=1}^{N-1} \left(PU_m \left(\frac{1}{N}\right)^m \sum_{k=1}^{N-1} \binom{k-1}{m-1} \right) \\ &= PU_0 + \sum_{m=1}^{N-1} \left(PU_m \left(\frac{1}{N}\right)^m \sum_{j=0}^{N-2} \binom{j}{m-1} \right). \end{aligned} \tag{B.4}$$

Using the identity $\sum_{k=0}^{n} \binom{k}{b} = \binom{n+1}{b+1}$, the above equation turns to:

$$Pr\left(W \leq N-1\right) = \sum_{m=0}^{N-1} PU_m \left(\frac{1}{N}\right)^m \binom{N-1}{m}. \tag{B.5}$$

APPENDIX C

As $\Lambda \to \infty$, due to the effect of prioritization there will be only N active users of class 1. Thus, we will have:

$$\begin{aligned} &Pr\left(A_k\right) \to 0;\ k = 1, \cdots, N-1; \quad A_N = \left\{\overline{m} = (N, 0, \cdots, 0)_{1\times N}\right\}, \\ &Pr\left(Y = k\right) \to \delta\left(N-k\right);\ k = 1, \cdots, N, \\ &Pr\left(miss|Y = k\right) \to \delta\left(N-k\right)\frac{1}{k}\left(\overline{m}\cdot\overline{P}_{miss}\right);\ k = 1, \cdots, N, \end{aligned} \tag{C.1}$$

where $\delta\left(k\right)$ is the Dirac delta function. Hence, the floor of $Pr\left(miss\right)$ as Λ goes to infinity regardless of the type of requesting distribution and N is:

$$Pr\left(miss\right) \to P_{miss,1}. \tag{C.2}$$

APPENDIX D

As $\Lambda \to \infty$, due to the effect of prioritization and regardless of requesting distribution, the only primary user configuration is N active primary users of class 1. Therefore, we have:

$$\begin{aligned} &Pr\left(C_k\right) \to 0;\ k = 1, \cdots, N;\quad C_N = \left\{\overline{m} = \left(N, 0, \cdots, 0\right)_{1\times N}\right\} \\ &P_{OCC}\left(OCC = k\right) \to \delta\left(N - k\right), \end{aligned} \tag{D.1}$$

and for $P\left(X_i \middle| OCC\right)$ in (3.45):

$$P\left(X_i = x_i \middle| OCC = N\right) \to \delta\left(x_i - N\right)\delta\left(i - 1\right). \tag{D.2}$$

In this case for (3.35), (3.36), (3.38), and (3.40) we have, respectively:

$$\begin{aligned} &Pr\left(miss | OCC = N, X_1 = N\right) \to P_{miss,1} \\ &Pr\left(\text{CDE} = k | OCC = N\right) \to \delta\left(k\right) \\ &Pr\left(Int_{class\ i} | J, OCC = N, X_i = x_i\right) \to \delta\left(x_i - N\right)\delta\left(i - 1\right) f\left(j\right) \\ &P\left(J | OCC = N, X_1 = N\right) \to f\left(j\right). \end{aligned} \tag{D.3}$$

Hence, (3.45) changes to:

$$Pr\left(Int_i \middle| OCC = N\right) \to \delta\left(i - 1\right) \sum_{j=1}^{N} \frac{1}{N} f\left(j\right)^2. \tag{D.4}$$

Consequently, (3.43) and (3.44) respectively converge to:

$$\begin{aligned} &T_{P|OCC=N} \rightarrow N\tau_{P,1|OCC=N} \\ &\tau_{P,1|OCC=N} \rightarrow \sum_{j=1}^{N} \frac{1}{N} f\left(j\right)^2 C_{P,1}^{int} + \left(1 - \sum_{j=1}^{N} \frac{1}{N} f\left(j\right)^2\right) C_{P,1}. \end{aligned} \tag{D.5}$$

Thus, the limit point for the throughput of the primary network is:

$$T_p \rightarrow \sum_{j=1}^{N} f\left(j\right)^2 C_{P,1}^{int} + \left(N - \sum_{j=1}^{N} f\left(j\right)^2\right) C_{P,1}. \tag{D.6}$$

APPENDIX E

As $P_T \to \infty$, probabilities of miss detection of an occupied subcarrier and interference on a primary user become zero:

$$\begin{aligned} &Pr\left(miss|OCC\right) \to 0 \\ &Pr\left(Int_i\middle|OCC\right) \to 0 \\ &Pr\left(\text{num of miss} = l|OCC\right) \to \delta\left(l\right) \end{aligned} \tag{E.1}$$

Thus for (3.54) and (3.55) we have:

$$\begin{aligned} &T_{S|OCC=k}^{int} \to 0 \\ &T_{S|OCC=k}^{no\ int} \to \sum_{j=1}^{N} g\left(j\right) C_S = \sum_{j=1}^{N-k} g\left(j\right) C_S = \left(1 - g\left(0\right)\right) C_S = \left(1 - P_f^{N-k}\right) C_S. \end{aligned} \tag{E.2}$$

Hence, the throughput of the secondary user as the primary transmit power goes to infinity converges to

$$T_S \to C_S \left(1 - \sum_{k=0}^{N} P_f^{N-k} P_{OCC}\left(OCC = k\right)\right). \tag{E.3}$$

APPENDIX F

As large $\Lambda \to \infty$, due to the effect of prioritization and regardless of requesting distribution, the only primary user configuration is N active primary users of class 1 and all N subcarriers are occupied ($P_{OCC}\left(OCC = k\right) \to \delta\left(N - k\right)$). Hence, if the secondary user detects an idle subcarrier it will definitely cause interference on a primary user. Considering that there are no empty subcarriers and using the results in Appendix B for $Pr\left(Int_1 \middle| OCC = N\right) \to \sum_{j=1}^{N} \frac{1}{N} f\left(j\right)^2$, we have:

$$\begin{aligned} T_{S|OCC=N}^{no\ int} &\to 0 \\ T_{S|OCC=N}^{int} &\to N\tau_{S,1|OCC=N}^{int} \\ \tau_{S,1|OCC=N}^{int} &\to \sum_{j=1}^{N} \frac{1}{N} f\left(j\right)^2 C_{S,1}^{int}. \end{aligned} \tag{F.1}$$

Hence, the throughput of the secondary user at large primary network traffic converges to:

$$T_S \to \sum_{j=1}^{N} f\left(j\right)^2 C_{S,1}^{int}. \tag{F.2}$$